AD_____

Award Number: W81XWH-06-1-0673

TITLE: ErbB2 Trafficking and Signaling in Human Vestibular Schwannomas

PRINCIPAL INVESTIGATOR: Marlan R. Hansen, M.D.

CONTRACTING ORGANIZATION: The University of Iowa
                                             Iowa City, IA 52242

REPORT DATE: October 2009

TYPE OF REPORT: Annual

PREPARED FOR: U.S. Army Medical Research and Materiel Command
                        Fort Detrick, Maryland 21702-5012

DISTRIBUTION STATEMENT: Approved for Public Release;
                                        Distribution Unlimited

The views, opinions and/or findings contained in this report are those of the author(s) and should not be construed as an official Department of the Army position, policy or decision unless so designated by other documentation.

REPORT DOCUMENTATION PAGE

1. REPORT DATE	2. REPORT TYPE	3. DATES COVERED
1 Oct 2009	Annual	15 SEP 2008 – 14 SEP 2009

4. TITLE AND SUBTITLE

ErbB2 Trafficking and Signaling in Human Vestibular Schwannomas

5a. CONTRACT NUMBER

5b. GRANT NUMBER
W81XWH-06-1-0673

5c. PROGRAM ELEMENT NUMBER

6. AUTHOR(S)

Marlan R. Hansen, M.D., J. Jason Clark, Wie Ying Yue, Prabhat C. Goswami, Bruce J. Gantz

E-Mail: marlan-hansen@uiowa.edu

5d. PROJECT NUMBER

5e. TASK NUMBER

5f. WORK UNIT NUMBER

7. PERFORMING ORGANIZATION NAME(S) AND ADDRESS(ES)

The University of Iowa
Iowa City, IA, 52242

8. PERFORMING ORGANIZATION REPORT NUMBER

9. SPONSORING / MONITORING AGENCY NAME(S) AND ADDRESS(ES)
U.S. Army Medical Research and Materiel Command
Fort Detrick, Maryland 21702-5012

10. SPONSOR/MONITOR'S ACRONYM(S)

11. SPONSOR/MONITOR'S REPORT NUMBER(S)

12. DISTRIBUTION / AVAILABILITY STATEMENT
Approved for Public Release; Distribution Unlimited

13. SUPPLEMENTARY NOTES

14. ABSTRACT

We find that the ErbB2 receptor tyrosine kinase is active in vestibular schwannoma (VS) cells and drives proliferation. Our overall hypothesis is that defects in merlin lead to constitutive ErbB2 activation at the cell membrane and that inhibition of ErbB2 will reduce the survival of VS cells and potentiate the effects of radiation on VSs. In this report we show that VS cells, which lack functional merlin, constitutively express activated ErbB2 in lipid rafts contributing to their proliferative potential. Furthermore, protein kinase A inactivates merlin by phosphorylation in Schwann cells in vitro and in vivo following denervation, correlated with movement of ErbB2 into lipids rafts and re-entry into the cell cycle. VS cells are relatively radioresistance, due at least in part, to persistent JNK activity which promotes cell survival and limits oxidative stress. Finally, inhibition of ErbB2 reduces VS cell radiosensitivity whereas activation of ErbB2 enhances radiosensitivity, likely by regulating cell proliferation.

15. SUBJECT TERMS
Vestibular schwannoma, neurofibromatosis, radiation, merlin, ErbB2

16. SECURITY CLASSIFICATION OF:			17. LIMITATION OF ABSTRACT	18. NUMBER OF PAGES	19a. NAME OF RESPONSIBLE PERSON USAMRMC
a. REPORT	b. ABSTRACT	c. THIS PAGE			
U	U	U	UU	95	19b. TELEPHONE NUMBER *(include area code)*

Table of Contents

Introduction:

Neurofibromatosis type II (NF2) results from mutation in the tumor suppressor gene, *merlin*, leading to the development of multiple intracranial and spinal tumors including schwannomas. Schwann cells (SCs) of the vestibular nerve are most commonly affected and bilateral vestibular schwannomas (VSs) is a hallmark of NF2. We have begun exploring factors that contribute to VS growth. We find that the ErbB2 receptor tyrosine kinases is active in VS cells and drives proliferation. *Our overall hypothesis is that defects in merlin lead to constitutive ErbB2 activation at the cell membrane and that inhibition of ErbB2 will reduce the survival of VS cells and potentiate the effects of radiation on VSs*. Our object is to test this hypothesis using cultured primary human VS cells.

Body:

During the third year of the award we have made substantial progress in achieving the aims of the proposal. Below we discuss the progress for each aim of the proposal.

Specific aim 1. Determine the ability of merlin to regulate ErbB2 localization and activity in vestibular schwannoma (VS) cells. We initially focused on correlating the status of merlin phosphorylation with ErbB2 trafficking in normal Schwann cells (SCs). First, we determined that the trafficking of ErbB2 into lipid rafts in SCs correlates with loss of axonal contact, phosphorylation of merlin on Serine 518, and proliferation (Figs. 1 and 2, and Brown and Hansen 2007).[1] Thus, phosphorylation of merlin on Serine 518 (S518), which inhibits its growth suppressive function, is correlated with the movement of ErbB2 into lipid rafts in the cell membrane. We also found that ErbB2 constitutively resides in lipid rafts in human VS cells that lack functional merlin.[1] Both results are consistent with our hypothesis that merlin regulates ErbB2 trafficking in VS cells. In the coming year we will use cultured VS

Figure 1. **A**. Immunoblots of contralateral nerve (**CL**), proximal (**P**) and distal (**D**) segments of the rat sciatic nerve 4 and 7 days post-axotomy (**PA**) probed with anti-merlin S518 phosphorylation (**p-merlin**) and non-phosphospecific merlin antibodies. **B**. Immunostaining of frozen sections from contralateral and distal nerve segments with anti-pmerlin (green) and anti-neurofilament 200 (NF200, red) antibodies.

cells to determine the extent to which replacement of merlin in human vestibular schwannoma cells regulates the trafficking of ErbB2 within the cell membrane. To accomplish this we have generated adenoviral vectors expressing wild-type and S518 mutated merlin. These effectively replace merlin in VS cells and reduce their proliferative capacity (Fig. 3). Our next task is to use biotinylation of cell surface proteins in cultures expressing the merlin constructs to determine the extent to which merlin regulates ErbB2 cell surface expression. In our preliminary experiments we have had difficulty biotinylating cell surface proteins in primary VS cultures. This primarily reflects the relatively small number of cells that can be generated from primary tumors. As an alternative to primary VS cultures, we have generated 2 cells lines derived from human VSs resected from 2 patients with NF2. These cell lines were generated by transfection with HPV E6/E7, similar to the HEI193 cells, in collaboration with Dr. John Lee.
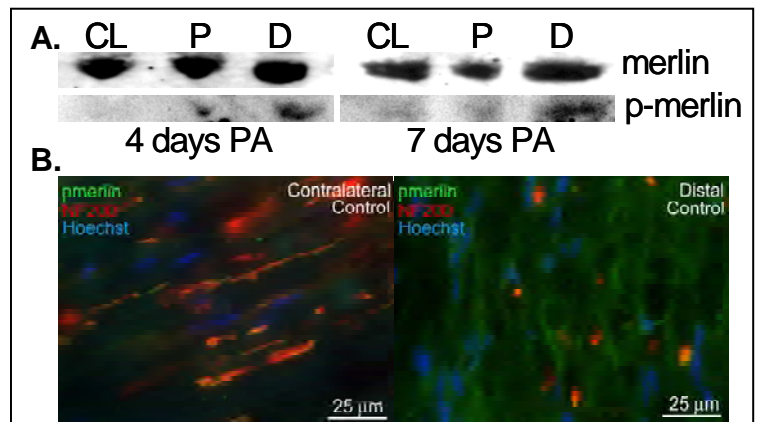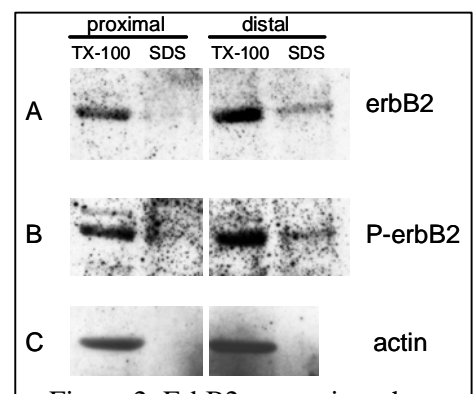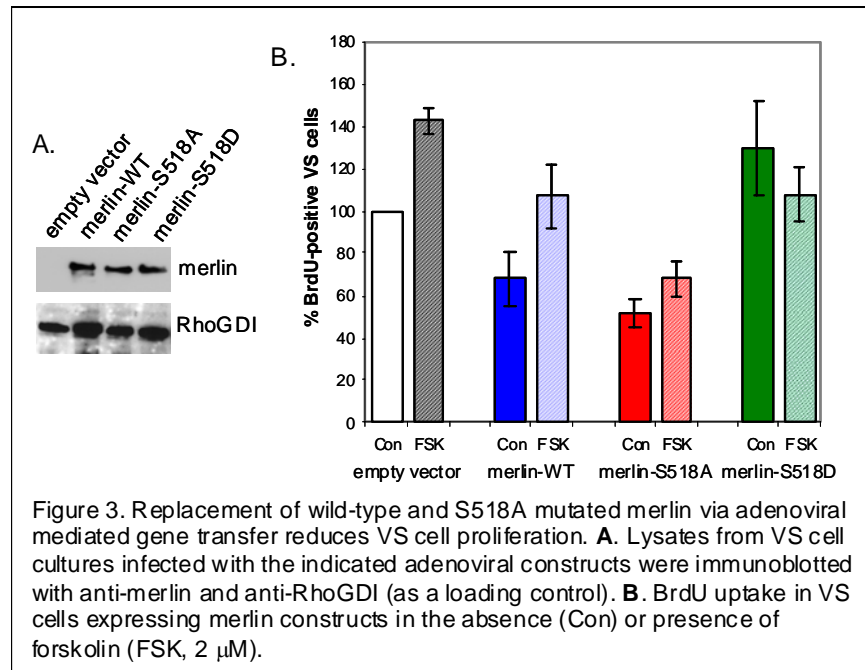

Figure 2. ErbB2 moves into the Triton-X-100 insoluble (lipid raft) fraction and becomes phosphorylated (p-ErbB2) in denervated Schwann cells (distal) following axotomy.

We have already verified that our Ad-merlin vectors effectively replace merlin in these cells (Fig. 4) and will use these cell lines if we continue to have difficulty biotinylating proteins in the primary cultures. We have recently found that mutation of merlin increases ErbB2 expression in sciatic nerve Schwann cells before and after denervation.

We have also examined the contribution of ErbB2 activity to activation of downstream pro-growth signals including MEK/Erk, PI-3-K/AKT, and JNK. In contrast to our original hypothesis, activation of these downstream kinases does not depend on ErbB2 signaling (see Yue, WY submitted manuscript). Nevertheless, these kinases are active in VS

Figure 3. Replacement of wild-type and S518A mutated merlin via adenoviral mediated gene transfer reduces VS cell proliferation. **A**. Lysates from VS cell cultures infected with the indicated adenoviral constructs were immunoblotted with anti-merlin and anti-RhoGDI (as a loading control). **B**. BrdU uptake in VS cells expressing merlin constructs in the absence (Con) or presence of forskolin (FSK, 2 μM).

cells and contribute to proliferative potential of the cells. JNK signaling also promotes VS cell survival by limiting the accumulation of mitochondrial superoxides. These later observations extend beyond the scope of the original proposal and result from our exploration of the consequences of ErbB2 signaling in VS cells.

In conclusion we have firmly established that ErbB2 signaling contributes to VS growth *in vitro* and *in vivo* and that trafficking of ErbB2 into lipids rafts of the cell membranes correlates with loss of merlin function, either by mutation or phosphorylation. We have also established that activation of several downstream kinases critical for VS cell growth including MEK/Erk, PI-3-K/AKT, and JNK, does not depend on ErbB2 activity.

Specific aim 2. Determine whether phosphorylation of merlin on serine 518 (S518) by protein kinase A (PKA) inhibits merlin's ability to regulate ErbB2 trafficking and suppress VS cell proliferation. We first demonstrated that activation of protein kinase A (PKA) with forskolin (FSK, 2-5 μM) leads to merlin S518 phosphorylation in rat SCs (Fig. 5) and that this correlates with
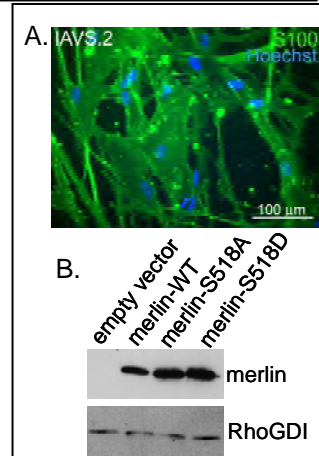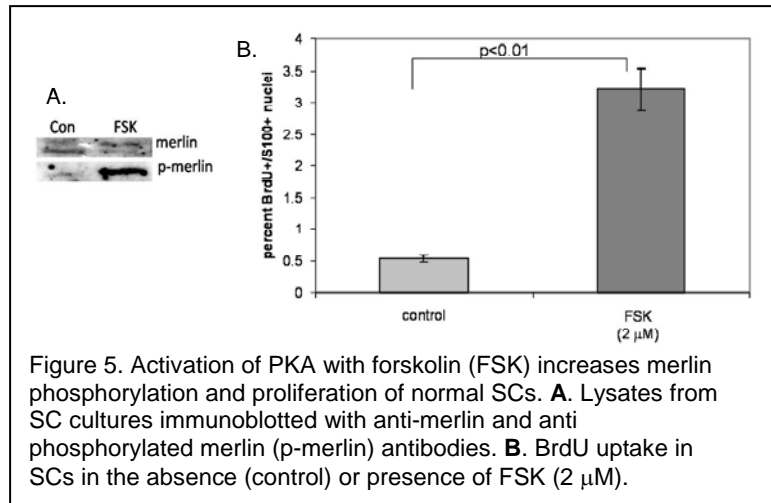

Figure 4. IAVS2 NF2 cell line generated by HPV E6/E7 transformation of cultured VS cells from an NF2 patient. **A.** Immunostaining with anti-S100, a SC marker. **B.** Replacement of merlin isoforms using adenoviral vectors.

proliferation and with movement of ErbB2 to the cell membrane (see above). Furthermore, we found that treatment of sectioned sciatic nerves with the PKA inhibitor, KT5720, reduces merlin phosphorylation following axotomy, verifying that PKA phosphorylates merlin in proliferating SCs *in vivo* (Fig. 6). Furthermore, treatment of VS

Figure 5. Activation of PKA with forskolin (FSK) increases merlin phosphorylation and proliferation of normal SCs. **A**. Lysates from SC cultures immunoblotted with anti-merlin and anti phosphorylated merlin (p-merlin) antibodies. **B**. BrdU uptake in SCs in the absence (control) or presence of FSK (2 μM).
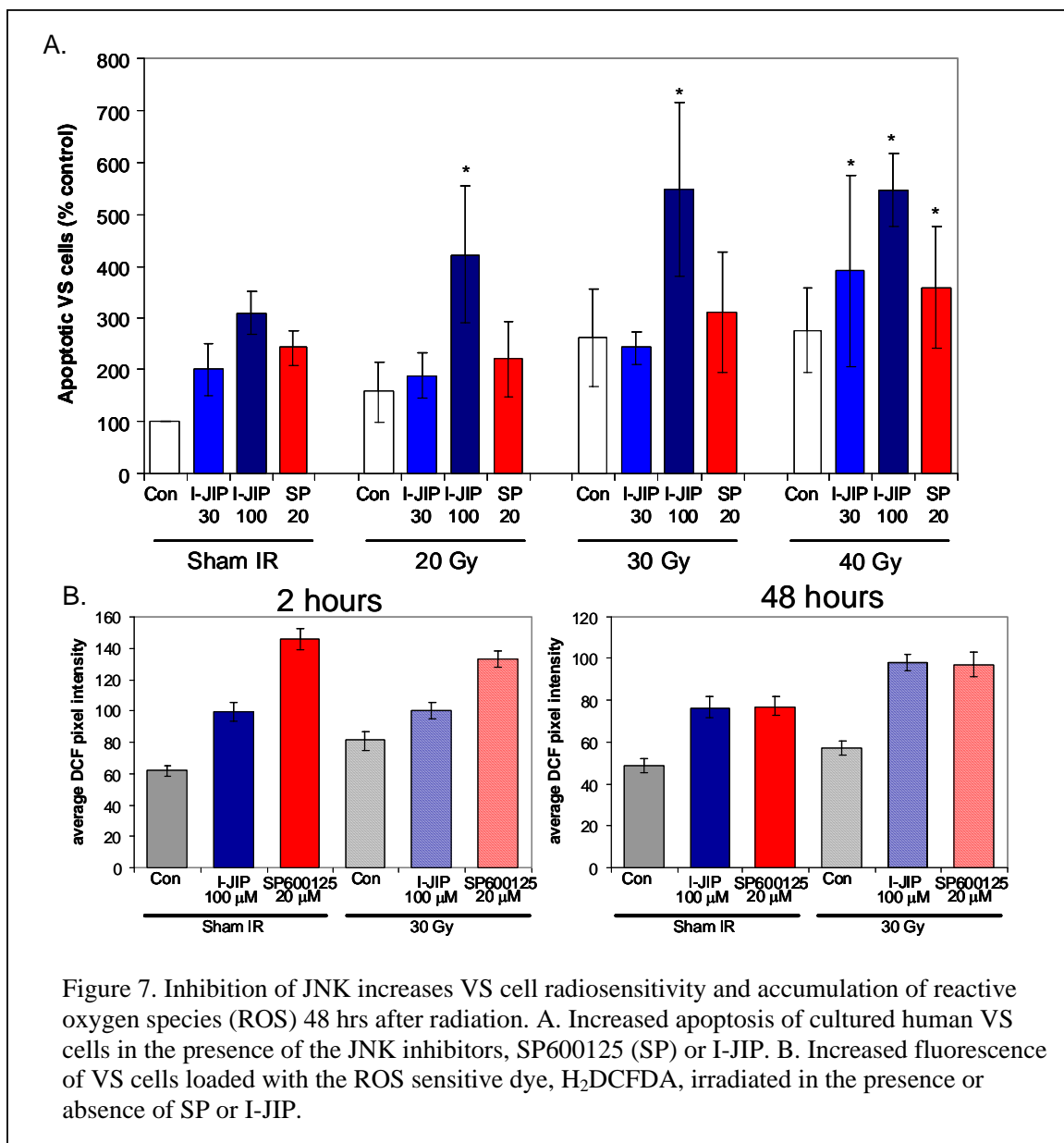
cells expressing wild-type merlin with FSK promotes VS cell proliferation and replacement of S518D mutated merlin, which is phosphomimetic, in VS cells fails to suppress VS cell proliferation (Fig. 3). These results are consistent with the hypothesis that PKA inactivates merlin by phosphorylation to promote SC proliferation. Nevertheless, FSK may also promote proliferation of VS cells expressing

Figure 6. Inhibition of PKA with KT5720 prevents merlin S518 phosphorylation in the distal segment of rat sciatic nerves following axotomy.

S518A mutated merlin (Fig. 3), suggesting that the ability of PKA to promote proliferation is not entirely due to merlin S518 phosphorylation. To verify these results with statistical significance we will repeat the experiment in at least 2 more VS cultures.
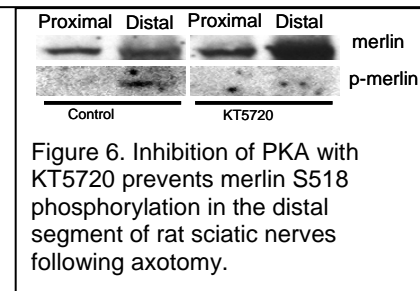
In the coming year, we will return to cultured VS cells to directly test the role of S518 phosphorylation by PKA in regulating ErbB2 trafficking. This depends on our ability to biotinylate cell surface proteins in primary VS cultures as in aim 1. If we are unable to successfully perform the experiments in primary cultures we will use our NF2 cell lines as outlined above.

Specific aim 3. Determine whether ErbB2 inhibitors potentiate the ability of radiation therapy (RT) to induce VS apoptosis and reduce proliferation. We have been able to perform radiation experiments on several cultured human VS specimens. We demonstrate that doses of ≥30 Gy are required to limit VS cell proliferation and that doses ≥40 Gy are required to induce apoptosis. We found that sublethal doses of radiation (10 Gy) induce DNA damage in VS cells, evidenced by histone 2AX phosphorylation, implying that VS cells possess intrinsic mechanisms to repair radiation induced DNA damage without undergoing apoptosis. Furthermore, we show that inhibition of ErbB2, which reduces VS cell proliferation, protects VS cells against radiation induced cell death. Conversely, activation of ErbB2 by treatment with neuregulin, which promotes VS cell proliferation, increases the radiosensitivity of human VS cells. These results imply that (1) VS are radioresistant relative to most neoplasms, (2) the radiosensitivity of human VS cells depends on proliferative status, and (3) ErbB2 signaling

sensitizes VS cells to radiation by promoting proliferation. This work is now published.[2] Thus, we have been able to make substantial progress on the proposed experiments in this aim. To extend these observations, we have examined the effects of merlin-sensitive downstream kinases, MEK, Akt, and c-Jun N-terminal kinase (JNK) on VS cell proliferation, apoptosis and radiosensitivity. We find that JNK is active in VS cells and promotes cell proliferation and survival by limiting the accumulation of reactive oxygen species (see attached submitted manuscript, Yue, WY, et. al., J Neurosci). Further, JNK confers a radioprotective effect on VS cells evidenced by increased apoptosis in VS cultures treated concurrently with γ-irradiation and JNK inhibitors, SP600125 or I-JIP (Fig. 7). Finally, we have found that ErbB2 inhibitors reduce the growth of VS xenografts in nude mice, demonstrating the therapeutic relevance and potential of these investigations.[3]

Figure 7. Inhibition of JNK increases VS cell radiosensitivity and accumulation of reactive oxygen species (ROS) 48 hrs after radiation. A. Increased apoptosis of cultured human VS cells in the presence of the JNK inhibitors, SP600125 (SP) or I-JIP. B. Increased fluorescence of VS cells loaded with the ROS sensitive dye, H$_2$DCFDA, irradiated in the presence or absence of SP or I-JIP.

Key Research Accomplishments:

1- Demonstration that ErbB2 constitutively resides in lipid rafts in VS cells and translocates into lipid rafts in denervated Schwann cells, correlated with loss of merlin function.

2- Demonstration that protein kinase A phosphorylates merlin in Schwann cells *in vitro* and *in vivo* following denervation, correlated with proliferation and movement of ErbB2 into lipid rafts.

3- Demonstration that activation of PKA promotes proliferation of VS cells expressing merlin.

4- Demonstration that VS cells are relatively radioresistant. Inhibition of ErbB2 signaling further increases their radioresistance while activation of ErbB2 promotes radiosensitivity.

5- Demonstration of persistent activation of JNK in VS cells that promotes cell proliferation and survival by reducing oxidative stress. Further, persistent JNK activity accounts, at least in part, for the radioresistance of VS cells.

6- In collaboration with Dr. Joseph Cioffi, Medical College of Wisconsin, we have demonstrated that microRNA 21, a downstream effector of ErbB2 signaling, is upregulated in vestibular schwannoma tissue and promotes VS cell proliferation.

Reportable Outcomes:

Abstracts/Presentations:

Gurgel, R, Clark, J, Provenzano, M, Hansen, M. Merlin phosphorylation on serine 518 by protein kinase A contributes to spiral ganglion and sciatic nerve Schwann cell proliferation following denervation. Association for Research in Otolaryngology, Baltimore, Maryland, February 2009.

Cho, C-H, Xu, N, Han, GC, Green, S, Hansen, M. c-Jun N-terminal kinase is required for neurite growth in dissociated spiral ganglion neurons. Association for Research in Otolaryngology, Baltimore, Maryland, February 2009.

Hansen, MR, Clark, JJ, Gantz, BJ, Goswami, PC. Effects of ErbB2 signaling on the response of vestibular schwannoma cells to γ-irradiation. Triologic Society, Orlando, Florida, May 2008—Fowler Award for Best Basic Science Thesis.

Woodson, EA, Clark, JJ, Xu, N, Provenzano, MJ, Hansen, MR. Constitutive ERK and PI3-K activity each promote proliferation in vestibular schwannoma cells while constitutive JNK activity and p75NTR signaling protect against apoptosis. Association for Research in Otolaryngology, Phoenix, Arizona, February 2008.

Clark, JJ, Brown, KD, Gantz, BJ, Hansen MR. Contribution of ErbB2 signaling to vestibular schwannoma cell proliferation and radiosensitivity. 5th International Conference on Vestibular Schwannomas and Other CPA Lesions, Barcelona, Spain, June 2007

Brown, KD, Clark, J, Hansen MR. Differential lipid raft localization of ErbB2 in vestibular schwannoma cells and Schwann cells. Combined Sections Meeting, Triologic Society, Marco Island, Florida, February 2007.

Brown, KD, Clark, J, Hansen MR. Differential lipid raft localization of ErbB2 in vestibular schwannoma cells and Schwann cells. Association for Research in Otolaryngology, Denver, Colorado, February 2007.

Manuscripts:

Hansen, MR, Clark, JJ, Gantz, BJ, Goswami, PC. (2008) Effects of ErbB2 signaling on the response of vestibular schwannoma cells to γ-irradiation. Laryngoscope, 118(6):1023-30.

Brown, KD, Hansen, MR. (2008) Lipid raft localization of erbB2 in vestibular schwannoma and Schwann cells. Otol Neurotol, 29(1):79-85.

Clark, JJ, Provenzano, M, Diggelmann, HR, Xu, N, Hansen, SS, Hansen, MR. The ErbB inhibitors, trastuzumab and erlotinib, inhibit growth of vestibular schwannoma xenografts in nude mice: a preliminary study. Otology&Neurotology 2008, 29(6):846-53.

Funding applied for based on work supported by this award:

Plastic Surgery Education Foundation/AAONHS   Richard Gurgel (PI)
Contribution of merlin inactivation by protein kinase A to facial nerve Schwann cell regenerative responses
The objectives are to determine the role of protein kinase A in the inactivation of merlin and Schwann cell mitosis following facial nerve injury.

Status: funded

NIH/NIDCD   Marlan Hansen (PI)
Contribution of c-Jun N-terminal kinase activity to vestibular schwannoma growth
The objectives are to determine the mechanisms leading to persistent c-Jun N-terminal kinase activity in vestibular schwannoma and the cellular consequences of inhibiting this activity.

Status: funded

Conclusions:

In summary, we have shown that VS cells, which lack functional merlin, constitutively express activated ErbB2 in lipid rafts contributing to their proliferative potential. Furthermore, protein kinase A inactivates merlin by phosphorylation in SCs *in vitro* and *in vivo* following denervation, correlated with movement of ErbB2 into lipids rafts and re-entry into the cell cycle. VS cells are relatively radioresistance, due at least in part, to persistent JNK activity which promotes cell survival and limits oxidative stress. Finally, inhibition of ErbB2 reduces VS cell radiosensitivity whereas activation of ErbB2 enhances radiosensitivity, likely by regulating cell proliferation.

References:

1. Brown KD, Hansen MR. Lipid raft localization of erbB2 in vestibular schwannoma and Schwann cells. *Otol Neurotol.* 2008;29(1):79-85.
2. Hansen MR, Clark JJ, Gantz BJ, Goswami PC. Effects of ErbB2 signaling on the response of vestibular schwannoma cells to gamma-irradiation. *Laryngoscope.* Jun 2008;118(6):1023-1030.
3. Clark JJ, Provenzano M, Diggelmann HR, Xu N, Hansen SS, Hansen MR. The ErbB inhibitors trastuzumab and erlotinib inhibit growth of vestibular schwannoma xenografts in nude mice: a preliminary study. *Otol Neurotol.* Sep 2008;29(6):846-853.

Lipid Raft Localization of ErbB2 in Vestibular Schwannoma and Schwann Cells

Kevin D. Brown and Marlan R. Hansen

Department of Otolaryngology—Head and Neck Surgery, University of Iowa College of Medicine, Iowa City, Iowa, U.S.A.

Hypothesis: ErbB2 resides in lipid rafts (regions of receptor regulation) in vestibular schwannoma (VS) cells.

Background: ErbB2 is a growth factor receptor critical for Schwann cell (SC) proliferation and development. ErbB2 localization and activity may be regulated by merlin, an adaptor protein deficient in VS. Lipid rafts are microdomains in the plasma membrane that amplify and regulate receptor signaling. Persistence of erbB2 in lipid rafts in VS due to merlin deficiency may explain increased VS cell growth.

Methods: Protein extracts from VS or rat sciatic nerve (proximal or distal to a crush injury) were isolated into lipid raft and nonraft fractions and immunoblotted for erbB2, phosphorylated erbB2, and merlin (for sciatic nerve). Cultured VS cells were probed with anti-erbB2 antibody and a lipid raft marker, cholera toxin B (CTB).

Results: ErbB2 moves to lipid rafts in proliferating SCs and is persistently localized to lipid rafts in VS cells. ErbB2 is phosphorylated (activated) in lipid rafts. ErbB2 colocalized with CTB in cultured VS cells, confirming raft targeting. Merlin also persistently localized to lipid rafts in SCs, and its relative phosphorylation increased in proliferating cells.

Conclusion: Lipid raft localization of erbB2 in proliferating SCs and in VS cells supports a critical role for lipid rafts in amplifying/regulating erbB2 signaling. Merlin resides in lipid rafts in SCs, and its phosphorylation increases in proliferating SCs, suggesting it regulates cell proliferation within lipid rafts. The absence of merlin in VS may therefore lead to persistent erbB2 localization to lipid rafts and increased cell proliferation. **Key Words:** Vestibular schwannoma—ErbB2—Merlin—Signal transduction—Lipid rafts.

Otol Neurotol **29:**79–85, 2008.

Vestibular schwannomas (VSs) represent benign neoplasms arising from Schwann cells (SCs) of the vestibular nerves. Two forms of the disease exist, a sporadic form and a form associated with the genetic disease neurofibromatosis type 2 (NF-2). Both forms share in common mutations in the *NF2* gene known as merlin or schwannomin (1). The merlin protein shares a high degree of homology with the ezrin-radixin-moesin family of proteins. This family of proteins functions as intermediates that integrate signaling between cell surface scaffolding proteins and cytoplasmic signaling cascades [reviewed in Bretscher et al. (2)]. Specifically, merlin appears to mediate contact inhibition of cell growth (3,4).

Of relevance to SC tumorigenesis, merlin has been implicated in regulating the subcellular localization and activity of the glial growth factor receptor, erbB2. In SCs, heterodimers composed of erbB2 and erbB3 function as receptors for the glial growth factor, neuregulin 1 (NRG1) (5). NRG1-induced dimerization of this pair leads to receptor phosphorylation followed by activation of intracellular pathways critical for SC survival and proliferation. These include the mitogen-activated protein kinase and phosphatidylinositol-3 kinase pathways (6). In the absence of erbB2 and erbB3, SCs fail to develop (7–9). ErbB2 signaling also contributes to the proliferation of SCs following axotomy, indicating that SCs critically depend on this receptor for normal development and proliferation (10).

In addition to its role in SC development and response to injury, erbB2 signaling contributes to the development and progression of SC neoplasms. Overexpression of NRG1 results in malignant peripheral nerve sheath tumors in transgenic mice, and human malignant peripheral nerve sheath tumor proliferation depends on erbB signaling (11,12). Of particular interest, recent investigations revealed that constitutive erbB2 activity contributes

to VS proliferation in vitro, further supporting a central role for erbB2 in human SC tumorigenesis (13–16).

Signaling by receptor tyrosine kinases, such as erbB2, is regulated at multiple levels including expression, degradation, access to ligand, and, in particular, subcellular localization. Cholesterol-enriched microdomains of the cell membrane, known as lipid rafts, concentrate receptors with intermediate molecules critical for amplifying and regulating signaling pathways [reviewed in Hancock (17)]. Cell surface receptors traffic in and out of these microdomains as they are engaged by their respective ligands, initiate their signaling cascades, and are ultimately removed. ErbB2 localizes to lipid rafts in other cell systems, suggesting that it may intermittently reside in lipid rafts in SCs and VS cells (18,19). Likewise, merlin localizes to lipid rafts in fibroblasts and has been implicated in regulating the intracellular localization and activity of receptor tyrosine kinases, including cell contact–dependent sequestration of erbB2 in SCs (4,20). These observations suggest a model wherein merlin regulates SC proliferation by regulating the subcellular localization of erbB2, among other molecules, in response to cell-cell contact cues (4).

Aberrant localization of growth-promoting receptors in lipid rafts may predispose to neoplasia (21). Persistent localization of erbB2 to lipid rafts (due to merlin deficiency) may therefore contribute to the dysregulated growth of VS cells. Here we evaluate the extent to which erbB2 localizes to lipid rafts in quiescent and proliferating SCs and in VS cells.

MATERIALS AND METHODS

Vestibular Schwannoma Collection

All patients provided written, informed consent for use of tumor harvested at the time of surgery. The institutional review board at the University of Iowa approved the study protocol. VS specimens were collected at the time of surgical removal and placed in ice-cold culture media (Dulbecco modified Eagle medium with 10% fetal calf serum and N2 additives) until either soluble and insoluble fractions were isolated (see below) or cells were cultured. A total of 8 tumors (sporadic form of disease) were examined (4 tumors for Western blots and 4 tumors for immunofluorescence studies).

Rat Sciatic Nerve Collection

The institutional animal care and use committee at the University of Iowa approved all protocols used in the study. Previous work has demonstrated increased erbB2 expression in denervated, proliferating rat sciatic nerve SCs beginning at 3 days after axotomy (10). We therefore selected 4 days as the period to evaluate erbB2 localization in proliferating SCs. Adult female Sprague-Dawley rats were anesthetized with ketamine/xylazine, and the sciatic nerve was exposed in the mid–gluteal region. The sciatic nerve was crushed for 10 seconds with a small hemostat (hematoma formation at the crush site facilitated easy future identification of this site), and the wound was closed. Four days later, the animals were killed, the operative site reopened, and proximal and distal nerve segments to the crush site collected. These segments were then pooled in 3 separate experiments of 3 animals each. Protein extracts for Western blotting were isolated into soluble and insoluble fractions as described below.

Primary Vestibular Schwannoma Cell Culture

The culture of human VS cells has been previously described (14). Briefly VS specimens were cut into approximately 1-mm pieces and digested in collagenase and trypsin. They were then further dissociated by trituration through small-bore pipettes. The cells were initially resuspended in culture media (Dulbecco modified Eagle medium with 10% fetal calf serum and N2 additives) and plated onto 4-well tissue culture slides precoated with polyornithine and laminin. The cells were maintained in serum-free N2 media, following the initial media exchange until they reached greater than 70% confluency.

Bromodeoxyuridine Labeling of Sciatic Nerve

Four days following sciatic nerve crush injury, animals received 4 injections of bromodeoxyuridine (BrdU; 10 mg/mL in phosphate-buffered saline [PBS], 50 µg/g weight intraperitoneally) spaced over a 24-hour interval. The animals were killed, perfused with 4% paraformaldehyde transcardiac, and the distal and proximal sciatic nerve segments were harvested and fixed in 4% paraformaldehyde for 20 minutes. The nerve segments were stripped of the epineurium, and the fascicles were gently teased apart. Following treatment with 2 N HCl, the nerve segments were permeabilized with 0.8% Triton-X100 in PBS, blocked, and immunostained with anti-BrdU monoclonal antibody (1:1,000, clone G3G4, hybridoma core, University of Iowa) and rabbit anti-S100 (1:800; Sigma, St. Louis, MO, USA) followed by Alexa 488– and Alexa 546–conjugated secondary antibodies (Molecular Probes, Eugene, OR, USA). Nuclei were labeled with Hoescht 3342 (10 µg/mL; Sigma). BrdU labeling was quantified by counting the percent of BrdU-positive SCs (S100-positive) nuclei in 3 randomly selected fields for each nerve segment from 3 separate animals. Differences in the mean percent of BrdU-positive cells were determined by the 2-tailed Student's t test using Excel software (Microsoft Corp., Redmond, WA, USA). Nerve segments were imaged using Leica SP5 confocal microscope using Leica software (Leica Microsystems Inc., Bannockburn, IL, USA).

Western Blotting of Vestibular Schwannoma and Rat Sciatic Nerve Extracts (Isolation of Soluble and Insoluble Fractions)

Isolation of soluble and insoluble fractions as well as the equivalence of the insoluble fraction with lipid rafts has been previously described (21). After washing the tissue pellet (either VS or sciatic nerve) with ice-cold PBS, the pellet was resuspended in ice-cold Triton-X100 (TX-100) buffer (1% TX-100, 150 mmol/L NaCl, 20 mmol/L Tris, pH 7.4 plus). Minicomplete protease inhibitors as well as phosphatase inhibitors were added, as per manufacturer's instructions, to all lysis buffers (Roche Diagnostics Corp., Indianapolis, IN, USA). The tissue was then sonicated to break connective tissue, and cells were then allowed to incubate 30 minutes on ice to allow dissolution of the nonlipid raft fraction. After this incubation, the lysates was centrifuged, and the supernatant removed. This supernatant constituted the soluble (nonlipid raft) fraction. The remaining pellet was then resuspended in an equal volume of sodium dodecyl sulfate (SDS) lysis buffer (0.5% SDS, 1% β-mercaptoethanol, 1% TX-100, 150 mmol/L NaCl, 20 mmol/L Tris, pH 7.4). By using equal volumes of buffer for each

isolated fraction, the relative amount of erbB2 in each fraction reflects its distribution between the soluble and insoluble fractions. Accurate comparisons as to the relative distribution (between soluble, nonlipid raft fractions and insoluble lipid raft fractions) of erbB2, phospho-erbB2, and merlin can then be made. The sample was then again sonicated to aid in resuspending the pellet from centrifugation and incubated for 30 minutes on ice to allow dissolution of lipid rafts. The resulting lysate constituted the insoluble (lipid raft) fraction. Both lysates then had an equivalent volume of SDS running buffer added. Lysates were then separated under denaturing conditions on a 7.5% SDS–polyacrylamide gel electrophoresis (PAGE) gel and were subsequently transferred to nitrocellulose paper. Blots were then blocked with 5% dried milk in   Tris-buffered saline + Tween and immunoblotted with the following antibodies: anti-erbB2 (5 µg/mL AB-17; Lab Vision, Freemont, CA, USA), anti-phospho-erbB2 (2.5 µg/mL Ab-18, Lab Vision), anti-actin (1:5,000 Ab-5; BD Biosciences, Mississauga, ON, Canada), and anti–NF-2/schwannomin/merlin (1:10,000, sc-331; Santa Cruz Biotechnology, Santa Cruz, CA, USA). All blots were washed and then treated with either goat antimouse or goat antirabbit horseradish peroxidase–conjugated antibody at a 1:20,000 dilution (BioRad, Hercules, CA, USA). Blots were washed again and then developed with electrochemiluminescence solution, as per manufacturer's instructions (Pierce, Rockford, IL, USA) and exposed to film.

Immunostaining of Vestibular Schwannoma Cells

To verify colocalization of erbB2 with lipid rafts, VS cultures were washed twice with ice-cold PBS. Cells were then incubated with cholera toxin B (CTX-B)–Alexa Fluor 555 (red, 2.5 µg/mL) for 30 minutes at 4°C. Cholera toxin B binds GM1 ganglioside and is a marker for lipid rafts (Molecular Probes). Cells were light protected from this point on. After this incubation, cells were then washed 3 times with ice-cold PBS for 5 minutes each. Cells were then fixed with 4% paraformaldehyde/0.4% TX-100/PBS, pH 7.2, for 10 minutes. After fixation, cells were then washed 3 times with wash buffer (0.4% TX-100, PBS) for 5 minutes for each wash and blocked with blocking buffer (0.4% TX-100, 5% goat serum, 2% bovine serum albumin, PBS) for 30 minutes at room temperature. Cells were then washed once with wash buffer for 5 minutes. Mouse anti-erbB2 (Ab-2, 1:400; Oncogene Research Products, San Diego, CA, USA), diluted in blocking buffer, was then incubated overnight at 4°C. After 3 washes, Alexa Fluor 488 goat antimouse secondary antibody (1:1,000; Molecular Probes) was then incubated for 1 hour at room temperature. Cells were then washed 3 times and cover-slipped with 1 to 2 drops of Aquamount (Lerner Laboratories, Pittsburgh, PA, USA). Fluorescent digital images were captured using Zeiss LSM 510 confocal microscope. Images were prepared for publication with Adobe Photoshop (San Jose, CA, USA).

RESULTS

To better understand the role of erbB2 trafficking to lipid rafts in SC proliferation, we initially evaluated erbB2 localization in proliferating and quiescent normal SCs. Denervated SCs distal to the site of a sciatic nerve crush injury proliferate and increase expression of erbB2 within 3 days after injury, whereas those in the proximal segment remain quiescent (10). Therefore, we compared erbB2 localization to lipid rafts in nerve segments prox-

imal and distal to a crush injury. Four days after crushing the sciatic nerve, proximal and distal segments were collected and pooled from 3 animals in each of the 3 experiments. Protein extracts from the sciatic nerve segments were then isolated into TX-100 soluble and insoluble fractions. Equal volumes of lysate buffer were used to suspend these fractions to permit evaluation of the relative distribution of erbB2 between these fractions. These fractions were then separated by SDS-PAGE, transferred to nitrocellulose paper, and immunoblotted for erbB2, phosphorylated erbB2, and actin (to permit comparisons of protein content between proximal and distal segments). As shown in Figure 1C, erbB2 appeared exclusively in the nonlipid raft fraction (TX-100 soluble) in the proximal (nonproliferating) segment. The distal (proliferating) segment demonstrated an increase in overall erbB2 expression as previously reported (10) and also demonstrated the movement of erbB2 into the lipid raft (insoluble) fraction. This suggests that erbB2 moves to lipid rafts in proliferating SCs and supports the physiological importance of this localization in dividing cells. Furthermore, erbB2 is phosphorylated in the lipid raft fraction (Fig. 1D). As expected, the cytosolic protein actin remained in the TX-100 fraction verifying the adequacy of the TX-100 extraction (Fig. 1E). Proliferation of SCs in the distal segment was verified by BrdU labeling (Fig. 1, A and B). Together these data suggest that localization of erbB2 into lipid rafts is an important feature of SC proliferation and that erbB2 is activated in lipid rafts as demonstrated by its phosphorylation within these fractions.

Previous studies have suggested that merlin regulates erbB2 trafficking in SCs as merlin is present in erbB2 immunoprecipitates from SCs (4). Furthermore, merlin resides within lipid rafts in cultured fibroblasts (20). The data above demonstrate inducible erbB2 trafficking to lipid rafts in SCs that have lost axonal contact and re-enter the cell cycle. We then sought to determine if merlin also localizes to lipid rafts in SCs and if that localization varied between quiescent and proliferating nerve segments. TX-100 soluble and insoluble fractions derived from sciatic nerve segments proximal and distal to the crush injury were separated by SDS-PAGE, transferred to nitrocellulose paper, and immunoblotted for merlin. Merlin has been previously demonstrated to present as 2 dominant bands with the upper band representing its phosphorylated form (22,23). Merlin was exclusively found in the lipid raft (insoluble) fraction in rat sciatic nerve in both the distal (proliferating) and proximal (quiescent) segments of the nerve (Fig. 2). This finding was confirmed in 3 replicate experiments and is consistent with previous reports in other cell systems (20). Thus, merlin constitutively localizes to lipid rafts in normal SCs, implying that it likely plays a fundamental role in regulating the trafficking of key signaling molecules into and out of these microdomains of the cell membrane. Interestingly, the relative amount of phosphorylated merlin is higher in proliferating nerve, consistent with previous reports
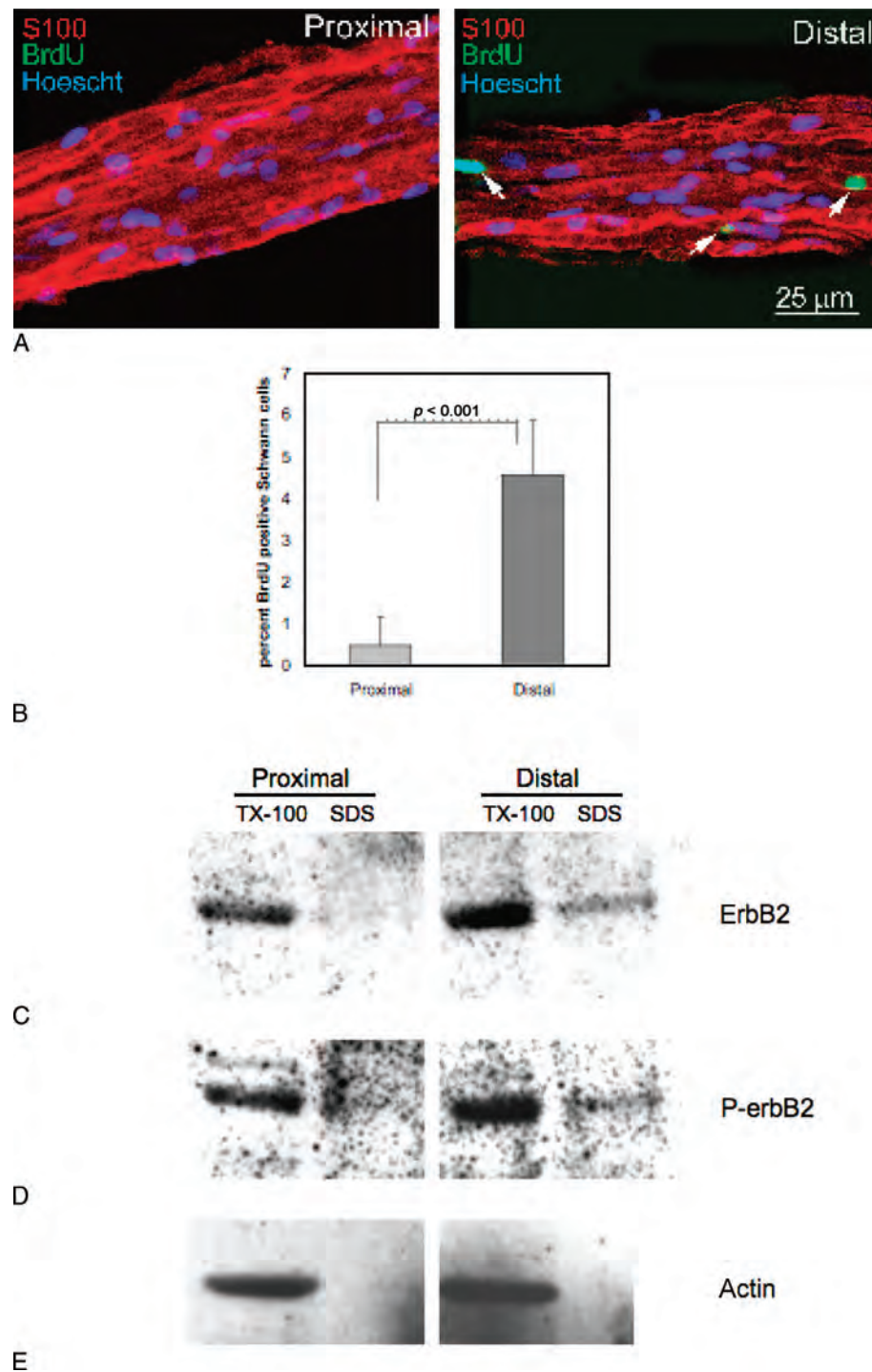
13

FIG. 1. Lipid raft localization of erbB2 in sciatic nerve. *A–B*, Four days after a crush injury, animals were labeled with BrdU as described in Materials and Methods. Proximal and distal segments were collected and immunostained with anti-BrdU monoclonal antibody (1:1,000, clone G3G4, hybridoma core, University of Iowa) and rabbit anti-S100 (1:800; Sigma) followed by Alexa 488- and Alexa 546-conjugated secondary antibodies (Molecular Probes). Nuclei were labeled with Hoescht 3342 (10 μg/mL; Sigma). BrdU labeling was quantified by counting the percent of BrdU-positive SC (S100 positive) nuclei in 3 randomly selected fields for each nerve segment from 3 separate animals. Differences in the mean percent of BrdU-positive cells were determined by the 2-tailed Student's *t* test and demonstrated significance at $p < 0.001$. *C–E*, Four days after a crush injury to the sciatic nerve, proximal (quiescent) and distal (proliferating) segments were collected, and soluble (TX-100/nonlipid raft) and insoluble (SDS/lipid raft) fractions were prepared. Fractions were separated by SDS-PAGE, transferred to nitrocellulose, and blotted for erbB2 (*C*) and phospho-erbB2 (*D*). Fractions were also blotted for actin (*E*) to verify equal protein loading and complete extraction of TX-100 soluble proteins. Data are representative of pooled nerve segments from 3 animals for each of 3 independent experiments.
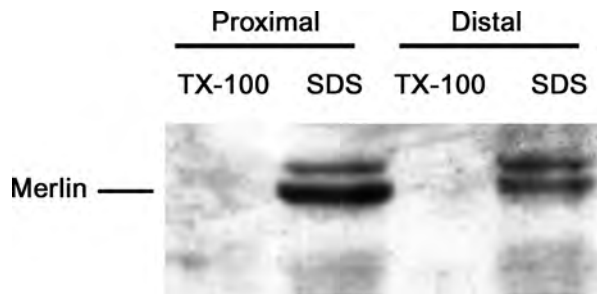
FIG. 2. Lipid raft localization of merlin in sciatic nerve. Four days after a crush injury to the sciatic nerve, proximal (quiescent) and distal (proliferating) segments were collected, and soluble (TX-100/nonlipid raft) and insoluble (SDS/lipid raft) fractions were prepared. Fractions were separated by SDS-PAGE, transferred to nitrocellulose, and blotted for merlin. The characteristic 2 dominant bands of merlin are seen. Data are representative of pooled nerve from 3 animals for each of 3 independent experiments.

indicating that phosphorylated merlin promotes cell proliferation (24).

Because merlin is implicated in erbB2 trafficking and is deficient in VS cells and because erbB2 activation contributes to VS proliferation, we next evaluated the lipid raft distribution of erbB2 in acutely resected human VS. VS tissue was harvested and isolated into TX-100 soluble and insoluble fractions (21,25). As demonstrated previously, the insoluble fraction corresponds to the lipid raft–containing fraction of the cell (21). Each of these fractions was then separated by SDS-PAGE, transferred to nitrocellulose paper, and immunoblotted for erbB2. The blot was then stripped and reprobed with an anti–phosphorylated erbB2 antibody. Equal volumes of buffer were used for each isolated fraction, and equal volumes were loaded into the gel for each fraction; therefore, the relative amount of erbB2 in each fraction reflects its distribution between the soluble and insoluble fractions. Remarkably, erbB2 exclusively localized within the lipid raft (TX-100 insoluble) fraction in VS tissue (Fig. 3A). The phosphorylated form of erbB2 is likewise localized to the lipid raft fraction (Fig. 3B), suggesting that the erbB2 in TX-100 insoluble fraction exists in an activated state consistent with the observation of constitutive erbB2 activation in VS tissue (14). Similar findings were seen in VS specimens from 4 patients. These data together demonstrate that in VS, which lacks functional merlin, activated erbB2 localizes to lipid rafts to a greater extent than that seen in denervated SCs and suggests the possibility that constitutive erbB2 localization in lipid rafts in VS contributes to their growth potential.

Although the TX-100 insoluble fraction has been previously demonstrated to contain lipid rafts, other subcellular domains such as caveolae and insoluble cytoskeletal components are likewise present within this fraction. To verify that erbB2 in the TX-100 insoluble fraction is due to its distribution into lipid rafts, we used colocalization studies with fluorophore-labeled CTX-B, which specifically binds to GM1 ganglioside

and is a reliable marker for lipid rafts and anti-erbB2 immunofluorescence. VS cultures near confluency were labeled with Alexa Fluor 555–conjugated CTB (red) followed by fixation and immunolabeling with anti-erbB2 and an Alexa Fluor 488 secondary antibody (green). Cells were imaged with confocal microscopy, and images were combined to evaluate for overlap of the fluorophores. As shown in Figure 4, erbB2 immunofluorescence is predominantly restricted to the cell membrane where it extensively overlaps with CTX-B labeling, confirming that erbB2 localization to the TX-100 insoluble (lipid raft) fraction is due to its localization to lipid rafts.

DISCUSSION

Lipid rafts are proposed to serve as hubs of activity by which signals of cell growth are amplified and/or regulated before being transduced into the cell (26). Merlin is the deficient or mutated protein in VS, and previous studies suggest that merlin may localize to lipid rafts in fibroblasts (1,20). Similarly, in other cell systems, erbB2 appears to localize to lipid rafts (18). ErbB2 and its binding partner erbB3 have been proposed to promote the proliferation of schwannoma cells (13–16). We therefore hypothesized that differences in lipid raft localization of erbB2 may, in part, explain the constitutive activation of erbB2 in VS.

Our evaluation revealed that erbB2 is constitutively localized to lipid rafts in VS tissue. This was demonstrated both biochemically by extracting a lipid raft fraction (Fig. 3) as well as by imaging, demonstrating that erbB2 colocalizes with CTX-B, a marker for lipid rafts
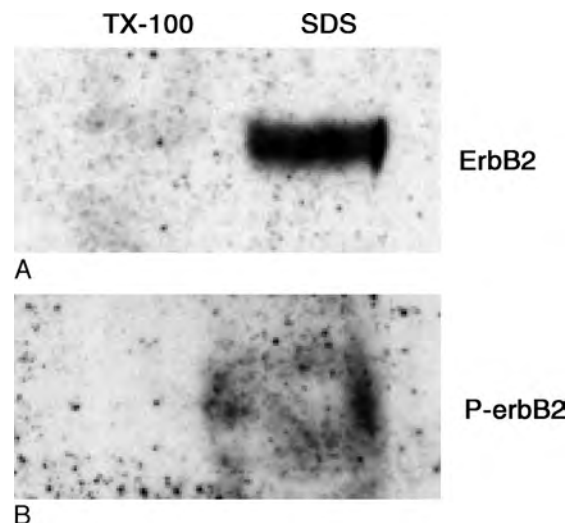

FIG. 3. Lipid raft localization of erbB2 in VS cells. Soluble (TX-100/nonlipid raft) and insoluble (SDS/lipid raft) fractions were prepared from freshly harvested tumor specimens. Fractions were separated by SDS-PAGE, transferred to nitrocellulose, and blotted for erbB2 (*A*) and phospho-erbB2 (*B*). Data are representative of 4 independent experiments performed on 4 separate tumors.
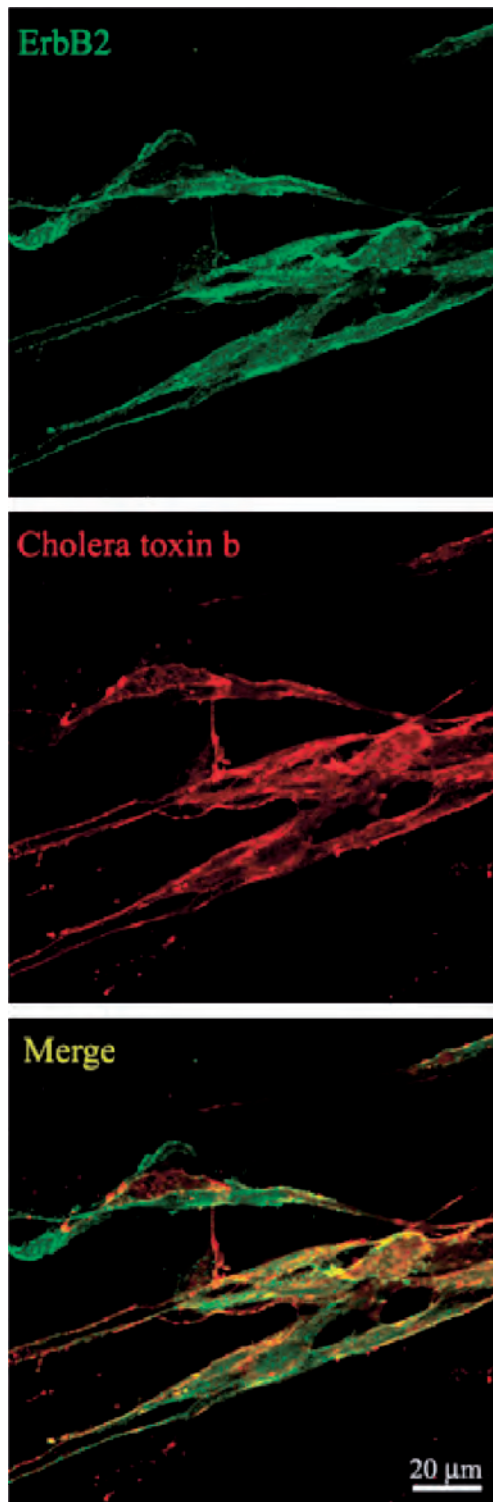
15

FIG. 4. Colocalization of erbB2 with lipid rafts. VS cells were cultured and labeled with Alexa Fluor 555–conjugated CTX-B (*red*), a lipid raft marker, and anti-erbB2 with Alexa Fluor 488 secondary antibody (*green*). Fluorescence was detected with confocal microscopy. Overlap of the *red* and *green* labeling produces a *yellow* color indicating colocalization of the molecules. Data are representative of 4 independent experiments performed on 4 separate tumors.

(Fig. 4). Activation of erbB2 in this fraction is demonstrated by its phosphorylation (Fig. 3). ErbB2 has previously been suggested to play a key role in SC proliferation as well as proliferation of VS cells (10,13,14,27). The constitutive presence of activated erbB2 in lipid rafts (which are an axis for growth-promoting receptors to initiate their signal transduction cascades) is a novel finding and provides a key piece of evidence for how disordered growth may occur in VS cells.

The significance of this finding is further underscored by our demonstration that SCs in proliferating sciatic nerve distal to a crush injury site not only increase erbB2 expression, but also translocate erbB2 to the insoluble lipid raft fraction (Fig. 1). This correlation between proliferating SCs and the presence of erbB2 in lipid rafts suggests that movement of erbB2 into lipid rafts following loss of axonal contact is a physiological response of SCs that promotes proliferation. Taken with our observation of constitutive erbB2 localization to lipid rafts in VS cells, these results suggest a mechanism for constitutive erbB2 signaling in VS cells that contributes to their proliferative potential (14).

Merlin exists in 2 states: an open, phosphorylated form that promotes cell proliferation and growth and a closed hypophosphorylated form that inhibits cell growth (24). The presence of merlin in lipid rafts has been previously suggested to be crucial for the ability of merlin to intercede and disrupt positive growth cues emanating from the plasma membrane (20). We demonstrate in our work for the first time that merlin is localized to lipid rafts in SCs and that its relative phosphorylation increases within this fraction in proliferating SCs. These data together suggest that merlin regulation of receptor kinases such as ErbB2 occurs in lipid rafts. Merlin interacts with the erbB2 binding protein, erbin, via the anchoring protein EBP50 (28), and has been proposed to regulate the membrane localization of erbB2 in SCs in response to cell-cell contact signals (4). In this model, merlin mediates the assembly of transmembrane and intracellular signaling hubs based on cell-cell contact signals (4). In subconfluent SCs in vitro or denervated SCs in vivo, merlin is phosphorylated and "open." In this state, merlin interacts with several transmembrane, scaffolding and signaling molecules including erbB2, facilitating the assembly of a complex of signaling molecules. In confluent cells in vitro or in the presence of axons, merlin is hypophosphorylated and closed. This leads to disruption of the signaling complex, sequestration of erbB2 from lipid rafts and cell cycle arrest. As VS cells lack functional merlin (1), they would be unable to accomplish this disruption of signaling complexes leading to a state of constitutive activation in which erbB2 remains localized in lipid rafts despite increased cell density. Although further study is necessary to fully validate this model, it offers an appealing explanation for how erbB2 activity could contribute to the disordered growth of VS cells.

16

Together, these data demonstrate that activated erbB2 is constitutively localized to lipid rafts in VS in both whole tissue and cell culture. ErbB2 is also inducibly localized to rafts in denervated, proliferating SC sciatic nerve, suggesting a critical role for erbB2 in SC proliferation. Merlin may regulate erbB2 trafficking in lipid rafts and its absence in VS cells may, in part, explain the increased growth potential of VS cells.

REFERENCES

1. Welling DB. Clinical manifestations of mutations in the neurofibromatosis type 2 gene in vestibular schwannomas (acoustic neuromas). *Laryngoscope* 1998;108:178–89.
2. Bretscher A, Edwards K, Fehon RG. ERM proteins and merlin: integrators at the cell cortex. *Nat Rev Mol Cell Biol* 2002;3:586–99.
3. Morrison H, Sherman LS, Legg J, et al. The NF2 tumor suppressor gene product, merlin, mediates contact inhibition of growth through interactions with CD44. *Genes Dev* 2001;15:968–80.
4. Fernandez-Valle C, Tang Y, Ricard J, et al. Paxillin binds schwannomin and regulates its density-dependent localization and effect on cell morphology. *Nat Genet* 2002;31:354–62.
5. Marchionni MA, Goodearl AD, Chen MS, et al. Glial growth factors are alternatively spliced erbB2 ligands expressed in the nervous system. *Nature* 1993;362:312–8.
6. Holbro T, Civenni G, Hynes NE. The ErbB receptors and their role in cancer progression. *Exp Cell Res* 2003;284:99–110.
7. Woldeyesus MT, Britsch S, Riethmacher D, et al. Peripheral nervous system defects in erbB2 mutants following genetic rescue of heart development. *Genes Dev* 1999;13:2538–48.
8. Garratt AN, Voiculescu O, Topilko P, Charnay P, Birchmeier C. A dual role of erbB2 in myelination and in expansion of the Schwann cell precursor pool. *J Cell Biol* 2000;148:1035–46.
9. Riethmacher D, Sonnenberg-Riethmacher E, Brinkmann V, Yamaai T, Lewin GR, Birchmeier C. Severe neuropathies in mice with targeted mutations in the ErbB3 receptor. *Nature* 1997;389:725–30.
10. Carroll SL, Miller ML, Frohnert PW, Kim SS, Corbett JA. Expression of neuregulins and their putative receptors, ErbB2 and ErbB3, is induced during Wallerian degeneration. *J Neurosci* 1997;17:1642–59.
11. Frohnert PW, Stonecypher MS, Carroll SL. Constitutive activation of the neuregulin-1/ErbB receptor signaling pathway is essential for the proliferation of a neoplastic Schwann cell line. *Glia* 2003;43:104–18.
12. Huijbregts RP, Roth KA, Schmidt RE, Carroll SL. Hypertrophic neuropathies and malignant peripheral nerve sheath tumors in transgenic mice overexpressing glial growth factor beta3 in myelinating Schwann cells. *J Neurosci* 2003;23:7269–80.
13. Hansen MR, Linthicum FH Jr. Expression of neuregulin and activation of erbB receptors in vestibular schwannomas: possible autocrine loop stimulation. *Otol Neurotol* 2004;25:155–9.
14. Hansen MR, Roehm PC, Chatterjee P, Green SH. Constitutive neuregulin-1/ErbB signaling contributes to human vestibular schwannoma proliferation. *Glia* 2006;53:593–600.
15. Stonecypher MS, Byer SJ, Grizzle WE, Carroll SL. Activation of the neuregulin-1/ErbB signaling pathway promotes the proliferation of neoplastic Schwann cells in human malignant peripheral nerve sheath tumors. *Oncogene* 2005;24:5589–605.
16. Stonecypher MS, Chaudhury AR, Byer SJ, Carroll SL. Neuregulin growth factors and their ErbB receptors form a potential signaling network for schwannoma tumorigenesis. *J Neuropathol Exp Neurol* 2006;65:162–75.
17. Hancock JF. Lipid rafts: contentious only from simplistic standpoints. *Nat Rev Mol Cell Biol* 2006;7:456–62.
18. Nagy P, Vereb G, Sebestyen Z, et al. Lipid rafts and the local density of ErbB proteins influence the biological role of homo- and heteroassociations of ErbB2. *J Cell Sci* 2002;115:4251–62.
19. Frenzel KE, Falls DL. Neuregulin-1 proteins in rat brain and transfected cells are localized to lipid rafts. *J Neurochem* 2001;77:1–12.
20. Stickney JT, Bacon WC, Rojas M, Ratner N, Ip W. Activation of the tumor suppressor merlin modulates its interaction with lipid rafts. *Cancer Res* 2004;64:2717–24.
21. Brown KD, Hostager BS, Bishop GA. Differential signaling and tumor necrosis factor receptor–associated factor (TRAF) degradation mediated by CD40 and the Epstein-Barr virus oncoprotein latent membrane protein 1 (LMP1). *J Exp Med* 2001;193:943–54.
22. Kissil JL, Johnson KC, Eckman MS, Jacks T. Merlin phosphorylation by p21-activated kinase 2 and effects of phosphorylation on merlin localization. *J Biol Chem* 2002;277:10394–9.
23. Hughes SC, Fehon RG. Phosphorylation and activity of the tumor suppressor Merlin and the ERM protein Moesin are coordinately regulated by the Slik kinase. *J Cell Biol* 2006;175:305–13.
24. Gutmann DH, Haipek CA, Hoang Lu K. Neurofibromatosis 2 tumor suppressor protein, merlin, forms two functionally important intramolecular associations. *J Neurosci Res* 1999;58:706–16.
25. Brown KD, Hostager BS, Bishop GA. Regulation of TRAF2 signaling by self-induced degradation. *J Biol Chem* 2002;277:19433–8.
26. Simons K, Toomre D. Lipid rafts and signal transduction. *Nat Rev Mol Cell Biol* 2000;1:31–9.
27. Hayworth CR, Moody SE, Chodosh LA, Krieg P, Rimer M, Thompson WJ. Induction of neuregulin signaling in mouse Schwann cells in vivo mimics responses to denervation. *J Neurosci* 2006;26:6873–84.
28. Rangwala R, Banine F, Borg JP, Sherman LS. Erbin regulates mitogen-activated protein (MAP) kinase activation and MAP kinase–dependent interactions between Merlin and adherens junction protein complexes in Schwann cells. *J Biol Chem* 2005;280:11790–7.

◆ CANDIDATE'S THESIS

Fowler Award Presentation

Effects of ErbB2 Signaling on the Response of Vestibular Schwannoma Cells to γ-Irradiation

Marlan R. Hansen, MD; J. Jason Clark, MS; Bruce J. Gantz, MD; Prabhat C. Goswami, PhD

Objective: For vestibular schwannomas (VSs) that require treatment, options are limited to microsurgery or irradiation (IR). Development of alternative therapies that augment or replace microsurgery or IR would benefit patients not suitable for current therapies. This study explored the ability of ErbB2 inhibitors to modulate the effects of IR on VS cells.

Study Design: Prospective study using primary cultures derived from human VSs.

Methods: Primary cultures of VS cells were derived from acutely resected tumors. Cultures received single escalating doses (15–40 Gy) of γ-irradiation from a ^{137}Cs γ-irradiation source. Cell proliferation was determined by BrdU uptake and apoptosis by terminal deoxynucleotidyl transferase dUTP nick end labeling (TUNEL). Trastuzumab (Herceptin) and PD158780 were independently used to inhibit ErbB2 signaling while neuregulin-1β (NRG-1) was used to activate ErbB2.

Results: IR induces VS cell cycle arrest and apoptosis in doses greater than 20 Gy, demonstrating that VS cells are relatively radioresistant. This radioresistance likely arises from their low proliferative capacity as a sublethal dose of IR (10 Gy) strongly induces deoxyribonucleic acid (DNA) damage evidenced by histone H2AX phosphorylation. Inhibition of ErbB2, which decreases VS cell proliferation, protects VS cells from radiation-induced apoptosis, while NRG-1, an ErbB2 ligand and VS cell mitogen, increases radiation-induced VS cell apoptosis.

Conclusions: Compared with many neoplastic conditions, VS cells are relatively radioresistant. The radio-protective effect of ErbB2 inhibitors implies that the sensitivity of VS cells to IR depends on their proliferative capacity. These results hold important implications for current and future treatment strategies.

Key Words: Proliferation, apoptosis, acoustic neuroma, radiotherapy, histone H2AX.

Laryngoscope, **118:1023–1030, 2008**

INTRODUCTION

Vestibular schwannomas (VSs) represent benign neoplasms arising from the Schwann cells (SCs) within the vestibular nerves. Most occur as sporadic, isolated tumors; however, patients with neurofibromatosis type 2 (NF2) develop multiple intracranial and spinal neoplasms, including bilateral VSs.[1] Management of VSs remains controversial. For many patients, observation with serial imaging to monitor for further growth suffices.[2,3] For patients who elect or require treatment, options are limited to microsurgical resection or irradiation (IR).[4] Estimates predict that in the coming decade, most VSs will be managed with IR.[5] Typically, IR is provided as stereotactic radiosurgery (SRS) in a single dose delivered from a gamma knife or linear accelerator (LINAC) or as fractionated stereotactic radiotherapy (FSR) delivered in fractionated doses.[6] Both microsurgery and SRS/FSR are generally well tolerated, yet occasionally result in significant morbidity and, in rare cases, even malignant transformation.[7–11] Further, some patients are not good candidates for either microsurgery or SRS/FSR. Understanding the mechanisms that regulate VS growth and their response to IR will hopefully lead to the development of effective alternative therapies that specifically limit schwannoma growth or increase their response to current therapies.

Vestibular schwannomas result from defects in the tumor suppressor gene, merlin. Both sporadic and familial (NF2) forms of VSs are associated with defects in the tumor suppressor gene, *schwannomin/merlin.*[12–14] The merlin protein shares a high degree of homology to the ezrin-radixin-moesin family of proteins believed to function by associating transmembrane and signaling molecules with

cytoskeletal actin, and so affecting cell-cell attachments, cell motility, and localization of cell signaling molecules.[15] Recent investigations have begun to identify mechanisms by which lack of merlin function may promote tumor growth. Merlin inhibits several intracellular signals implicated in cell proliferation and tumor formation, including Ras, Rac1/Cdc42, Raf, p21-activated kinases 1 and 2, extracellular regulated kinase/mitogen activated protein kinase (ERK/MAPK), and phosphatidyl-inositol 3-kinase (PI3-K)/Akt.[15] In addition to its effects on intracellular signals, merlin also regulates receptor tyrosine kinase trafficking and activity, including platelet-derived growth factor receptor[16] and ErbB2.[17,18] The extent to which these mechanisms contribute to SC neoplasia is unknown.

ErbB2 signaling contributes to Schwann cell development, proliferation, survival, and tumorigenesis. ErbB2 and ErbB3 are members of the epidermal growth factor (EGF) family of receptor tyrosine kinases, and both are required for normal SC development and survival.[19,20] They function as heterodimeric receptors for neuregulin-1 (NRG1), a potent axonally-derived SC mitogen that is essential for normal SC development and survival.[21] NRG1-induced ErbB2 and ErbB3 phosphorylation leads to activation of intracellular signals, including PI3 K/Akt and ERKs, which are necessary for SC proliferation and survival.[21–25]

Similar to denervated SCs, VS cells constitutively express NRG1 and its receptors ErbB2 and ErbB3. In VS cells, ErbB2 resides in detergent-resistant microdomains of the cell membrane associated with enhanced signal transduction known as lipid rafts, are constitutively active, and promotes VS cell proliferation.[26–28] Additional lines of evidence suggest that constitutive NRG1:ErbB2 signaling contributes to SC neoplasia. Mice genetically engineered to overexpress NRG1β in SCs develop malignant SC tumors[29] and constitutive NRG1:ErbB signaling contributes to cell proliferation in malignant SC tumors.[30,31] Thus, NRG1:ErbB2 signaling offers a potential therapeutic target for VS intervention.[27]

Effects of irradiation on vestibular schwannomas. In an effort to avoid surgical complications, SRS/FSR are increasingly used in the management of VSs. SRS/FSR typically do not result in complete VS regression; rather, in most cases, they result in partial tumor reduction or prevent further growth.[32,33] With the recent rise in the number of VSs treated with SRS/FSR and with longer periods of follow-up, an increasing number of treatment failures are being reported[34] and tumors from NF2 patients may be particularly radioresistant.[35–37] The lack of complete tumor regression in most VSs and the continued growth of selected VSs following SRS/FSR highlight the fact that compared with many neoplastic conditions, VSs are relatively resistant to IR. Despite the dramatic rise in the number of VSs treated with SRS/FSR recently,[5] the effects of IR on VS cells themselves remain largely unknown. Further, there are no known reagents that modify the response of VS cells to IR.

Constitutive ErbB2 activity in VS cells raises the possibility of using ErbB2 inhibitors in the management of VSs, especially those in patients with NF2, which are less amenable to microsurgical resection or SRS/FSR.[35–37] In addition to VSs, ErbB2 contributes to the growth of several other neoplastic conditions, most notably, breast carcinoma where up to 30% overexpress ErbB2.[38] In these cells, ErbB2 signaling appears to confer a radioprotective effect, and concurrent treatment with ErbB2 inhibitors increases the radiosensitivity of the tumor cells.[39,40] VSs that grow after SRS demonstrate persistent ErbB2 activation,[26] suggesting that ErbB2 activity may contribute to their radioresistance. Alternatively, since dividing cells are most sensitive to IR, ErbB2 signaling could increase VS cell radiosensitivity by promoting proliferation.

This study sought to determine the extent to which ErbB2 signaling modulates the response of cultured VS cells to IR. The data show that inhibition of ErbB2, which decreases VS cell proliferation, reduces radiation-induced VS cell apoptosis. By contrast, the ErbB2 ligand, NRG-1, a VS cell mitogen, enhances VS cell radiosensitivity. These results demonstrate that the response of VS cells to IR depends on their proliferation rate, which is regulated by ErbB2 signaling, and have important implications for current and future VS management strategies.

METHODS

Vestibular Schwannoma Cultures

All patients provided written consent and the procedures for obtaining VS samples were approved by the Institutional Review Board. Primary VS cultures were prepared as has been previously described.[27] Briefly, acutely resected tumors were minced into ~1 mm³ fragments, treated with 0.25% trypsin and 0.1% collagenase for 30 to 40 minutes at 37°C, and dissociated by tituration through narrow bore-glass pipets. Cell suspensions were plated on four-well plastic culture slides (Nalge Nunc International, Rochester, NY) coated with poly-ornithine followed by laminin (20 μg/mL) in Dulbecco's modified Eagle's medium (DMEM) with N2 supplements (Sigma, St. Louis, MO), bovine insulin (Sigma, 10 μg/mL) and 10% fetal calf serum (FCS). The medium was exchanged 1 to 2 days later and the cells were subsequently maintained in serum-free conditions until used for experiments, typically after 7 to 10 days. Cultures were maintained in a humidified incubator with 6.0% CO_2 at 37°C. Trastuzumab (Herceptin, HCN 10 μg/mL), PD158780 (Calbiochem, San Diego, CA, 20 μmol/L), or neuregulin 1β (LabVision, Fremont, CA, 3 nM) was added to the indicated cultures 24 hours prior to irradiation and maintained throughout the duration of the experiment. A total of 10 VS cultures, each derived from separate patients, were used in these studies.

Immunocytochemistry

Following fixation with 4% paraformaldehyde, the cultures were washed in phosphate buffered saline (PBS) and permeabilized with 0.8% Triton-×100 in PBS for 15 minutes. Nonspecific antibody binding was blocked with 5% goat serum, 2% bovine serum albumin (BSA), in phosphate buffered saline (PBS) with 0.8% Triton-×100. The cultures were then treated with primary antibodies overnight at 4C and then rinsed three times in PBS with 0.8% Triton-×100. The following primary antibodies were used in various combinations: Rabbit polyclonal antiS100 antibody (Sigma, 1:800), monoclonal antiBrdU antibody (University of Iowa Hybridoma Bank, Iowa City, IA, clone G3G4, 1:1,000), and monoclonal antiphosphorylated Ser[139] histone H2AX (Upstate Cell Signaling Solutions, Charlottesville, VA, 1:500). Secondary detection of primary antibody labeling was accomplished

using goat, antirabbit, and antimouse secondary antibodies conjugated to Alexa 488 or Alexa 568 (Invitrogen, Carlsbad, CA, 1:1,000). Following immunostaining, nuclei were stained with Hoescht 3342 (Sigma, 10 μg/mL) in PBS for 10 minutes at room temperature. Immunostaining was detected using an inverted Leica DMRIII microscope (Leica Microsystems, Bannockburn, IL) equipped with epifluorescence filters, and digital images were captured with a charge-coupled device Leica DFC 350FX camera (Leica Microsystems) using Leica FW4000 software. Images were analyzed in Image J (NIH, Bethesda. MD) and prepared for publication using Adobe PhotoShop (Adobe, San Jose, CA).

Determination of Vestibular Schwannoma Cell Proliferation

VS cultures were labeled with BrdU (Sigma, St. Louis, MO, 10 μg/mL) for 48 hours prior to fixation. Fixed cultures were treated with 2N HCl for 15 minutes prior to immunostaining and BrdU uptake was detected by immunostaining as above. The percent of BrdU positive VS cells (S100 positive) nuclei was determined by counting 10 randomly selected fields for each condition. Only S100 positive cells were scored. The average number of cells per field was 103.04 ± 4.23 (standard deviation). Since there is variability in the proliferation rate of individual tumors, the percent BrdU uptake was expressed as a percent of the control condition defined as 100%. The average percent of BrdU positive VS cells in the control condition was 13.17% ± 3.22 standard error of the mean (SEM). Each condition was repeated on at least three VS cultures derived from separate patients.

Determination of Vestibular Schwannoma Cell Apoptosis

Following fixation and immunostaining with antiS100, apoptotic cells were detected by terminal deoxynucleotidyl transferase dUTP nick end labeling (TUNEL) using the In Situ Cell Death Detection Kit, TMR red kit (Roche Diagnostics, Indianapolis, IN) according to the manufacturer's instructions. Nuclei were labeled with Hoescht 3342 as above. The percent of apoptotic VS cell (S100 positive) nuclei was determined by counting 10 randomly selected fields for each condition. Criteria for scoring were a TUNEL-positive nucleus with typical condensed morphology in an S100 positive cell. The percent of apoptotic VS cells was expressed as a percent of the control condition defined as 100%. The average percent of apoptotic VS cells in the control condition was 4.65% ± 0.80 (SEM). Each condition was repeated on 3 or more VS cultures derived from separate patients.

Irradiation of Vestibular Schwannoma Cultures

Primary VS cultures were irradiated by using a cesium-137 gamma radiation source set at dose rate of 0.84 Gy/minute. Control cultures, receiving sham IR, were treated in an identical manner but were not exposed to radiation.

Statistical Analyses

Evaluation for statistical differences in mean percent apoptotic and percent BrdU-positive VS cells among the various conditions was performed by analysis of variance (ANOVA) with post hoc Hidak-Solm analysis using SigmaStat software (Systat Software, Richmond, CA). For evaluation of differences of the mean percent apoptotic VS cells in 30 Gy versus 30 Gy positiveNRG1, the Student t test was used.

RESULTS

Single Doses of γ-Irradiation of 30 Gy or Greater Result in VS Cell Apoptosis

The objective of this study was to determine the effects of ErbB2 signaling on the response of VS cells to IR.

Despite the widespread use of SRS/FSR to treat VSs, the effects of IR on VS cells are not well characterized. Thus, investigation of the effects of ErbB2 signaling on VS radiosensitivity first required definition of the response of VS cells to IR. Primary VS cultures derived from acutely resected tumors were used for these purposes. These cultures contain over 98% schwannoma cells as determined by S100 immunoreactivity (Figs. 1, 2, and 3). Since the dose response of VS cells to IR has not been well defined, we evaluated the response of cultures derived from eight separate VSs treated with escalating doses (15–40 Gy) of γ-irradiation from a ^{137}Cs γ-irradiation source. Control cultures received sham IR. The clonogenic assay remains the gold standard assay for radiation-induced cell death.[41]

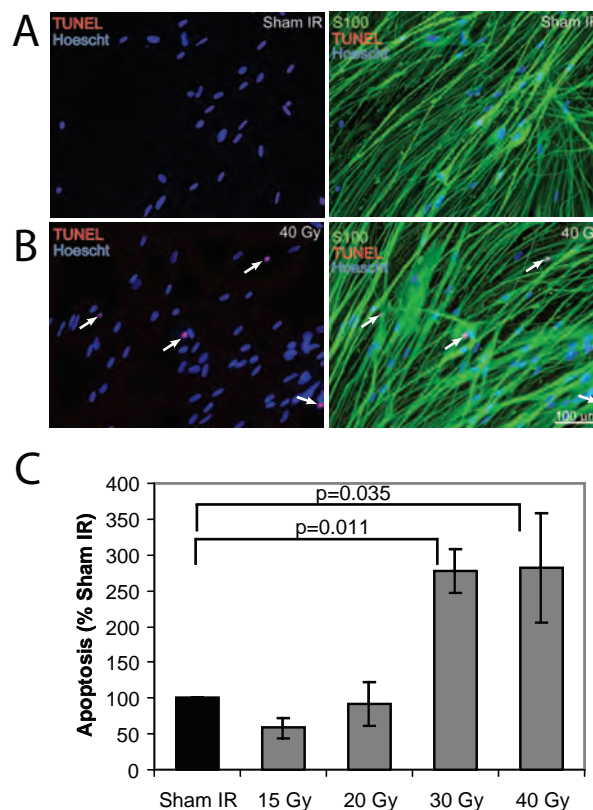Fig. 1. Vestibular schwannoma (VS) cell apoptosis is induced by γ-irradiation (IR). Primary VS cultures were irradiated with 15–40 Gy. Control cultures received sham IR. Seven days later, the cultures were fixed, immunolabeled with antiS100 antibodies followed by Alexa 488 secondary antibody (green) and labeled with terminal deoxynucleotidyl transferase dUTP nick end labeling (TUNEL) using TRITC-labeled dUTP (red). Nuclei were identified with Hoescht 3342 (blue). (A and B) Representative images from cultures receiving sham IR (A) or 40 Gy IR (B). Left panels: composite images of TUNEL (red) and Hoescht (blue) labeling. Right panels: composite images of antiSl00 (green), TUNEL, and Hoescht labeling. Arrows indicate TUNEL positive nuclei determined by overlap of red and blue channels. Scale bar = 100 μm. (C) Quantification of percent TUNEL-positive VS cells. The percent of TUNEL-positive VS cells in each condition was determined from 10 randomly selected fields and is expressed as a percent relative to cultures receiving sham IR, defined as 100%. Each condition was performed on at least three tumors derived from separate patients. Error bars present standard error of the mean (SEM). P values indicate significant differences by analysis of variance (ANOVA) with post hoc Hidak-Solm analysis.
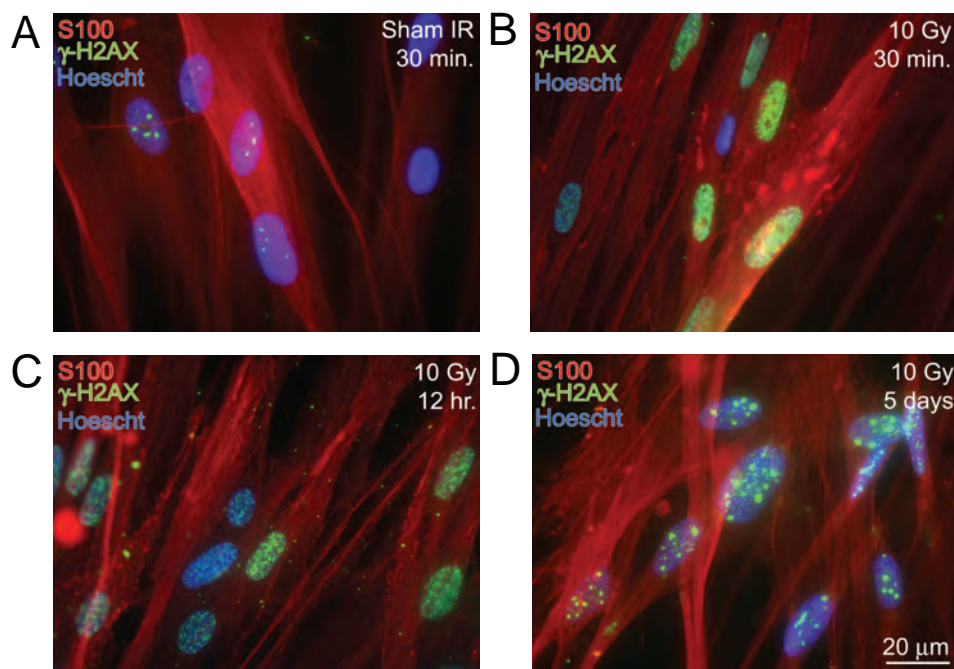
Fig. 2. Ten Gy γ-irradiation (IR) induces histone 2A phosphorylation (γ-H2AX) in vestibular schwannoma (VS) cells. Primary VS cultures received sham IR (A) or 10 Gy IR and were fixed 30 minutes (B), 12 hours (C), or 5 days (D) later. The cultures were immunolabeled with a monoclonal antibody that recognizes γ-H2AX followed by an Alexa 488 secondary antibody (green) and antiS100 antibody followed by Alexa 568 secondary antibody (red). Nuclei were identified with Hoescht staining. Scale bar = 20 μm.

However, VS cells are not transformed and do not form clones, making this assay impossible. Therefore, we used apoptosis as a marker for radiation-induced cell death.[41] Irradiation also induces necrotic cell death; however, since ErbB2 signaling regulates apoptosis in Schwann cells,[42] we focused on defining the apoptotic response of VS cells to IR.

Seven days following IR, the cultures were fixed and immunostained with antiS100 antibodies followed by an Alexa 488 (green) conjugated secondary antibody to specifically identify VS cells. The cells were then labeled with terminal deoxynucleotidyl transferase dUTP nick end labeling (TUNEL). TUNEL identifies apoptotic cells in situ by using terminal deoxynucleotidyl transferase (TdT) to transfer TRITC labeled dUTP (red) to strand breaks of cleaved deoxyribonucleic acid (DNA) (Fig. 1). Nuclei were identified with Hoescht 3342 (blue) labeling. The percent TUNEL positive VS cell (S100 positive) nuclei was determined from 10 randomly selected fields for each well. All TUNEL-positive nuclei were condensed, typical of apoptotic cell death. Thirty Gy and 40 Gy resulted in a nearly threefold increase in VS cell apoptosis compared with cultures receiving sham IR (277% ± 30 and 282% ± 77, respectively, mean ± SEM), which was statistically significant ($P < .05$), while the percent of apoptotic VS cells in cultures treated with 20 Gy or less was not significantly different from those in cultures receiving sham IR (Fig. 1). These results suggest that, compared with most malignant cells, VS cells are relatively resistant to IR.

Two possible explanations for the relative radioresistance of VS cells are that either higher doses of IR are needed to damage the VS cells' DNA or that the cells are capable of repairing DNA damage prior to re-entering cell cycle.[41] In the latter case, cells that successfully repair the damaged DNA prior to re-entering cell cycle would be less likely to undergo apoptosis. To determine if sublethal doses of IR are capable of damaging VS cell DNA, we immunostained cultures treated with 10 Gy IR with an antibody that recognizes phosphorylated histone H2AX (γ-H2AX). H2AX is phosphorylated following double-stranded breaks in DNA and is a sensitive indicator of radiation-induced DNA damage.[43] Within 30 minutes of IR, over 90% VS cells exhibit robust γ-H2AX immunoreactivity compared with cells receiving sham IR (Fig. 2). The intensity of the γ-H2AX immunoreactivity declines and becomes more punctate, but persists over the subsequent 5 days in over 80% of the VS cells (Fig. 2). These results demonstrate that sublethal doses of IR damage VS cell DNA and suggest that VS cells are capable of repairing damaged DNA due to sublethal doses of IR prior to re-entering cell cycle.

40 Gy γ-Irradiation Reduces Vestibular Schwannoma Cell Proliferation

A main consequence of SRS/FSR on VSs in vivo appears to be a lack of further tumor growth. One possible explanation for this decreased growth rate is that IR causes cell cycle arrest. We therefore asked to what extent IR induced cell cycle arrest in cultured VS cells. Primary VS cultures were irradiated with escalating doses of IR. Five days later, the cultures were treated with BrdU (10 μmol/L) for a further 48 hours. The cultures were then fixed and immunostained with antiBrdU and antiS100 antibodies. Nuclei were stained with Hoescht (Sigma-Aldrich, St. Louis, MO). The percent of BrdU positive VS cell (S100 positive) nuclei was determined from 10 randomly selected fields for each well. A total of seven VS tumors were used in these studies.

As shown in Figure 3, 40 Gy IR significantly reduced the percent of BrdU positive VS cells to 68% ± 15% (mean ± SEM) of cultures receiving sham IR ($P = .035$),

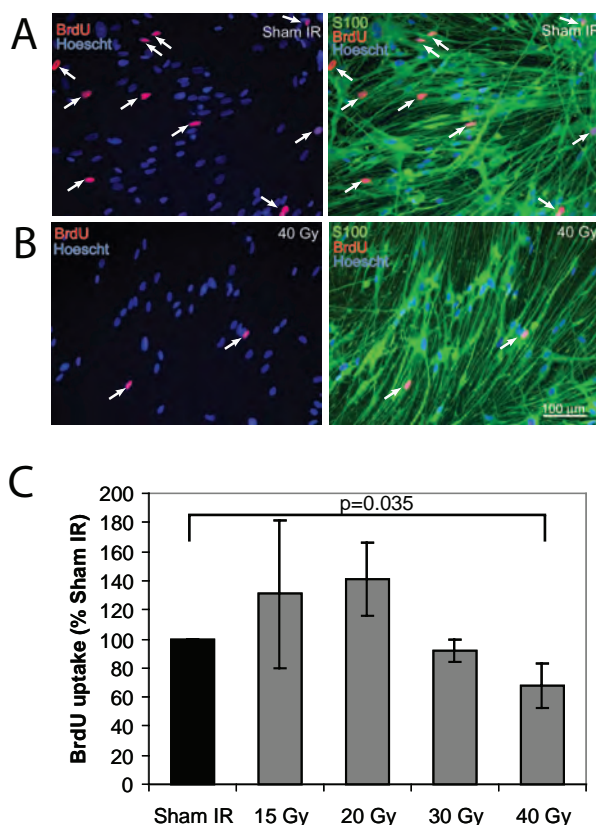Hansen et al.: ErbB2 Signaling and Irradiation of Vestibular Schwannoma Cells

Fig. 3. Forty Gy γ-irradiation (IR) reduces vestibular schwannoma (VS) cell proliferation. Primary VS cultures were irradiated with doses from 10 to 40 Gy. Control cultures received sham IR. Five days following irradiation the cultures were treated with BrdU (10 μmol/L) for an additional 48 hours, fixed, and immunolabeled with antiS100 antibodies followed by Alexa 488 secondary antibody (green) and antiBrdU monoclonal antibody followed by an Alexa 568 secondary antibody (red). Nuclei were identified with Hoescht 3342 (blue). (A and B) Representative images from cultures receiving sham IR (A) or 40 Gy IR (B). Left panels: composite images of BrdU (red) and Hoescht (blue) labeling. Right panels: composite images of antiS100 (green), BrdU, and Hoescht labeling. Arrows indicate BrdU positive nuclei determined by overlap of red and blue channels. Scale bar = 100 μm. (C) Quantification of percent BrdU positive VS cells. The percent BrdU positive VS cells in each condition was determined from 10 randomly selected fields and is expressed as a percent relative to cultures receiving sham IR, defined as 100%. Each condition was performed on a minimum of five tumors derived from separate patients. Error bars present standard error of the mean (SEM). *P* value indicates significant difference by analysis of variance (ANOVA) with post hoc Hidak-Solm analysis.

while lower doses did not significantly reduce VS cell proliferation. Thus, 40 Gy IR reduces VS cell proliferation in vitro.

ErbB2 Inhibitors Reduce Vestibular Schwannoma Cell Proliferation and Protect Vestibular Schwannoma Cells From Irradiation-Induced Apoptosis

Compared with many malignancies, VSs are relatively resistant to IR.[44,45] One explanation for the relative radioresistance of VS cells is their low proliferation rate. Another possible contributing factor is constitutive activation of protective signaling pathways such as

those recruited by ErbB2.[26,27,40,46] Conversely, by increasing proliferation, ErbB2 activity could enhance the response of VS cells to IR. Therefore, we asked to what extent ErbB2 signaling modulated the response of VS cells to IR.

To inhibit ErbB2 signaling we used two separate molecules: 1) trastuzumab (Herceptin, HCN, a humanized antiErbB2 monoclonal antibody used to treat breast carcinomas that overexpress ErbB2, and 2) PD158780, a small molecule ErbB2 inhibitor. Both molecules inhibit ErbB2 signaling in cultured VS cells.[27] To determine if ErbB2 activity modulated VS radiosensitivity, VS cultures were treated with trastuzumab (100 μg/mL) or PD158780 (20 μmol/L) 24 hours prior to receiving 30 or 40 Gy of IR. We have previously shown that these doses effectively reduce VS cell proliferation and inhibit SC proliferation in response to neuregulin-1 (NRG-1), an ErbB2 ligand and SC mitogen. For cultures used in proliferation assays, BrdU was added for the final 48 hours in culture. Seven days following IR, the cultures were fixed and the percent of apoptotic and proliferating VS cells was determined as before. As previously shown,[27] trastuzumab (100 μg/mL) and PD158780 (20 μmol/L) each significantly reduced VS proliferation ($P < .05$) in cultures receiving sham IR (Fig. 4). Neither inhibitor caused a significant further reduction in cell proliferation in cultures treated with 30 Gy or 40 Gy ($P > .05$), indicating a lack of additive benefit of ErbB2 inhibition with higher doses of IR in reducing cell proliferation.

With regards to modifying the apoptotic response, PD158780, but not trastuzumab, significantly increased VS cell apoptosis ($P = .033$) in cultures receiving sham IR (Fig. 5). There was no additional apoptosis when PD158780 was combined with 30 Gy or 40 Gy IR. Trastuzumab significantly reduced the percent of apoptotic VS cells in response to 30 Gy and 40 Gy ($P < .05$), indicating
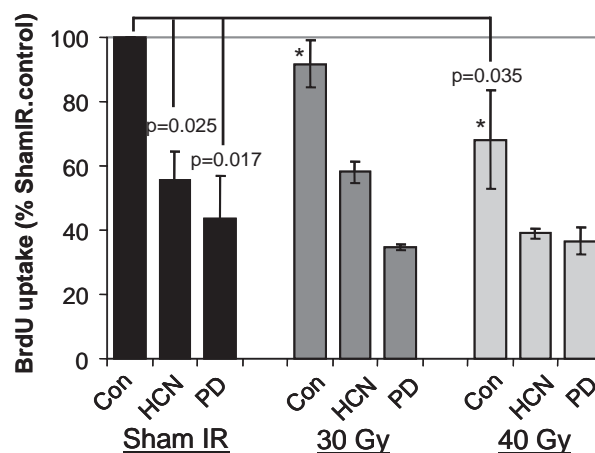

Fig. 4. Combination of irradiation (IR) with ErbB2 inhibitors provides no further decrease in vestibular schwannoma (VS) cell proliferation. Primary VS cultures were irradiated as above in the presence or absence (control, CON) of trastuzumab (Herceptin, HCN 100 μg/mL) or PD158780 (PD, 20 μmol/L). Control cultures received sham IR. BrdU uptake was determined as above. *P* values indicate significant differences by analysis of variance (ANOVA) with post hoc Hidak-Solm analysis. *Data also presented in Figure 4.

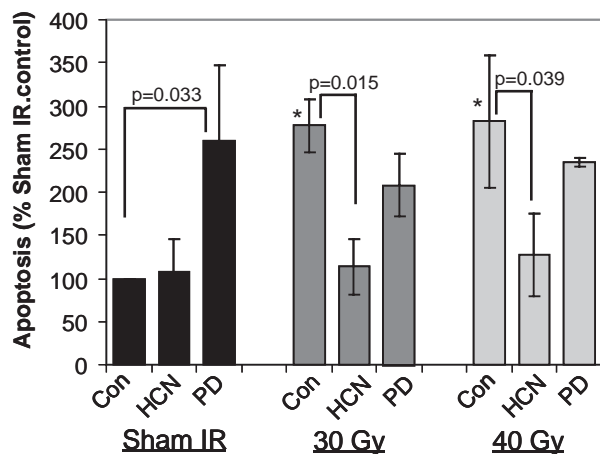Hansen et al.: ErbB2 Signaling and Irradiation of Vestibular Schwannoma Cells

1027

Fig. 5. ErbB2 inhibitors protect vestibular schwannoma (VS) cells from radiation-induced apoptosis. Primary VS cultures were irradiated as above in the presence or absence (control, CON) of trastuzumab (Herceptin, HCN 100 μg/mL) or PD158780 (PD, 20 μmol/L). Control cultures received sham IR. Apoptosis was determined as above with terminal deoxynucleotidyl transferase dUTP nick end labeling (TUNEL). *P* values indicate significant differences by analysis of variance (ANOVA) with post hoc Hidak-Solm analysis. *Data also presented in Figure 2.
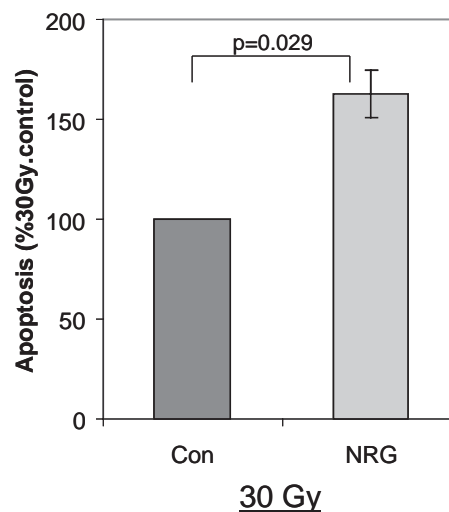

Fig. 6. Neuregulin-1 (NRG1) increases radiation-induced vestibular schwannoma (VS) cell apoptosis. Primary VS cultures were irradiated with 30 Gy as above in the presence or absence NRG1 (3 nM) and the percent of apoptotic VS cells was determined as before with terminal deoxynucleotidyl transferase dUTP nick end labeling (TUNEL). NRG1 significantly increased the percent of VS apoptotic cells (*P* = .029) by Student *t* test.

a cytoprotective effect of the ErbB2 inhibitor (Fig. 5) and suggesting that constitutive ErbB2 signaling does not significantly contribute to the relative radioresistance of VS cells.

Vestibular Schwannoma Cell Radiosensivity Depends on Proliferation Rate

ErbB2 inhibitors decrease VS cell proliferation[27] (Fig. 4) and trastuzumab decreases VS cells' sensitivity to radiation-induced apoptosis (Fig. 5), suggesting that the apoptotic response of VS cells to IR depends on their proliferation status. To further test this possibility, we treated VS cultures with the ErbB2 ligand, NRG-1 (3 nM), a SC mitogen that we have previously shown to promote VS cell proliferation.[27] NRG-1 significantly increased the percent of apoptotic VS cells following 30 Gy IR (Fig. 6) (*P* = .029, Student *t* test) indicating that increased ErbB2 signaling enhances VS cell sensitivity to IR, likely by promoting mitosis. Taken together these results imply that the apoptotic response of VS cells to IR depends on their proliferative capacity. ErbB2 activation by exogenous NRG-1 promotes proliferation and radiation-induced apoptosis, while ErbB2 inhibition reduces proliferation and radiation-induced apoptosis.

DISCUSSION

Effects of Irradiation on Vestibular Schwannoma Cells

An increasing number of VSs are being treated with SRS/FSR;[5] however, the effects of IR on the VS cells themselves are not well understood. Here we evaluated the apoptotic and proliferative response of cultured primary VS cells to increasing doses of IR. Our data demonstrate that compared to most neoplastic conditions, VS cells in vitro are relatively radioresistant, requiring over 20Gy IR

(e.g., 30–40 Gy) to induce apoptosis and cell cycle arrest. Further, in doses up to 40 Gy, the reduction in proliferation is less than that seen with ErbB2 inhibition. These findings correlate well with those of Anniko,[45] who also noted that cultured VS cells respond only to high doses of IR. While it is difficult to extrapolate dose response relations from cultured cells to those for VSs in patients, these data are consistent with a lack of complete tumor regression in many VSs using current SRS/FSR protocols, and raise the possibility that the response of VSs to SRS/FSR may not be due to direct cytotoxic effects on the VS cells. Rather, the central necrosis seen on magnetic resonance imaging in some cases, and the reduced tumor growth in many cases may reflect indirect effects, for example, by decreasing tumor vascularity. Lee et al.[47] found viable, typical schwannoma cells in four VSs resected for growth following SRS and noted increased fibrosis of the tumor bed and surrounding tissues. In a separate study, the proliferation rate of 6 VSs resected for continued growth following SRS was less than the proliferation rate in 15 VSs resected for growth following incomplete microsurgical resection.[48] However, two irradiated VSs in that study showed markedly increased proliferation.[48] Thus, the effect of SRS/FSR on VS cell proliferation in vivo at the doses currently used clinically, whether direct or indirect, remains to be defined.

The relative radioresistance of VS cells to IR likely reflects their low proliferative capacity rather than an increased resistance to DNA damage.[41] We find that sublethal doses of IR rapidly induce double-stranded DNA breaks, evidenced by H2AX phosphorylation, in over 90% of VS cells. The potential for additional radiation-induced genetic aberrations leading to malignant transformation or secondary neoplasia highlights the need for long-term follow-up of patients managed with SRS/FSR. In some

Hansen et al.: ErbB2 Signaling and Irradiation of Vestibular Schwannoma Cells

cases, late growth correlated with malignant transformation.[8,49] Radiation-induced DNA damage holds particular implications for management of patients with NF2 who harbor germline *merlin* defects and are prone to radiation-induced additional genetic aberrations[8,50] and neoplasia.[7,51]

Modern treatment strategies of unilateral, sporadic VSs employing microsurgery or SRS/FSR are highly effective with limited morbidity. By contrast, schwannomas in patients with NF-2 present significant treatment challenges. They are less responsive to radiotherapy, more likely to recur following surgical removal, and carry higher morbidity with treatment.[35–37] Further, in NF2 patients with multiple, large schwannomas, surgical and SRS/FSR options become limited. Development of alternative therapies that improve or replace microsurgery or SRS/FSR would greatly benefit these patients.

One strategy to increase tumor responsiveness to IR is to provide radiosensitizing agents. Since most do not specifically target tumor cells, they have the disadvantage of also increasing the radiation-induced damage to non-tumor cells, raising the likelihood of side effects. An alternative strategy is to use reagents that specifically target tumor growth in combination with IR in an effort to achieve an additive response. Here we evaluated ErbB2 signaling, which provides a radioprotective effect for some carcinomas[40,46] as one potential target to enhance VS cell radiosensitivity.

Effect of ErbB2 Inhibitors on Vestibular Schwannomas Cells

Previous work has shown that ErbB2 is constitutively active in VS cells and that this contributes to their proliferative response,[27] and the data here confirm these findings since both trastuzumab and PD158780 reduced VS cell proliferation in these cultures. Several mechanisms possibly contribute to this constitutive ErbB2 signaling, including increased receptor expression, increased receptor trafficking to the cell membrane,[17] and autocrine NRG-1 ligand expression.[27]

In addition to promoting SC and VS cell proliferation, ErbB2 signaling promotes SC survival. We find that at the doses used in this study, PD158780, a pharmacologic ErbB2 inhibitor, induces VS cell apoptosis, but trastuzumab, a humanized ErbB2 inhibitory monoclonal antibody, did not. This difference may reflect more effective ErbB2 inhibition by PD158780 or non-specific effects of the pharmacologic compound such as inhibition of other tyrosine kinases (e.g., EGF receptor) required for VS cell survival. Thus, the role of ErbB2 signaling in VS cell survival will require further investigation with additional specific ErbB2 inhibitors.

Response of Vestibular Schwannomas Cells to γ-Irradiation Depends on Proliferation Status

Two observations from these studies demonstrate that the sensitivity of VS cells to IR depends on their proliferation rate. First, trastuzumab, which reduces VS cell proliferation, decreases the percent of apoptotic VS cells following lethal doses of IR. Second, NRG-1, a potent SC and VS cell mitogen,[27] increases the apoptotic re-

sponse to IR. In so far as these in vitro data can be extrapolated to the response of VSs in patients, they suggest that SRS/FSR would be more likely to induce apoptosis in growing VSs compared with static tumors. Further, concurrent treatment with ErbB2 inhibitors and SRS/FSR may reduce, rather than augment, the apoptotic response.

Despite our observation that the sensitivity of VS cells to IR depends on their proliferation rate, several reports indicate that VSs in patients with NF2, which presumably have an increased proliferative capacity, are more likely to grow following SRS/FSR than sporadic VSs.[35–37] Whether this reflects an underlying greater radioresistance of VSs from NF2 patients compared with sporadic VSs or is simply due to the greater growth potential of the remaining viable tumor cells requires further investigation.

CONCLUSIONS

With the rapidly increasing use of SRS/FSR to treat VSs, the effects of IR on VS cells require definition. We show that IR induces cultured VS cell apoptosis and cell cycle arrest in doses exceeding 20 Gy. Increasing VS cell proliferation with the ErbB2 ligand NRG1 enhances the apoptotic effect, while ErbB2 inhibitors, which reduce proliferation, protect VS cells from radiation-induced apoptosis. The relative radioresistance of VS cells likely reflects their low proliferative capacity and raises the possibility that the effects of SRS/FSR on VSs are predominantly indirect.

BIBLIOGRAPHY

1. Baser ME, R Evans DG, Gutmann DH. Neurofibromatosis 2. *Curr Opin Neurol* 2003;16:27–33.
2. Smouha EE, Yoo M, Mohr K, Davis RP. Conservative management of acoustic neuroma: a meta-analysis and proposed treatment algorithm. *Laryngoscope* 2005;115:450–454.
3. Battaglia A, Mastrodimos B, Cueva R. Comparison of growth patterns of acoustic neuromas with and without radiosurgery. *Otol Neurotol* 2006;27:705–712.
4. Wackym PA. Stereotactic radiosurgery, microsurgery, and expectant management of acoustic neuroma: basis for informed consent. *Otolaryngol Clin North Am* 2005;38:653–670.
5. Pollock BE, Lunsford LD, Noren G. Vestibular schwannoma management in the next century: a radiosurgical perspective. *Neurosurgery* 1998;43:475–481; discussion 481–473.
6. Flickinger JC, Barker FG 2nd. Clinical results: radiosurgery and radiotherapy of cranial nerve schwannomas. *Neurosurg Clin N Am* 2006;17:121–128, vi.
7. Evans DG, Birch JM, Ramsden RT, Sharif S, Baser ME. Malignant transformation and new primary tumours after therapeutic radiation for benign disease: substantial risks in certain tumour prone syndromes. *J Med Genet* 2006;43: 289–294.
8. Bari ME, Forster DM, Kemeny AA, Walton L, Hardy D, Anderson JR. Malignancy in a vestibular schwannoma. Report of a case with central neurofibromatosis, treated by both stereotactic radiosurgery and surgical excision, with a review of the literature. *Br J Neurosurg* 2002;16:284–289.
9. Wilkinson JS, Reid H, Armstrong GR. Malignant transformation of a recurrent vestibular schwannoma. *J Clin Pathol* 2004;57:109–110.
10. Lanman TH, Brackmann DE, Hitselberger WE, Subin B. Report of 190 consecutive cases of large acoustic tumors (vestibular schwannoma) removed via the translabyrinthine approach. *J Neurosurg* 1999;90:617–623.
11. Meyer TA, Canty PA, Wilkinson EP, Hansen MR, Rubinstein JT, Gantz BJ. Small acoustic neuromas: surgical outcomes

versus observation or radiation. *Otol Neurotol* 2006;27:
380–392.

12. Rouleau GA, Merel P, Lutchman M, et al. Alteration in a new gene encoding a putative membrane-organizing protein causes neuro-fibromatosis type 2. *Nature* 1993;363:515–521.

13. Trofatter JA, MacCollin MM, Rutter JL, et al. A novel moesin-, ezrin-, radixin-like gene is a candidate for the neurofibromatosis 2 tumor suppressor. *Cell* 1993;72:791–800.

14. Welling DB. Clinical manifestations of mutations in the neurofibromatosis type 2 gene in vestibular schwannomas (acoustic neuromas). *Laryngoscope* 1998;108:178–189.

15. McClatchey AI, Giovannini M. Membrane organization and tumorigenesis–the NF2 tumor suppressor, Merlin. *Genes Dev* 2005;19:2265–2277.

16. Fraenzer JT, Pan H, Minimo L Jr, Smith GM, Knauer D, Hung G. Overexpression of the NF2 gene inhibits schwannoma cell proliferation through promoting PDGFR degradation. *Int J Oncol* 2003;23:1493–1500.

17. Fernandez-Valle C, Tang Y, Ricard J, et al. Paxillin binds schwannomin and regulates its density-dependent localization and effect on cell morphology. *Nat Genet* 2002;31:354–362.

18. Rangwala R, Banine F, Borg JP, Sherman LS. Erbin regulates mitogen-activated protein (MAP) kinase activation and MAP kinase-dependent interactions between merlin and adherens junction protein complexes in Schwann cells. *J Biol Chem* 2005;280:11790–11797.

19. Riethmacher D, Sonnenberg-Riethmacher E, Brinkmann V, Yamaai T, Lewin GR, Birchmeier C. Severe neuropathies in mice with targeted mutations in the ErbB3 receptor. *Nature* 1997;389:725–730.

20. Woldeyesus MT, Britsch S, Riethmacher D, et al. Peripheral nervous system defects in erbB2 mutants following genetic rescue of heart development. *Genes Dev* 1999;13:2538–2548.

21. Adlkofer K, Lai C. Role of neuregulins in glial cell development. *Glia* 2000;29:104–111.

22. Li Y, Tennekoon GI, Birnbaum M, Marchionni MA, Rutkowski JL. Neuregulin signaling through a PI3K/Akt/Bad pathway in Schwann cell survival. *Mol Cell Neurosci* 2001;17:761–767.

23. Hansen MR, Vijapurkar U, Koland JG, Green SH. Reciprocal signaling between spiral ganglion neurons and Schwann cells involves neuregulin and neurotrophins. *Hear Res* 2001;161:87–98.

24. Monje PV, Bartlett Bunge M, Wood PM. Cyclic AMP synergistically enhances neuregulin-dependent ERK and Akt activation and cell cycle progression in Schwann cells. *Glia* 2006;53:649–659.

25. Sliwkowski MX, Schaefer G, Akita RW, et al. Coexpression of erbB2 and erbB3 proteins reconstitutes a high affinity receptor for heregulin. *J Biol Chem* 1994;269:14661–14665.

26. Hansen MR, Linthicum FH Jr. Expression of neuregulin and activation of erbB receptors in vestibular schwannomas: possible autocrine loop stimulation. *Otol Neurotol* 2004;25:155–159.

27. Hansen MR, Roehm PC, Chatterjee P, Green SH. Constitutive neuregulin-1/ErbB signaling contributes to human vestibular schwannoma proliferation. *Glia* 2006;53:593–600.

28. Brown KD, Hansen MR. Lipid raft localization of erbB2 in vestibular schwannoma and Schwann cells. *Otol Neurotol* 2008;29:79–85.

29. Huijbregts RP, Roth KA, Schmidt RE, Carroll SL. Hypertrophic neuropathies and malignant peripheral nerve sheath tumors in transgenic mice overexpressing glial growth factor beta3 in myelinating Schwann cells. *J Neurosci* 2003;23:7269–7280.

30. Frohnert PW, Stonecypher MS, Carroll SL. Constitutive activation of the neuregulin-1/ErbB receptor signaling pathway is essential for the proliferation of a neoplastic Schwann cell line. *Glia* 2003;43:104–118.

31. Stonecypher MS, Byer SJ, Grizzle WE, Carroll SL. Activation of the neuregulin-1/ErbB signaling pathway promotes the proliferation of neoplastic Schwann cells in human malignant peripheral nerve sheath tumors. *Oncogene* 2005;24:5589–5605.

32. Lunsford LD, Niranjan A, Flickinger JC, Maitz A, Kondziolka D. Radiosurgery of vestibular schwannomas: summary of experience in 829 cases. *J Neurosurg* 2005;102(Suppl):195–199.

33. Hasegawa T, Kida Y, Kobayashi T, Yoshimoto M, Mori Y, Yoshida J. Long-term outcomes in patients with vestibular schwannomas treated using gamma knife surgery: 10-year follow up. *J Neurosurg* 2005;102:10–16.

34. Friedman RA, Brackmann DE, Hitselberger WE, Schwartz MS, Iqbal Z, Berliner KI. Surgical salvage after failed irradiation for vestibular schwannoma. *Laryngoscope* 2005;115:1827–1832.

35. Mathieu D, Kondziolka D, Flickinger JC, et al. Stereotactic radiosurgery for vestibular schwannomas in patients with neurofibromatosis type 2: an analysis of tumor control, complications, and hearing preservation rates. *Neurosurgery* 60: 460–468, 2007; discussion 468–470.

36. Rowe JG, Radatz M, Walton L, Kemeny AA. Stereotactic radiosurgery for type 2 neurofibromatosis acoustic neuromas: patient selection and tumour size. *Stereotact Funct Neurosurg* 2002;79:107–116.

37. Wowra B, Muacevic A, Jess-Hempen A, Hempel JM, Muller-Schunk S, Tonn JC. Outpatient gamma knife surgery for vestibular schwannoma: definition of the therapeutic profile based on a 10-year experience. *J Neurosurg* 2005;102(Suppl):114–118.

38. Peiro G, Aranda FI, Adrover E, et al. Analysis of HER2 by chromogenic in situ hybridization and immunohistochemistry in lymph node-negative breast carcinoma: prognostic relevance. *Hum Pathol* 2007;38:26–34.

39. Guo G, Wang T, Gao Q, et al. Expression of ErbB2 enhances radiation-induced NF-kappaB activation. *Oncogene* 2004;23:535–545.

40. Liang K, Lu Y, Jin W, Ang KK, Milas L, Fan Z. Sensitization of breast cancer cells to radiation by trastuzumab. *Mol Cancer Ther* 2003;2:1113–1120.

41. Pawlik TM, Keyomarsi K. Role of cell cycle in mediating sensitivity to radiotherapy. *Int J Radiat Oncol Biol Phys* 2004;59:928–942.

42. Syroid DE, Maycox PR, Burrola PG, et al. Cell death in the Schwann cell lineage and its regulation by neuregulin. *Proc Natl Acad Sci USA* 1996;93:9229–9234.

43. Burma S, Chen BP, Murphy M, Kurimasa A, Chen DJ. ATM phosphorylates histone H2AX in response to DNA double-strand breaks. *J Biol Chem* 2001;276:42462–42467.

44. Linskey ME, Martinez AJ, Kondziolka D, et al. The radiobiology of human acoustic schwannoma xenografts after stereotactic radiosurgery evaluated in the subrenal capsule of athymic mice. *J Neurosurg* 1993;78:645–653.

45. Anniko M. Early morphological changes following gamma irradiation. A comparison of human pituitary tumours and human acoustic neurinomas (schwannomas). *Acta Pathol Microbiol Scand [A]* 1981;89:113–124.

46. Sato S, Kajiyama Y, Sugano M, et al. Monoclonal antibody to HER-2/neu receptor enhances radiosensitivity of esophageal cancer cell lines expressing HER-2/neu oncoprotein. *Int J Radiat Oncol Biol Phys* 2005;61:203–211.

47. Lee DJ, Westra WH, Staecker H, Long D, Niparko JK, Slattery WH 3rd. Clinical and histopathologic features of recurrent vestibular schwannoma (acoustic neuroma) after stereotactic radiosurgery. *Otol Neurotol* 2003;24:650–660; discussion 660.

48. Lee F, Linthicum F Jr, Hung G. Proliferation potential in recurrent acoustic schwannoma following gamma knife radiosurgery versus microsurgery. *Laryngoscope* 2002;112:948–950.

49. Shin M, Ueki K, Kurita H, Kirino T. Malignant transformation of a vestibular schwannoma after gamma knife radiosurgery. *Lancet* 2002;360:309–310.

50. Warren C, James LA, Ramsden RT, et al. Identification of recurrent regions of chromosome loss and gain in vestibular schwannomas using comparative genomic hybridisation. *J Med Genet* 2003;40:802–806.

51. Baser ME, Evans DG, Jackler RK, Sujansky E, Rubenstein A. Neurofibromatosis 2, radiosurgery and malignant nervous system tumours. *Br J Cancer* 2000;82:998.

Persistent C-Jun N-terminal kinase activity contributes to the survival of human vestibular schwannoma cells by suppressing accumulation of mitochondrial superoxides

Authors: Wei Ying Yue[*,1], J. Jason Clark [*,1], Zana Ahmad[2], Joni K. Doherty[2], Frederick Domann[3], Marlan R. Hansen[1]
[*]These authors contributed equally to the study.

Departments of [1]Otolaryngology-Head and Neck Surgery and [3]Radiation Oncology, University of Iowa, Iowa City, Iowa 52242
[2]Department of Otolaryngology-Head and Neck Surgery, University of California-San Diego, San Diego, CA

Running title: JNK signaling in human vestibular schwannomas

Address correspondence to**:** Marlan R. Hansen, MD, Department of Otolaryngology-Head and Neck Surgery, University of Iowa Hospitals and Clinics, Iowa City, Iowa, 52242 Fax: (319) 356-4547 Email: marlan-hansen@uiowa.edu

Abstract: 250 words
Introduction: 451 words
Discussion: 1201 words

Keywords: acoustic neuroma, apoptosis, reactive oxygen species, cell signaling, merlin, cell proliferation

Abstract.

Vestibular schwannomas (VSs) result from mutations in the *merlin* tumor suppressor gene. Recent studies indicate that extracellular regulated kinase/mitogen activated protein kinase (ERK/MAPK) and phosphatidyl-inositol 3-kinase (PI3-K)/Akt are active in human VSs and here we show that c-Jun N-terminal kinases (JNKs) are also persistently active in human VS cells. Knock–down of merlin in normal human Schwann cells (SCs) by siRNA increased JNK phosphorylation confirming that merlin suppresses JNK activity in human SCs. Using cultures from human VSs, we investigated the contribution of ERKs, Akt, and JNKs to the proliferative and survival response of VS cells. Inhibition of ERK or Akt signaling reduced VS cell proliferation, but did not increase apoptosis, whereas inhibition of JNK with pharmacological or peptide inhibitors reduced VS cell proliferation and survival by inducing apoptosis. By contrast, inhibition of JNK prevents apoptosis in normal SCs. Inhibition of JNK increased the fluorescence intensity of VS cells loaded with 5-(and-6)-chloromethyl-2',7'-dichlorodihydrofluorescein diacetate (H_2DCFDA), a probe for reactive oxygen species (ROS). Further, ebselen, a ROS scavenger, rescued VS cells with suppressed JNK from apoptosis suggesting that JNK activity protects VS cells by limiting accumulation of ROS. VS cultures treated with JNK inhibitors demonstrated significantly higher levels of MitoSOX Red fluorescence implying that JNK activity specifically suppresses superoxide production in the mitochondria. Overexpression of superoxide dismutase 2 (mitochondrial SOD) prevented apoptosis in VS cells with suppressed JNK signaling. Taken together these results indicate that persistent JNK activity enhances VS cell survival, at least in part, by suppressing accumulation of mitochondrial superoxides.

Introduction

Vestibular schwannomas (VSs) represent benign tumors that arise from the Schwann cells (SCs) lining the vestibular nerve and comprise 10% of all intracranial neoplasms. VSs occur in either sporadic or familial (neurofibromatosis type 2, NF2) forms. Both are associated with defects in the tumor suppressor gene, *schwannomin (Sch)/merlin* (Rouleau et al., 1993; Trofatter et al., 1993; Bianchi et al., 1994; Bourn et al., 1994; Scoles et al., 1996; Stemmer-Rachamimov et al., 1997; Welling, 1998). Germline defects in *merlin*, as occur in NF2, result in bilateral VSs and multiple other intracranial and spinal tumors including schwannomas (Trofatter et al., 1993; Baser et al., 2003).

Recent investigations have identified potential mechanisms by which lack of functional merlin protein promotes tumor growth. Merlin inhibits several intracellular signals implicated in cell proliferation and tumor formation including Ras, Rac1/Cdc42, RhoA, Src, Raf, p21-activated kinases 1 and 2 (PAK1/2), extracellular regulated kinase/mitogen activated protein kinase (ERK/MAPK), c-Jun N-terminal kinase (JNK), and phosphatidyl-inositol 3-kinase (PI3-K)/Akt (Tikoo et al., 1994; Gutmann et al., 2001; Shaw et al., 2001; Kim et al., 2002; Fraenzer et al., 2003; Kaempchen et al., 2003; Kissil et al., 2003; Lim et al., 2003; Chadee and Kyriakis, 2004; Hirokawa et al., 2004; Lee et al., 2004; Rong et al., 2004; Chadee et al., 2006; Lim et al., 2006; Jones et al., 2008; Yi et al., 2008; Flaiz et al., 2009; Houshmandi et al., 2009). In addition to its effects on intracellular signals, merlin also regulates receptor tyrosine kinase trafficking and activity including platelet derived growth factor (PDGF) receptor (Fraenzer et al., 2003), epidermal growth factor receptor (EGFR/ErbB1) (Curto et al., 2007) and ErbB2 (Fernandez-Valle et al., 2002; Rangwala et al., 2005; Thaxton et al., 2007; Houshmandi et al., 2009). Due to

28

limited access and ability to culture primary human tumors, most of these studies used

transformed cell lines or cultures derived from merlin-deficient mice to examine the

consequences of merlin deficiency on cell growth. Thus, the extent to which these mechanisms

contribute to the development and growth of human VSs, the primary tumors resulting from

merlin deficiency, is unknown.

We have begun to investigate the merlin-sensitive signaling cascades that contribute to

the growth potential of human VS cells. Using tumor lysates and primary cultures derived from

acutely resected human VSs, we find that JNK is persistently phosphorylated in VS cells. Along

with MEK/ERK and PI3-K/Akt signaling, JNK activity promotes VS cell proliferation.

Additionally, JNK activity appears to protect VS cells from apoptosis by suppressing superoxide

production in the mitochondria. Thus, in contrast to normal SCs where activation of JNK leads to

apoptosis following denervation, persistent JNK activity in VS cells appears to contribute to their

ability to grow and survive in the absence of axons.

Experimental procedures

VS collection- The institutional review board of the University of Iowa approved the study

protocol. VS specimens and greater auricular nerve specimens from separate patients undergoing

neck dissection were collected following surgical removal and immediately placed in ice-cold

Hank's balanced salt solution (HBSS) until used for cultures or snap frozen in liquid nitrogen

until used for protein extracts.

Primary VS cell cultures- Primary VS cultures were prepared as previously described (Hansen et

al., 2006; Hansen et al., 2008). Briefly, acutely resected tumors were cut into 1 mm^3 fragments,

digested with collagenase (2 mg/ml, Sigma, St. Louis, MO) and 0.25% trypsin (Sigma) for 45–

60 min at 37C, and then put in 10% fetal bovine serum (FBS). Following centrifugation at 800 rpm for 3 min, the cells were resuspended and dissociated by trituration through narrow pipettes. Cell suspensions were plated in tissue culture plates (Corning Incorporated, Corning, NY) or 4-well culture slides (Nalge Nunc International, Rochester, NY) pretreated with polyornithine, followed by laminin (20 μg/ml). Cultures were maintained in Dulbecco's modified Eagle's medium (DMEM) with N2 supplements (Sigma), bovine insulin (Sigma, 1 mg/ml) and 10% FBS. The medium was exchanged 2 to 3 days later and when the cells reached 50–70% confluency, they were subsequently maintained in serum-free conditions until used for experiments, typically after 7-10 days. Over 90% of the cells in the cultures were S100-positive. Cultures were maintained in a humidified incubator with 6.0% CO_2 at 37C. Ebselen (EMD Bioscience, San Diego, CA) and/or kinase inhibitors including PD98059, U0126, LY294002, SP600125 (JNK Inhibitor II), cell permeable I-JIP (JNK Inhibitor VII) and PD158780 (all from EMD Bioscience) were added to the indicated cultures 4 h prior to experimental manipulation and maintained throughout the duration of the experiment.

For adenoviral mediated gene transfer, VS cultures were incubated with AdCMVEmpty (AdCon, $2x10^8$ pfu/ml) or AdSOD2 (superoxide dismutase 2, MnSOD, $2x10^8$ pfu/ml) manufactured by Viraquest, Inc. (North Liberty, IA). Treatment of parallel cultures with AdGFP confirmed that over 85% of VS cells are transduced by adenoviral vectors at this titer (not shown). Experimental manipulation began 48 h after viral transduction to allow time for transgene expression.

Western blotting- Protein extracts were prepared from VS tissue or culture lysates in ice-cold denaturing lysis buffer (50 mM Tris-HCl, pH 7.4, 1% Nonidet P-40 [NP-40], 150 mM NaCl, 1 mM EDTA, Minicomplete protease inhibitors (Roche Diagnostics Corp., Indianapolis, IN) as

well as phosphatase inhibitors (Sigma) were added, as per manufacturer's instructions, to all

lysis buffers. Lysates were sonicated, incubated for 30 min. on ice and centrifuged at 14000 rpm

for 10 min. at 4°C. Protein concentration was quantified using the Qubit flurometer (Invitrogen)

and 30-100 µg protein from each sample was dissolved in sample buffer (2% sodium dodecyl

sulfate [SDS], 5% β-mercaptoethanol, 62.5 mM Tris-HCl, 0.5% bromophenol blue), heated to

100°C for 5 min, and applied to 7.5% or 10% SDS-polyacrylamide gel electrophoresis (SDS-

PAGE) gels in running buffer. After electrophoresis, proteins were transferred to nitrocellulose

membranes (Bio-Rad, Hercules, CA) and the membranes were blocked with 5% nonfat dried

milk in TBST buffer (200 mM Tris-HCl, 1.37 M NaCl, 1% Tween 20, pH 7.5) for 30 min at

room temperature (RT). The blots were then incubated overnight at 4°C with primary antibodies

in blocking buffer. Primary antibodies used were: anti phosphorylated JNK (pJNK, Cell

Signaling #9251, Danvers, MA), pERK (Cell Signaling #9106), pAKT (Cell Signaling #9721),

JNK1 (Santa Cruz sc-474, Santa Cruz, CA), JNK2 (Cell Signaling,#4672), ERK(Cell Signaling

#9102), Akt (Cell Signaling #9272), pJUN (Cell Signaling #9261) and Rho-GDI (1:1000). The

membranes were washed 3 times with TBST and then incubated for 1 h at RT with horseradish-

peroxidase-conjugated secondary antibodies (1:5,000–1:50,000; Santa Cruz) diluted in blocking

buffer. The membranes were then washed 3 times with TBST, twice with TBS and developed

using Super Signal West Femto kit (Thermo Scientific,Rockford, IL) and exposed to film

(Amersham Hyperfilm TM ECL, GE Healthcare Limited, Buckinghamshire, UK). As needed,

membranes were stripped and re-probed with other primary and secondary antibody

combinations. Due to limited amounts of culture material that can be prepared from each tumor,

we did not have sufficient protein lysate to probe for all combinations of antibodies and selected

those that best controlled for the experimental conditions. Digital images of gels were captured

were captured on an Alpha Innotech gel imaging system (San Leandro, CA) and band pixel intensity was quantified using Image J software (NIH, Bethesda, MD).

siRNA knock down of merlin in normal human Schwann cells- Human Schwann cells (hSC; ScienCell, Carlsbad, CA) grown to 40% confluence were maintained in antibiotic-free media 24 hours prior to transfection. Small interfering RNA (siRNA) molecules (neurofibromin 2 ON-TARGETplus SMARTpool; Dharmacon, Lafayette, CO) were diluted in Opti-MEM reduced serum media (Invitrogen) and incubated with Lipofectamine-2000™ transfection reagent (Invitrogen) at room temperature for 20 minutes before being dropped onto cells at a final concentration of 40 nmol/L. Media was changed after 24 hours to minimize toxicity. Initial transfection was carried out on day 0, and repeat transfection was performed on day 4. Cells were harvested from duplicate plates on each day following siRNA transfection up to day 7 and Western blot techniques were then performed, as described (Ahma et al., 2010).

Immunostaining- Small fragments of VS or normal vestibular nerve specimens (removed for treatment of intractable Meniere's disease or temporal bone malignancies not affecting the inner ear) were fixed in 4% paraformaldehyde (PF), cryoprotected by in serial sucrose gradients, mounted in OCT and frozen sections (6-10 µm) were made on a cryostat. Cultures were fixed with 4% PF. Frozen section and cultured cells were washed with phosphate-buffered saline (PBS), permeabilized with PBS with 0.1% Triton X-100 for 10 min, blocked with blocking buffer (5% goat serum, 2% bovine serum albumin [BSA], 0.1% Triton- X in PBS) for 30–60 min, and then incubated with combinations of the following primary antibodies diluted in blocking buffer overnight at 4°C: anti-pJNK (1:500), anti-pJUN (1:500), anti-BrdU (1:800; clone G3G4, Hybridoma core, University of Iowa, Iowa City, IA), anti-cleaved caspase 3 (1:400 Cell Signaling #9664S), and anti-S100 (1:400, Sigma # S-2644). Alexa 488, Alexa 546, Alexa 568,

and Alexa 647 labeled secondary antibodies (1:800; Invitrogen, Carlsbad, CA), as indicated, were incubated at 37C for 1 h. Nuclei were labeled with Hoechst 33342 (10 μg/ml, Sigma) for 15 min.

Fluorescence images were captured using an inverted Leica DMRIII microscope (Leica, Bannockburn, IL) equipped with epifluorescence filters and a charge coupled device camera using Leica FW4000 software or with a Leica SP5 confocal microscope and prepared for publication using Adobe Photoshop (Adobe, San Jose, CA).

VS cell proliferation and apoptosis- Due to the limited number of cells that can be cultured from each tumor, we were not able to use flow cytometry or perform clonogenic or MTT assays to assay cell proliferation or apoptosis. Rather we scored the percent of 5-bromo-2-deoxyuridine (BrdU)-positive and terminal deoxynucleotidyl transferase dUTP nick end labeling (TUNEL)–positive VS cells to determine the extent of proliferation and apoptosis, respectively. VS cultures were labeled with BrdU (10 μM, Sigma) for 24 h prior to fixation. Fixed cultures were treated with 2N HCl for 15 min. prior to immunostaining and BrdU uptake was detected by immunostaining as above. The percent of BrdU positive VS cells (S100-positive) nuclei was determined by counting 10 randomly selected fields for each condition. Only S100-positive cells were scored. Given the variability in basal proliferation rates for each primary tumor, the percent of BrdU-positive VS cells was expressed as a percent of the control condition defined as 100%. Apoptotic cells were detected by TUNEL using the In Situ Cell Death Detection Kit, TMR red kit (Roche Diagnostics) according to the manufacturer's instructions. The percent of apoptotic VS cell (S100-positive) nuclei was determined by counting 10 randomly selected fields for each condition. Criteria for scoring were a TUNEL-positive nucleus with typical condensed morphology in an S100-positive cell. Apoptosis was confirmed in a subset of cultures by

immunostaining for cleaved caspase 3. The percent of apoptotic VS cells was expressed as a percent of the control condition defined as 100%. Each condition was repeated on 3 or more VS cultures derived from separate tumor.

Detection of reactive oxygen species- VS cultures in 4-well slides were loaded with 25 μM 5-(and-6)-chloromethyl-2′,7′-dichlorodihydrofluorescein diacetate, acetyl ester (CM-H$_2$DCFDA, Invitrogen, Eugene, OR) 30-45 min at 37C according to the manufacturer's instructions. During the final 5 min Hoechst 3342 (1.0 μM) was added label nuclei. JNK inhibitors (SP600125 or I-JIP) with or without ebselen were added to the indicated cultures 4-5 h prior to imaging. Digital epifluorescent images were captured from live cells using a Leica DMRIII inverted scope with exposure times set to a linear range based on cultures in control conditions and cells from cultures treated with 0.03% H$_2$O$_2$ or antimycin A (10 μM, Sigma). Fluorescent intensity was quantified from a circular selection within the cytoplasm of at least 30-50 cells using Image J software for each condition and the experiment was repeated on cultures from at least 4 separate tumors. Background fluorescence, determined from a similar sized circle placed outside cell boundaries, was substrated from each image.

To detect mitochondrial superoxide accumulation, VS cultures on 4 well glass coverslips were loaded with MitoSOX™ Red mitochondrial superoxide indicator (1 μM, Invitrogen) for 10 min. at 37C according to the manufacturer's instructions. JNK inhibitors were added to the indicated cultures 4 h prior to MitoSOX loading and maintained throughout the experiment. Fluorescent digital images were captured using Leica SP5 confocal microscope and fluorescent intensity was quantified as above using Image J.

Data and statistical analysis- Numerical data were managed and graphed in Excel (Microsoft, Redmond, WA) and SigmaStat (Systat Software, San Jose, CA) was used for statistical analyses.

Results

JNK is persistently phosphorylated in VS cells. Merlin suppresses the activity of several kinase

signaling cascades implicated in tumorigenesis including MEK/ERK, PI3-K/Akt, and JNK

(Tikoo et al., 1994; Gutmann et al., 2001; Shaw et al., 2001; Kim et al., 2002; Fraenzer et al.,

2003; Kaempchen et al., 2003; Kissil et al., 2003; Lim et al., 2003; Chadee and Kyriakis, 2004;

Hirokawa et al., 2004; Lee et al., 2004; Rong et al., 2004; Chadee et al., 2006; Lim et al., 2006;

Scoles, 2008). Recent studies demonstrate that PI3-K/Akt and MEK/ERK are persistently active

in human VS cells which lack functional merlin (Stemmer-Rachamimov et al., 1997; Ammoun et

al., 2008; Doherty et al., 2008; Jacob et al., 2008). To determine whether JNK is active in VS

cells, we immunostained frozen sections from acutely resected VSs and normal vestibular nerve

with antibodies that recognize the dually phosphorylated, or activated, JNK (pJNK) and with

anti-S100 antibodies to specifically label Schwann cells. S100-positive cells displayed pJNK

labeling indicating that JNK is phosphorylated in VS cells *in vivo* (Fig. 1). Conversely, pJNK

immunoreactivity was not detectable in the SCs of the normal vestibular nerve. Scarpa's

ganglion (vestibular) neurons demonstrated punctate pJNK immunoreactivity (Fig. 1).

Immunostaining with anti-neurofilament 200 (NF200) antibodies verified that the cells with

punctate pJNK immunoreactivity were neuronal. Thus, JNK is constitutively phosphorylated in

vestibular schwannoma cells and in vestibular neurons, but not normal vestibular SCs, *in vivo*.

To determine the extent of JNK phosphorylation in VSs, we probed immunoblots of

protein lysates from acutely resected VSs with anti-pJNK antibodies. Protein lysates from

acutely resected great auricular nerve (GAN) specimens served as a control to determine the

extent of activation of these kinases in mature SCs. The blots were stripped and reprobed with

non phospho-specific antibodies and subsequently with an antibody against Rho-GDI, a protein

with comparable expression in SCs and schwannoma cells (Ammoun et al., 2008).

Immunostaining intensity was quantified by densitometry and the levels of phosphorylated JNK1

and JNK2 were compared to non-phosphorylated JNK 1 and 2. The overall levels of JNK 1 and 2

were compared to Rho-GDI to determine if there are differences in kinase expression in VS

tissue compared to normal nerves. Data were quantified for 4VS and 4 GAN specimens, and are

representative of results from 4 additional VS and 3 GAN specimens. As shown in Fig. 1, both

JNK1 and JNK2 are expressed at significantly higher levels in the GAN compared to VS tissue.

The extent of JNK1, and to a lesser extent, JNK2 phosphorylation was significantly greater in

VS compared with GAN tissue. Thus, JNK is persistently active in VS cells compared with

normal SCs.

Persistent JNK phosphorylation in VS tissue suggests that merlin suppresses JNK

phosphorylation in human SCs. To test this hypothesis we immunoblotted lysates from primary

human SC cultures transfected with merlin targeted or scrambled siRNA with anti-pJNK

antibodies for seven days following transfection. We have previously shown that this

significantly reduces merlin expression in human SCs by probing these lysates with anti-merlin

antibodies (Ahma et al., 2010). Knock-down of merlin resulted in increased JNK

phosphorylation verifying that merlin suppresses JNK phosphorylation in human SCs (Fig. 2).

To verify persistent ERK, Akt and JNK phosphorylation in VS cells, we also probed

immunoblots prepared from primary human VS cell cultures maintained in basal medium

without serum with anti-pERK, anti-pAkt and anti-pJNK antibodies. Consistent with

observations in tumor lysates (Fig. 1) (Jacob et al., 2008), cultured VS cells demonstrate

persistent basal phosphorylation of these kinases (Fig. 3). ERK phosphorylation was specifically

suppressed by the MEK inhibitor U0126 (10 μM) and Akt phosphorylation was suppressed by the PI3-K inhibitor, LY294002 (20 μM). These blots are representative of similar results obtained from cultures derived from at least 3 separate VSs for each condition. Based on immunostaining, pJNK distributes diffusely in the cytoplasm and nucleus in cultured VS cells (Fig. 3). Thus, cultured primary VS cells retain active ERK, Akt and JNK similar to their counterparts *in vivo* suggesting that they represent a realistic model to study the contribution of these signals to VS tumorigenesis.

ErbB2, a receptor tyrosine kinase required for normal SC development and survival, constitutively resides in lipid rafts in VS cells and is active (Hansen and Linthicum, 2004; Hansen et al., 2006; Wickremesekera et al., 2007; Brown and Hansen, 2008). This constitutive ErbB2 activity contributes to the proliferative potential of VS cells and is required for Src activation (Hansen et al., 2006; Houshmandi et al., 2009). Further, merlin regulates ErbB2 trafficking and signaling (Fernandez-Valle et al., 2002; Rangwala et al., 2005). Since MEK/ERK, PI3-K/Akt, and JNKs are activated by ErbB2 (Li et al., 2001; Nuntharatanapong et al., 2005; Monje et al., 2006; Piechocki et al., 2007; Yamauchi et al., 2008), it is possible that the activation of these kinases in VS cells results from constitutive ErbB2 signaling. We compared ERK, Akt, and JNK phosphorylation status in protein lysates prepared from primary VS cultures maintained in the presence or absence of the ErbB2 inhibitor, PD158780 (100 nM) (Hansen et al., 2008). Lysates from primary rat sciatic nerve SC cultures confirmed that PD158780 inhibits the ability of NRG-1, an ErbB2 ligand, to induce ErbB2 phosphorylation (Supplemental Fig. 1). PD158780 failed to reduce pERK, pAkt, and pJNK levels in primary VS cells (Fig. 3). Similar results were obtained from at least 3 VS cultures derived from separate tumors. Similar results were obtained with AG825 (1 μM), a different ErbB2 inhibitor (not shown). These data suggest

that, in contrast to Src phosphorylation in merlin deficient glial cells (Houshmandi et al., 2009), persistent phosphorylation of ERKs, Akt, and JNK in VS cells does not require ErbB2 activity.

MEK/ERK and PI3-K/Akt promote VS proliferation- Given that MEK/ERK, PI3-K/Akt, and JNKs are active in VS cells, we sought to determine the extent to which these pro-growth signals contributed to the proliferative and survival response of primary VS cells. We scored BrdU-positive VS cells in cultures treated with either LY294002 (2, 20 μM), a PI3-K inhibitor, or with U0126 (10 μM) or PD98059 (2, 20 μM), MEK inhibitors. For each culture derived from separate tumor, the percent of BrdU-positive VS cells was expressed as a percent of the control condition defined as 100%. In control conditions 5.5%±2.5 (mean±SD) of VS cells were BrdU-positive. VS cell apoptosis was determined by scoring TUNEL (terminal deoxynucleotidyl transferase dUTP nick end labeling)-positive VS cells in parallel cultures. The percent of TUNEL-positive VS cells was likewise expressed as a percent of the control condition. Overall, 3.0%±1.6 of VS cells were TUNEL-positive in control conditions. Inhibition of MEK with U0126 or PD98059 significantly reduced VS cell proliferation but did not result in a significant difference in the percent of apoptotic cells (Fig. 4). Similarly, the PI3-K inhibitor, LY294002, significantly reduced VS cell proliferation but not survival (Fig. 4). These data suggest that both MEK/ERK and PI3-K/Akt activity contribute to VS cell proliferation *in vitro*, but are not independently required for cell survival.

JNK promotes VS proliferation and survival- SCs critically depend on axons for long-term survival and activation of JNK contributes to the apoptosis of denervated SCs following axotomy (Cheng et al., 2001; Parkinson et al., 2001; Parkinson et al., 2004). Conversely, JNK activity promotes survival of transformed rat RN22 schwannoma cells (Lopez-Sanchez et al., 2007).

Given that JNK remains active in primary human VS cells, we sought to determine if persistent

JNK activity contributes to the ability of VS cells to proliferate and survive in the absence of

axons. We quantified the percent of BrdU-positive and TUNEL-positive VS cells in cultures

treated with cell permeant peptide I-JIP (30, 100 µM) or SP 600125 (20 µM). I-JIP is a peptide

that competitively inhibits the binding of JNKs to the JIP scaffolding protein, thereby inhibiting

JNK activation (Dickens et al., 1997; Barr et al., 2002; Kuan and Burke, 2005). SP600125 is a

small molecule inhibitor of JNK (Bogoyevitch et al., 2004; Kuan and Burke, 2005). Treatment

with either I-JIP or SP600125 significantly decreased the percent of BrdU-positive and increased

the percent of TUNEL-positive VS cells (Fig. 5). Thus, inhibition of persistent JNK activity

reduces VS cell proliferation and survival.

Inhibition of JNK results in RN22 schwannoma cell necrosis, but not apparently

apoptosis (Lopez-Sanchez et al., 2007). However, we observed an increase in TUNEL-positive

human primary VS cells in the presence of JNK inhibitors implying that JNK inhibition leads to

apoptosis in these cells. To verify that JNK inhibition results in VS cell apoptosis we stained

primary VS cells cultures maintained in I-JIP (30 µM) or SP600125 (20 µM) with anti-active

caspase-3 antibody, which detects cleaved caspase-3, a hallmark of apoptosis (Hengartner,

2000), and TUNEL. As shown in Fig. 5, TUNEL-positive VS cells demonstrated cleaved

caspase-3 (active caspase) immunoreactivity in their cytoplasm, confirming that the TUNEL-

positive cells are apoptotic. Finally, to verify that the increase in apoptosis leads to an overall

decrease in cell survival, we counted the number of surviving cells 5 days after treatment with I-

JIP and SP600125. Both JNK inhibitors significantly reduced the number of surviving VS cells

(Fig. 5). Thus, inhibition of JNK induces VS cell apoptosis and decreases survival.

The results above imply that persistent JNK activity promotes VS cell survival. To verify that VS cells with persistent JNK activity are those that survive, we labeled primary VS cultures maintained in the presence or absence of I-JIP or SP600125 with anti-phosphorylated Jun (pJUN) antibodies and TUNEL. pJun immunofluorescence was determined from digital, epifluorescent images for each VS cell by measuring the mean pixel density in each nucleus (Alam et al., 2007). Background fluorescence/nonspecific labeling was determined by measuring the mean pixel intensity in the cytoplasm, taking advantage of the fact that pJun is an obligatorily nuclear protein so that any cytoplasmic fluorescence represents background labeling (Alam et al., 2007). Cells with a nuclear:cytoplasmic pJun immunofluorescence intensity ratio ≥5 were considered pJun-positive. We then compared the pJun and TUNEL status for each of >300 cells per condition and the results were verified in 3 VS cultures from separate tumors. As shown in Fig. 6, I-JIP and SP600125 both decreased the percent of pJun-positive cells and increased the percent of TUNEL-positive cells. None of the TUNEL-positive cells in any condition were also pJun-positive. These observations indicate that susceptibility to apoptosis highly correlates with loss of pJun immunoreactivity and support the hypothesis that persistent JNK activity protects VS cells from apoptosis.

JNK activity protects VS cells from apoptosis by limiting accumulation of reactive oxygen species (ROS)- Accumulation of ROS regulates a variety of cellular functions relevant to SC neoplasia including receptor tyrosine kinase signaling, proliferation, apoptosis, and senescence (Genestra, 2007; Ryter et al., 2007). Inhibition of JNK with SP600125 in RN22 schwannoma cells cultured in the absence of serum results in increased ROS and necrotic cell death (Lopez-Sanchez et al., 2007). To determine the effect of JNK activity on the ROS status of primary

human VS cells, we loaded primary cultures with 5-(and-6)-chloromethyl-2',7'-dichlorodihydrofluorescein diacetate (H$_2$DCFDA), a fluorescent probe for ROS. Oxidation of the nonfluorescent H$_2$DCFDA yields 2',7'-dichlorofluorescein (DCF), a highly fluorescent product that detects the generation of reactive oxygen intermediates in intact cells (Yuan et al., 1993; Oyama et al., 1994; Lopez-Sanchez et al., 2007). Following loading with H$_2$DCFDA, the cells were maintained in the presence or absence of I-IJP (30, 100 μM) or SP600125 (20 μM) for 4 h. DCF fluorescence intensity was quantified from digital images of live cultures by measuring the mean pixel density in the perinuclear cytoplasm of each cell. In cultures derived from 4 separate tumors, inhibition of JNK significantly increased DCF fluorescence (Fig. 7). Thus, JNK inhibitors increase ROS in VS cultures.

To determine if the increase in ROS accounts for the pro-apoptotic effects of JNK inhibitors, we treated 5 VS cultures derived from different tumors with ebselen (-phenyl-1,2-benzisoselenazol-3(2H)-one), a seleno-organic compound that acts as a glutathione peroxidase mimic and is an effective ROS scavenger (Fig. 6) (Ozaki et al., 1997; Nakamura et al., 2002), in combination with JNK inhibitors and determined the percent of apoptotic VS cells as above. Ebselen significantly protected VS cells from apoptosis due to JNK inhibition (Fig. 7). Taken together, these observations suggest that persistent JNK activity protects VS cells from apoptosis, at least in part, by limiting the accumulation of ROS.

To further explore the mechanisms of ROS suppression by JNK activity, we sought to identify the subcellular source and type of ROS in VS cells treated with JNK inhibitors. Mitochondria are a major source of ROS and JNK regulates several mitochondrial activities including ROS production. To determine if JNK regulates mitochondrial ROS production in VS cells, primary VS cultures were loaded with MitoSOX Red, a fluorogenic dye that specifically

detects superoxide in the mitochondria of live cells (Robinson et al., 2008). It fails to detect other ROS- or reactive nitrogen species-generating systems. Cells were maintained in the presence or absence of SP600125 or I-IJIP for 4 h and MitoSOX Red fluorescence was quantified. VS cultures treated with JNK inhibitors demonstrated significantly higher levels of MitoSOX Red fluorescence implying that persistent JNK activity suppresses superoxide production in VS cell mitochondria (Fig. 8).

To determine if this increase in mitochondrial superoxide production contributes to VS cell apoptosis, VS cultures were treated with an adenoviral vector encoding superoxide dismutase 2 (SOD2, MnSOD), a mitochondrially localized superoxide scavenger, or a control vector. Cultures were subsequently treated with I-JIP or SP600125 and the percent of TUNEL-positive VS cells was determined. Expression of SOD2 significantly suppressed VS cell apoptosis in the presence of JNK inhibitors (Fig. 8). Taken together, these results suggest that JNK activity protects VS cell from apoptosis specifically by suppressing mitochondrial superoxide production.

Discussion

Progrowth signals in VSs- As a tumor suppressor, the merlin protein regulates a wide variety of signaling events implicated in tumorigenesis including Ras, Rac1/Cdc42, RhoA, Src, Raf, p21-activated kinases 1 and 2 (PAK1/2), extracellular regulated kinase/mitogen activated protein kinase (ERK/MAPK), c-Jun N-terminal kinase (JNK), and phosphatidyl-inositol 3-kinase (PI3-K)/Akt, ErbB2 and PDGF receptor (Tikoo et al., 1994; Gutmann et al., 2001; Shaw et al., 2001; Kim et al., 2002; Fraenzer et al., 2003; Kaempchen et al., 2003; Kissil et al., 2003; Lim et al., 2003; Chadee and Kyriakis, 2004; Hirokawa et al., 2004; Lee et al., 2004; Rong et al., 2004;

Chadee et al., 2006; Lim et al., 2006; Ammoun et al., 2008; Jones et al., 2008; Yi et al., 2008; Flaiz et al., 2009; Houshmandi et al., 2009). Prior studies demonstrate increased ERK and Akt signaling in human VSs and here we verified that JNK is likewise active in human VS tissue (Ammoun et al., 2008; Lee et al., 2009). This persistent JNK activity likely results from merlin inactivation since knock-down of merlin in normal human SCs leads to increased JNK phosphorylation. Limited access to human specimens has hampered identification of which of these merlin-sensitive signals contribute to VS formation and growth. Using primary cultures derived from human VSs, we found that MEK/ERK, PI3-K/Akt, and JNK activity each promote VS cell proliferation. Consistent with these observations, recent studies found that proliferation of human VS cells depends on MEK/ERK and Akt signaling (Ammoun et al., 2008; Lee et al., 2009).

Merlin also regulates ErbB2 localization and activity and inhibition of ErbB2 reduces VS cell proliferation and growth of human VS xenografts in nude mice (Fernandez-Valle et al., 2002; Stickney et al., 2004; Hansen et al., 2006; Thaxton et al., 2007; Brown and Hansen, 2008; Clark et al., 2008; Houshmandi et al., 2009). Nevertheless, activation of ERK, Akt, and JNK appears independent of ErbB2 signaling in human VS cells (Fig. 2). By contrast, Src activity in merlin-deficient central nervous system glial cells depends on ErbB2 (Houshmandi et al., 2009). Recent evidence indicates that the persistent basal ERK phosphorylation in human VS cells likely results from focal adhesion kinase (FAK)/Src/Ras, but not Rac/PAK, signaling (Ammoun et al., 2008).

*JNK expression and activity in VS*s- JNK isoforms 1, 2 and 3 present diverse and often opposing effects on cell survival, apoptosis, and tumorigenesis (Bode and Dong, 2007). JNK1 and 2 are expressed ubiquitously, while JNK 3 is primarily expressed in neurons. We find that JNK2 and,

to a lesser extent, JNK1 are expressed at higher levels in normal nerve tissue compared with VSs. The significance of the lower levels of JNK1 and JNK2 expression in VS tissue compared to normal nerve remains unknown. In some cellular responses, JNK1 and JNK2 function redundantly while in other cases they differentially regulate cellular responses. For example, fibroblasts lacking JNK1 exhibit proliferation defects whereas lack of JNK2 confers a proliferative advantage (Tournier et al., 2000). Complete absence of both JNKs results in a dramatic proliferation defect, similar to cells lacking c-Jun (Schreiber et al., 1999). Despite increased levels of JNK expression, JNK is not phosphorylated in mature SCs whereas it is phosphorylated in VS cells. This persistent JNK phosphorylation appears to promote survival and proliferation in VS cells.

JNKs are activated by dual phosphorylation on threonine (T) 183 and tyrosine (Y) 185 by a kinase signaling cascade involving the MAPK kinases (MAP2K), MEK 4 and 7, and the MAPK kinase kinases (MAP3K), mixed lineage kinases (MLK) 1-3, classically in response to cellular stress such as irradiation (IR) or oxidative stress (reviewed in (Weston and Davis, 2007)). Significantly, merlin suppresses JNK activity in HEI 193 cells, a human schwannoma cell line transformed with viral oncogenes (Chadee and Kyriakis, 2004) although the exact mechanisms by which merlin regulates JNK activity in schwannoma cells is unknown. JNK is phosphorylated in response to Rac1/Cdc42 activation and merlin inhibits Rac1/Cdc42; hyperactivation of Rac1/Cdc42 signaling represents one potential mechanism contributing to persistent JNK phosphorylation in VS cells (Flaiz et al., 2009). Merlin also suppresses MLK-3 signaling by Thus, activation of MLK-3 in response to merlin deficiency represents another potential mechanism contributing to persistent JNK phosphorylation in VS cells.

JNK signaling is also regulated by subcellular localization and JIPs (JNK interacting proteins) and POSH (plenty of SH3s) are scaffolding proteins that bind JNKs tethering them near MLKs, MEKs, and specific substrates, thus regulating JNK's functional activity (Dickens et al., 1997; Kukekov et al., 2006; Whitmarsh, 2006). The observation that disruption of JNK binding to JIP by a specific competitive peptide (I-JIP) effectively inhibits JNK activity highlights the importance of JNK's interaction with scaffolding proteins for its activation in VS cells, similar to other cells (Dickens et al., 1997; Bonny et al., 2001).

Depending on the cell type and context, JNK activity can either promote or suppress cell survival, proliferation, and tumorigenesis (Chen et al., 1996; Chen et al., 2001; Kennedy and Davis, 2003; Liu and Lin, 2005; Bode and Dong, 2007). For example, JNKs suppress *ras*-induced tumorigenesis in fibroblasts but promote Bcr-Abl induced B-cell lymphoma (Hess et al., 2002; Kennedy and Davis, 2003). Both the physiological context and time course of kinase activation appear to determine whether JNK signaling promotes survival or apoptosis (Ventura et al., 2006; Bode and Dong, 2007). In SCs, JNKs are activated in response to nerve injury and promote SC apoptosis (Cheng et al., 2001; Parkinson et al., 2001; Parkinson et al., 2004; Ahn and Shin, 2006; Lee et al., 2006). Conversely, JNK activity promotes survival of transformed schwannoma cells and other glial neoplasms (Tsuiki et al., 2003; Cui et al., 2006; Lopez-Sanchez et al., 2007). Here we show that JNK promotes human VS cell proliferation and survival. Thus, JNK represents a potential specific therapeutic target for treatment of VSs that would likely reduce VS cell growth yet not harm normal SCs. Such treatment strategies may be especially suitable for patients with NF2 and multiple schwannomas that are difficult to manage with current treatment options.

ROS in VS cells- In many cells, JNK is activated by elevated ROS contributing to cell death (Shen and Liu, 2006); however, JNK appears to suppress ROS accumulation in rat RN22 schwannoma cells (Lopez-Sanchez et al., 2007) and here we show that JNK specifically suppresses mitochondrial superoxide accumulation in human VS cells. Three enzyme activities function to scavenge cellular ROS. SOD enzymes convert superoxides to hydrogen peroxide (H_2O_2), whereas catalase and glutathione peroxidase convert H_2O_2 to O_2 and H_2O (Halliwell and Gutteridge, 1999). SOD2 (MnSOD), a nuclear-encoded and mitochondria-localized homotetrameric enzyme, is the primary defense against mitochondrially generated ROS, whereas SOD1 (Cu/ZnSOD) is distributed in the cytosol and accounts for 70-80% of cellular SOD activity (McCord and Fridovich, 1969; Zelko et al., 2002). Overexpression of SOD2 protects human VS cells from apoptosis due to JNK inhibition confirming that the increase in mitochondrial superoxide contributes to the death of VS cells with suppressed JNK activity. Taken together, these observations suggest that the reduction in ROS stress due to persistent JNK activity may account, at least in part, for the ability of VS cells to grow and survive in the absence of axons in contrast to their normal SC counterparts which critically depend on axonal contact for long-term survival

References

Ahma Z, Brown CM, Patel AK, Ryan AF, Ongkeko R, Doherty JK (2010) Merlin knockdown in human Schwann cells: Clues to vestibular schwannoma tumorigenesis. Otol Neurotol:in press.

Ahn M, Shin T (2006) Increased phosphorylation of c-Jun NH (2)-terminal protein kinase in the sciatic nerves of Lewis rats with experimental autoimmune neuritis. J Vet Sci 7:13-17.

Alam SA, Robinson BK, Huang J, Green SH (2007) Prosurvival and proapoptotic intracellular signaling in rat spiral ganglion neurons in vivo after the loss of hair cells. J Comp Neurol 503:832-852.

Ammoun S, Flaiz C, Ristic N, Schuldt J, Hanemann CO (2008) Dissecting and targeting the growth factor-dependent and growth factor-independent extracellular signal-regulated kinase pathway in human schwannoma. Cancer Res 68:5236-5245.

Barr RK, Kendrick TS, Bogoyevitch MA (2002) Identification of the critical features of a small peptide inhibitor of JNK activity. J Biol Chem 277:10987-10997.

Baser ME, DG RE, Gutmann DH (2003) Neurofibromatosis 2. Curr Opin Neurol 16:27-33.

Bianchi AB, Hara T, Ramesh V, Gao J, Klein-Szanto AJ, Morin F, Menon AG, Trofatter JA, Gusella JF, Seizinger BR, et al. (1994) Mutations in transcript isoforms of the neurofibromatosis 2 gene in multiple human tumour types. Nat Genet 6:185-192.

Bode AM, Dong Z (2007) The functional contrariety of JNK. Mol Carcinog 46:591-598.

Bogoyevitch MA, Boehm I, Oakley A, Ketterman AJ, Barr RK (2004) Targeting the JNK MAPK cascade for inhibition: basic science and therapeutic potential. Biochim Biophys Acta 1697:89-101.

Bonny C, Oberson A, Negri S, Sauser C, Schorderet DF (2001) Cell-permeable peptide inhibitors of JNK: novel blockers of beta-cell death. Diabetes 50:77-82.

Bourn D, Carter S, Gareth D, Evans R, Strachan T (1994) Germline mutation in the neurofibromatosis type 2 tumour suppressor gene. Hum Mol Genet 3:813--816.

Brown KD, Hansen MR (2008) Lipid raft localization of erbB2 in vestibular schwannoma and Schwann cells. Otol Neurotol 29:79-85.

Chadee DN, Kyriakis JM (2004) MLK3 is required for mitogen activation of B-Raf, ERK and cell proliferation. Nat Cell Biol 6:770-776.

Chadee DN, Xu D, Hung G, Andalibi A, Lim DJ, Luo Z, Gutmann DH, Kyriakis JM (2006) Mixed-lineage kinase 3 regulates B-Raf through maintenance of the B-Raf/Raf-1 complex and inhibition by the NF2 tumor suppressor protein. Proc Natl Acad Sci U S A 103:4463-4468.

Chen N, Nomura M, She QB, Ma WY, Bode AM, Wang L, Flavell RA, Dong Z (2001) Suppression of skin tumorigenesis in c-Jun NH(2)-terminal kinase-2-deficient mice. Cancer Res 61:3908-3912.

Chen YR, Wang X, Templeton D, Davis RJ, Tan TH (1996) The role of c-Jun N-terminal kinase (JNK) in apoptosis induced by ultraviolet C and gamma radiation. Duration of JNK activation may determine cell death and proliferation. J Biol Chem 271:31929-31936.

Cheng HL, Steinway ML, Xin X, Feldman EL (2001) Insulin-like growth factor-I and Bcl-X(L) inhibit c-jun N-terminal kinase activation and rescue Schwann cells from apoptosis. J Neurochem 76:935-943.

Clark JJ, Provenzano M, Diggelmann HR, Xu N, Hansen SS, Hansen MR (2008) The ErbB inhibitors trastuzumab and erlotinib inhibit growth of vestibular schwannoma xenografts in nude mice: a preliminary study. Otol Neurotol 29:846-853.

Cui J, Han SY, Wang C, Su W, Harshyne L, Holgado-Madruga M, Wong AJ (2006) c-Jun NH(2)-terminal kinase 2alpha2 promotes the tumorigenicity of human glioblastoma cells. Cancer Res 66:10024-10031.

Curto M, Cole BK, Lallemand D, Liu CH, McClatchey AI (2007) Contact-dependent inhibition of EGFR signaling by Nf2/Merlin. J Cell Biol 177:893-903.

Dickens M, Rogers JS, Cavanagh J, Raitano A, Xia Z, Halpern JR, Greenberg ME, Sawyers CL, Davis RJ (1997) A cytoplasmic inhibitor of the JNK signal transduction pathway. Science 277:693-696.

Doherty JK, Ongkeko W, Crawley B, Andalibi A, Ryan AF (2008) ErbB and Nrg: Potential Molecular Targets for Vestibular Schwannoma Pharmacotherapy. Otol Neurotol 29:50-57.

Fernandez-Valle C, Tang Y, Ricard J, Rodenas-Ruano A, Taylor A, Hackler E, Biggerstaff J, Iacovelli J (2002) Paxillin binds schwannomin and regulates its density-dependent localization and effect on cell morphology. Nat Genet 31:354-362.

Flaiz C, Chernoff J, Ammoun S, Peterson JR, Hanemann CO (2009) PAK kinase regulates Rac GTPase and is a potential target in human schwannomas. Exp Neurol 218:137-144.

Fraenzer JT, Pan H, Minimo L, Jr., Smith GM, Knauer D, Hung G (2003) Overexpression of the NF2 gene inhibits schwannoma cell proliferation through promoting PDGFR degradation. Int J Oncol 23:1493-1500.

Genestra M (2007) Oxyl radicals, redox-sensitive signalling cascades and antioxidants. Cell Signal 19:1807-1819.

Gutmann DH, Hirbe AC, Haipek CA (2001) Functional analysis of neurofibromatosis 2 (NF2) missense mutations. Hum Mol Genet 10:1519-1529.

Halliwell B, Gutteridge JMC (1999) Free Radicals in Biology and Medicine, 3rd Edition. New York: Oxford University Press, Inc.

Hansen MR, Linthicum FH, Jr. (2004) Expression of neuregulin and activation of erbB receptors in vestibular schwannomas: possible autocrine loop stimulation. Otol Neurotol 25:155-159.

Hansen MR, Vijapurkar U, Koland JG, Green SH (2001) Reciprocal signaling between spiral ganglion neurons and Schwann cells involves neuregulin and neurotrophins. Hear Res 161:87-98.

Hansen MR, Roehm PC, Chatterjee P, Green SH (2006) Constitutive neuregulin-1/ErbB signaling contributes to human vestibular schwannoma proliferation. Glia 53:593-600.

Hansen MR, Clark JJ, Gantz BJ, Goswami PC (2008) Effects of ErbB2 signaling on the response of vestibular schwannoma cells to gamma-irradiation. Laryngoscope 118:1023-1030.

Hengartner MO (2000) The biochemistry of apoptosis. Nature 407:770-776.

Hess P, Pihan G, Sawyers CL, Flavell RA, Davis RJ (2002) Survival signaling mediated by c-Jun NH(2)-terminal kinase in transformed B lymphoblasts. Nat Genet 32:201-205.

Hirokawa Y, Tikoo A, Huynh J, Utermark T, Hanemann CO, Giovannini M, Xiao GH, Testa JR, Wood J, Maruta H (2004) A clue to the therapy of neurofibromatosis type 2: NF2/merlin is a PAK1 inhibitor. Cancer J 10:20-26.

Houshmandi SS, Emnett RJ, Giovannini M, Gutmann DH (2009) The neurofibromatosis 2 protein, merlin, regulates glial cell growth in an ErbB2- and Src-dependent manner. Mol Cell Biol 29:1472-1486.

Jacob A, Lee TX, Neff BA, Miller S, Welling B, Chang LS (2008) Phosphatidylinositol 3-kinase/AKT pathway activation in human vestibular schwannoma. Otol Neurotol 29:58-68.

Jones GN, Tep C, Towns WH, 2nd, Mihai G, Tonks ID, Kay GF, Schmalbrock PM, Stemmer-Rachamimov AO, Yoon SO, Kirschner LS (2008) Tissue-specific ablation of Prkar1a causes schwannomas by suppressing neurofibromatosis protein production. Neoplasia 10:1213-1221.

Kaempchen K, Mielke K, Utermark T, Langmesser S, Hanemann CO (2003) Upregulation of the Rac1/JNK signaling pathway in primary human schwannoma cells. Hum Mol Genet 12:1211-1221.

Kennedy NJ, Davis RJ (2003) Role of JNK in tumor development. Cell Cycle 2:199-201.

Kim H, Lim JY, Kim YH, Park SH, Lee KH, Han H, Jeun SS, Lee JH, Rha HK (2002) Inhibition of ras-mediated activator protein 1 activity and cell growth by merlin. Mol Cells 14:108-114.

Kissil JL, Wilker EW, Johnson KC, Eckman MS, Yaffe MB, Jacks T (2003) Merlin, the product of the Nf2 tumor suppressor gene, is an inhibitor of the p21-activated kinase, Pak1. Mol Cell 12:841-849.

Kuan CY, Burke RE (2005) Targeting the JNK signaling pathway for stroke and Parkinson's diseases therapy. Curr Drug Targets CNS Neurol Disord 4:63-67.

Kukekov NV, Xu Z, Greene LA (2006) Direct interaction of the molecular scaffolds POSH and JIP is required for apoptotic activation of JNKs. J Biol Chem 281:15517-15524.

Lee H, Jo EK, Choi SY, Oh SB, Park K, Kim JS, Lee SJ (2006) Necrotic neuronal cells induce inflammatory Schwann cell activation via TLR2 and TLR3: implication in Wallerian degeneration. Biochem Biophys Res Commun 350:742-747.

Lee JY, Kim H, Ryu CH, Kim JY, Choi BH, Lim Y, Huh PW, Kim YH, Lee KH, Jun TY, Rha HK, Kang JK, Choi CR (2004) Merlin, a tumor suppressor, interacts with transactivation-responsive RNA-binding protein and inhibits its oncogenic activity. J Biol Chem 279:30265-30273.

Lee TX, Packer MD, Huang J, Akhmametyeva EM, Kulp SK, Chen CS, Giovannini M, Jacob A, Welling DB, Chang LS (2009) Growth inhibitory and anti-tumour activities of OSU-03012, a novel PDK-1 inhibitor, on vestibular schwannoma and malignant schwannoma cells. Eur J Cancer 45:1709-1720.

Li Y, Tennekoon GI, Birnbaum M, Marchionni MA, Rutkowski JL (2001) Neuregulin signaling through a PI3K/Akt/Bad pathway in Schwann cell survival. Mol Cell Neurosci 17:761-767.

Lim JY, Kim H, Jeun SS, Kang SG, Lee KJ (2006) Merlin inhibits growth hormone-regulated Raf-ERKs pathways by binding to Grb2 protein. Biochem Biophys Res Commun 340:1151-1157.

Lim JY, Kim H, Kim YH, Kim SW, Huh PW, Lee KH, Jeun SS, Rha HK, Kang J (2003) Merlin suppresses the SRE-dependent transcription by inhibiting the activation of Ras-ERK pathway. Biochem Biophys Res Commun 302:238-245.

Liu J, Lin A (2005) Role of JNK activation in apoptosis: a double-edged sword. Cell Res 15:36-42.

Lopez-Sanchez N, Rodriguez JR, Frade JM (2007) Mitochondrial c-Jun NH2-terminal kinase prevents the accumulation of reactive oxygen species and reduces necrotic damage in neural tumor cells that lack trophic support. Mol Cancer Res 5:47-60.

McCord JM, Fridovich I (1969) Superoxide dismutase. An enzymic function for erythrocuprein (hemocuprein). J Biol Chem 244:6049-6055.

Monje PV, Bartlett Bunge M, Wood PM (2006) Cyclic AMP synergistically enhances neuregulin-dependent ERK and Akt activation and cell cycle progression in Schwann cells. Glia 53:649-659.

Nakamura Y, Feng Q, Kumagai T, Torikai K, Ohigashi H, Osawa T, Noguchi N, Niki E, Uchida K (2002) Ebselen, a glutathione peroxidase mimetic seleno-organic compound, as a multifunctional antioxidant. Implication for inflammation-associated carcinogenesis. J Biol Chem 277:2687-2694.

Nuntharatanapong N, Chen K, Sinhaseni P, Keaney JF, Jr. (2005) EGF receptor-dependent JNK activation is involved in arsenite-induced p21Cip1/Waf1 upregulation and endothelial apoptosis. Am J Physiol Heart Circ Physiol 289:H99-H107.

Oyama Y, Hayashi A, Ueha T, Maekawa K (1994) Characterization of 2',7'-dichlorofluorescin fluorescence in dissociated mammalian brain neurons: estimation on intracellular content of hydrogen peroxide. Brain Res 635:113-117.

Ozaki M, Nakamura M, Teraoka S, Ota K (1997) Ebselen, a novel anti-oxidant compound, protects the rat liver from ischemia-reperfusion injury. Transpl Int 10:96-102.

Parkinson DB, Bhaskaran A, Droggiti A, Dickinson S, D'Antonio M, Mirsky R, Jessen KR (2004) Krox-20 inhibits Jun-NH2-terminal kinase/c-Jun to control Schwann cell proliferation and death. J Cell Biol 164:385-394.

Parkinson DB, Dong Z, Bunting H, Whitfield J, Meier C, Marie H, Mirsky R, Jessen KR (2001) Transforming growth factor beta (TGFbeta) mediates Schwann cell death in vitro and in vivo: examination of c-Jun activation, interactions with survival signals, and the relationship of TGFbeta-mediated death to Schwann cell differentiation. J Neurosci 21:8572-8585.

Piechocki MP, Yoo GH, Dibbley SK, Lonardo F (2007) Breast cancer expressing the activated HER2/neu is sensitive to gefitinib in vitro and in vivo and acquires resistance through a novel point mutation in the HER2/neu. Cancer Res 67:6825-6843.

Provenzano MJ, Xu N, Ver Meer MR, Clark JJ, Hansen MR (2008) p75NTR and Sortilin Increase After Facial Nerve Injury. Laryngoscope 118:87-93.

Rangwala R, Banine F, Borg JP, Sherman LS (2005) Erbin Regulates Mitogen-activated Protein (MAP) Kinase Activation and MAP Kinase-dependent Interactions between Merlin and Adherens Junction Protein Complexes in Schwann Cells. J Biol Chem 280:11790-11797.

Robinson KM, Janes MS, Beckman JS (2008) The selective detection of mitochondrial superoxide by live cell imaging. Nat Protoc 3:941-947.

Rong R, Tang X, Gutmann DH, Ye K (2004) Neurofibromatosis 2 (NF2) tumor suppressor merlin inhibits phosphatidylinositol 3-kinase through binding to PIKE-L. Proc Natl Acad Sci U S A 101:18200-18205.

Rouleau GA, Merel P, Lutchman M, Sanson M, Zucman J, Marineau C, Hoang-Xuan K, Demczuk S, Desmaze C, Plougastel B, et al. (1993) Alteration in a new gene encoding a putative membrane-organizing protein causes neuro-fibromatosis type 2. Nature 363:515-521.

Ryter SW, Kim HP, Hoetzel A, Park JW, Nakahira K, Wang X, Choi AM (2007) Mechanisms of cell death in oxidative stress. Antioxid Redox Signal 9:49-89.

Schreiber M, Kolbus A, Piu F, Szabowski A, Mohle-Steinlein U, Tian J, Karin M, Angel P, Wagner EF (1999) Control of cell cycle progression by c-Jun is p53 dependent. Genes Dev 13:607-619.

Scoles DR (2008) The merlin interacting proteins reveal multiple targets for NF2 therapy. Biochim Biophys Acta 1785:32-54.

Scoles DR, Baser ME, Pulst SM (1996) A missense mutation in the neurofibromatosis 2 gene occurs in patients with mild and severe phenotypes. Neurology 47:544-546.

Shaw RJ, Paez JG, Curto M, Yaktine A, Pruitt WM, Saotome I, O'Bryan JP, Gupta V, Ratner N, Der CJ, Jacks T, McClatchey AI (2001) The Nf2 tumor suppressor, merlin, functions in Rac-dependent signaling. Dev Cell 1:63-72.

Shen HM, Liu ZG (2006) JNK signaling pathway is a key modulator in cell death mediated by reactive oxygen and nitrogen species. Free Radic Biol Med 40:928-939.

Stemmer-Rachamimov AO, Xu L, Gonzalez-Agosti C, Burwick JA, Pinney D, Beauchamp R, Jacoby LB, Gusella JF, Ramesh V, Louis DN (1997) Universal absence of merlin, but not other ERM family members, in schwannomas. Am J Pathol 151:1649-1654.

Stickney JT, Bacon WC, Rojas M, Ratner N, Ip W (2004) Activation of the tumor suppressor merlin modulates its interaction with lipid rafts. Cancer Res 64:2717-2724.

Thaxton C, Lopera J, Bott M, Fernandez-Valle C (2007) Neuregulin and laminin stimulate phosphorylation of the NF2 tumor suppressor in Schwann cells by distinct protein kinase A and p21-activated kinase-dependent pathways. Oncogene.

Tikoo A, Varga M, Ramesh V, Gusella J, Maruta H (1994) An anti-Ras function of neurofibromatosis type 2 gene product (NF2/Merlin). J Biol Chem 269:23387-23390.

Tournier C, Hess P, Yang DD, Xu J, Turner TK, Nimnual A, Bar-Sagi D, Jones SN, Flavell RA, Davis RJ (2000) Requirement of JNK for stress-induced activation of the cytochrome c-mediated death pathway. Science 288:870-874.

Trofatter JA, MacCollin MM, Rutter JL, Murrell JR, Duyao MP, Parry DM, Eldridge R, Kley N, Menon AG, Pulaski K, et al. (1993) A novel moesin-, ezrin-, radixin-like gene is a candidate for the neurofibromatosis 2 tumor suppressor. Cell 72:791-800.

Tsuiki H, Tnani M, Okamoto I, Kenyon LC, Emlet DR, Holgado-Madruga M, Lanham IS, Joynes CJ, Vo KT, Wong AJ (2003) Constitutively active forms of c-Jun NH2-terminal kinase are expressed in primary glial tumors. Cancer Res 63:250-255.

Ventura JJ, Hubner A, Zhang C, Flavell RA, Shokat KM, Davis RJ (2006) Chemical genetic analysis of the time course of signal transduction by JNK. Mol Cell 21:701-710.

Welling DB (1998) Clinical manifestations of mutations in the neurofibromatosis type 2 gene in vestibular schwannomas (acoustic neuromas). Laryngoscope 108:178-189.

Weston CR, Davis RJ (2007) The JNK signal transduction pathway. Curr Opin Cell Biol 19:142-149.

Whitmarsh AJ (2006) The JIP family of MAPK scaffold proteins. Biochem Soc Trans 34:828-832.

Wickremesekera A, Hovens CM, Kaye AH (2007) Expression of ErbB-1 and 2 in vestibular schwannomas. J Clin Neurosci 14:1199-1206.

Yamauchi J, Miyamoto Y, Chan JR, Tanoue A (2008) ErbB2 directly activates the exchange factor Dock7 to promote Schwann cell migration. J Cell Biol 181:351-365.

Yi C, Wilker EW, Yaffe MB, Stemmer-Rachamimov A, Kissil JL (2008) Validation of the p21-activated kinases as targets for inhibition in neurofibromatosis type 2. Cancer Res 68:7932-7937.

Yuan L, Inoue S, Saito Y, Nakajima O (1993) An evaluation of the effects of cytokines on intracellular oxidative production in normal neutrophils by flow cytometry. Exp Cell Res 209:375-381.

Zelko IN, Mariani TJ, Folz RJ (2002) Superoxide dismutase multigene family: a comparison of the CuZn-SOD (SOD1), Mn-SOD (SOD2), and EC-SOD (SOD3) gene structures, evolution, and expression. Free Radic Biol Med 33:337-349.

Figure Legends

Figure 1. JNK is phosphorylated in VS tissue but not SCs from mature nerve. **A-C**. Epifluorescence images of VS (**A**) or vestibular nerve (VN, **B,C**) frozen sections immunostained with anti-pJNK (green) and anti-S100 (red) antibodies. pJNK immunoreactivity is detected in VS cells (**A**) and Scarpa's ganglion neurons (**C**), but not VN SCs (**B,C**). Scale bars=25 μm. **D**. Confocal image of normal VN frozen section in the region of Scarpa's ganglion immunostained with anti-neurofilament 200 (NF200, red) and anti-pJNK (green) antibodies demonstrating punctate pJNK immunoreactivity in the neurons, but not SCs, of the VN. Scale bars=25 μm. **E**. Representative western blots of VS or great auricular nerve (GAN) lysates probed with antibodies against pJNK, JNK1/2, or Rho-GDI. **F** and **G**. Mean relative expression levels of JNK1/2 and pJNK from 4 VS and 4 GAN specimens. Error bars present standard error of the mean (SEM). * $p<0.05$ by Student's two-tailed t-test.

Figure 2. siRNA mediated knock down of merlin expression in normal human Schwann cells results in increased JNK phosphorylation. Western blot of human Schwann cell lysates (20 μg) over a time course (days) following merlin knockdown using merlin-targeted siRNA. As merlin is depleted, JNK phosphorylation (pJNK) increases in a time-dependent manner, while total JNK levels remain constant. Western blot for actin is shown as a loading control (bottom panel) and SKBR3 lysate (10 μg) was used as a positive control (far right lane).

Figure 3. ERKs, Akt, and JNK are persistently phosphorylated in human VS cells. **A-C**. Western blots of VS cell lysates from cultures maintained in serum free, basal medium treated with the

MEK inhibitor, U0126 (10 μM); the PI3-K inhibitor, LY294002 (20 μM); and/or the ErbB2

inhibitor PD158780 (100 nM) as indicated and probed with the indicated antibodies. **D**.

Immunostaining of cultured VS cells with anti-pJNK (red, upper and lower panel) and anti-S100

(green, lower panel). Scale bar=50 μm.

Figure 4. MEK/ERK and PI3-K/Akt activity contributes to VS cell proliferation. Primary VS

cultures were maintained in the presence of the MEK inhibitors, U1026 or PD98059, or the PI3-

K inhibitor, LY294002 for 24 h. **A, B**. Cell proliferation was determined by scoring the percent

of BrdU-positive, S100-positive VS cells from 10 randomly selected fields and is expressed as a

percent relative to control cultures, defined as 100%. **C, D**. Apoptosis was scored as the percent

of TUNEL-positive, S100-positive VS cells with condensed nuclei. Each condition was

performed on at least 4 cultures derived from separate tumors. Error bars present SEM. * $p<0.05$

by one way ANOVA with post-hoc Tukey analysis.

Figure 5. JNK activity promotes VS cell proliferation and survival. Primary VS cultures were

cultured in the presence or absence of JNK inhibitors (I-JIP or SP600125). **A**. Representative

cultures immunolabeled with anti-BrdU (red) and anti-S100 (green) antibodies. Nuclei were

identified with Hoescht 3342 (blue). Arrows indicate BrdU-positive nuclei determined by

overlap of red and blue channels. Scale bar=100 μm. **B, C**. Quantification of VS cell

proliferation apoptosis determined as in Fig. 3. **D**. VS cell survival determined by counting the

number of S100-positive cells remaining after 5 days in the absence or presence of JNK

inhibitors. Each condition was performed on at least 3 cultures derived from separate tumors.

Error bars present SEM. * $p<0.05$ by one way ANOVA with post-hoc Tukey analysis. **E**. VS

cultures treated with SP600125 or I-JIP and labeled with TUNEL (red), anti-cleaved caspase 3 antibody (green), and Hoechst (blue) demonstrating activation of caspase 3 in TUNEL-positive cells. Scale bar=20 μm.

Figure 6. VS cell apoptosis due to inhibition of JNK correlates with loss of c-JUN phosphorylation (pJUN). **A**. VS cultures were treated with JNK inhibitors (I-JIP, 100 μM or SP600125, 20 μM) for 24 h, fixed, immunostained with anti-pJUN (Alexa 488 secondary antibody, psuedocolored green, right panels) and S100 antibodies (Alexa 647 secondary antibody, psuedocolored green, left panels). Apoptotic cells were detected by TUNEL (red) and nuclei were labeled with Hoechst (blue). Scale bar=100 μm. **B**. The percent of pJUN-negative and TUNEL-positive, pJUN-negative and TUNEL-negative, and pJUN-positive and TUNEL-negative cells were scored. Cells were considered pJUN-positive if the nuclear:cytoplasmic ratio of pJUN immunofluorescence intensity exceeded 5. No cells were simultaneously pJUN-positive and TUNEL-positive in any condition. At least 300 cells were scored per condition and the results were repeated in cultures from 3 separate tumors. JNK inhibitors decreased the percent of pJUN-positive cells and increased the percent of TUNEL-positive cells.

Figure 7. Inhibition of JNK increases VS cell oxidative stress leading to cell death. **A**. Oxidative status of VS cells in the presence or absence of SP600125, I-JIP, or ebselen was determined by measuring the DCF fluorescence intensity in cultures loaded with CM-H_2DCFDA. Thirty to fifty cells were imaged per condition. Results are representative of 4 cultures derived from separate tumors. Error bars present SEM. * $p<0.05$ by one way ANOVA with post-hoc Tukey analysis. **B**. Representative images of DCF fluorescence in the indicated conditions. Scale bar=100 μm. **C**.

VS cultures were treated with SP600125 or I-JIP in the presence or absence of ebselen (Eb, 20 μM) and the percent of TUNEL-positive cells was determined as before. * $p<0.05$ by one way ANOVA with post-hoc Tukey analysis.
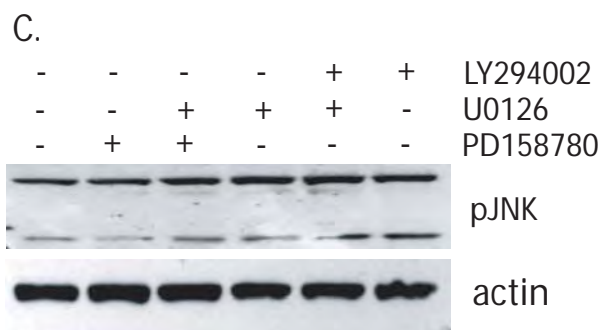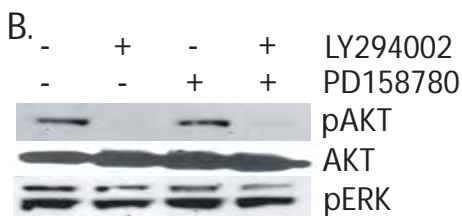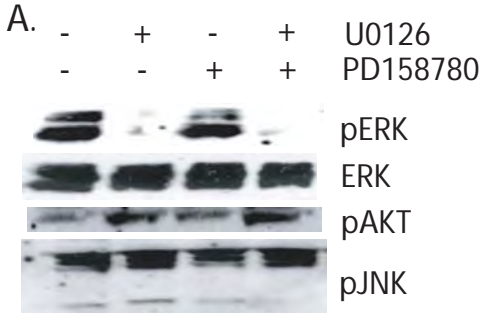
Figure 8. Inhibition of JNK increases VS cell mitochondrial superoxide accumulation leading to cell death. **A, B.** Mitochondrial superoxide accumulation was determined by measuring MitoSOX™ Red fluorescent intensity in VS cultures treated with SP600125 (20 μM) or I-JIP (100 μM). **A**. MitoSOX™ Red fluorescence is presented as a scaled image with intensity levels as indicated. Scale bar=25 μm. **B**. Mean MitoSOX™ Red fluorescence in indicated conditions. Thirty to fifty cells were imaged per condition. The results are representative of 3 cultures derived from separate tumors. Error bars present SEM. * $p<0.05$ by one way ANOVA with post-hoc Tukey analysis. **C**. VS cultures maintained in the presence or absence of JNK inhibitors were transduced with adenoviral vector expressing SOD2 (AdSOD2) or control vector (AdCon) and the percent of TUNEL-positive cells were scored as above. The results are from 4 cultures derived from separate tumors. Error bars represent SEM. * $p<0.05$ by one way ANOVA with post-hoc Tukey analysis. D. Representative images of VS cultures treated with I-JIP and either AdCon (left panel) or AdSOD2 (right panel). Cultures were immunostained with anti-S100 (green) antibody and labeled with TUNEL (red) and Hoechst (blue). Scale bar=100 μm.
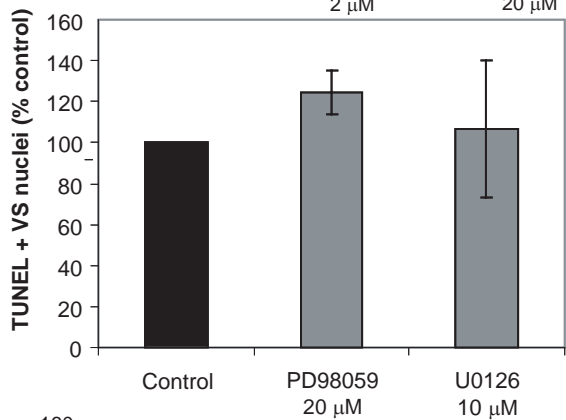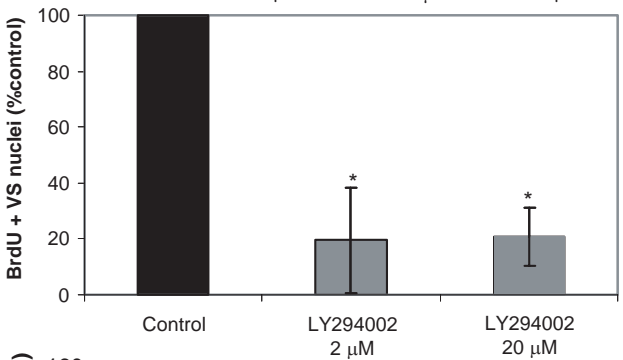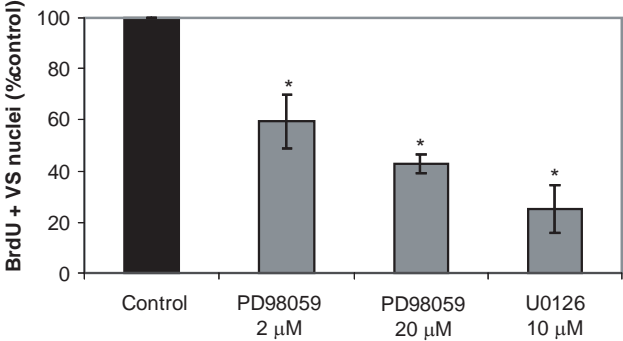
Supplemental Figure 1. PD158780 inhibits ErbB2 phosphorylation in rat Schwann cells (SCs). Protein lysates from neonatal rat sciatic nerve SCs, cultured as previously described (Hansen et al., 2001; Provenzano et al., 2008) and treated with neuregulin β1 (NRGβ1, 3 nM) in the

presence or absence of PD158780 (100 nM), were immunoblotted with anti-phosphorylated

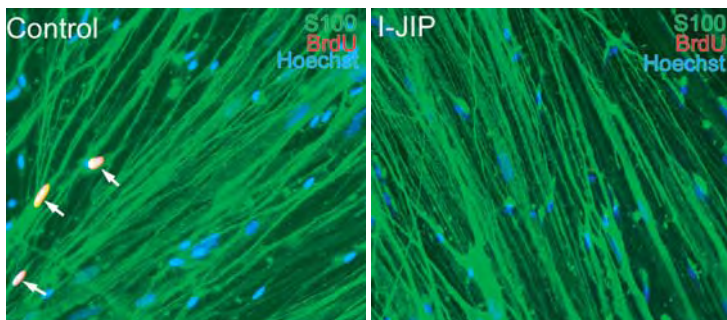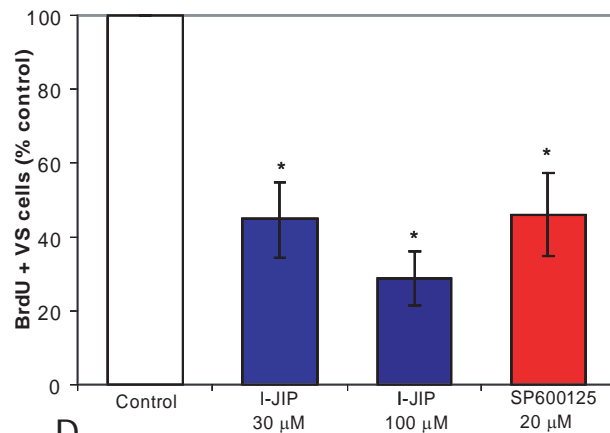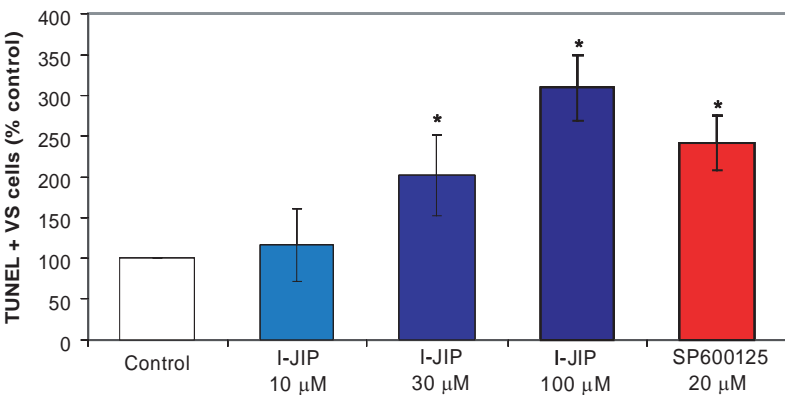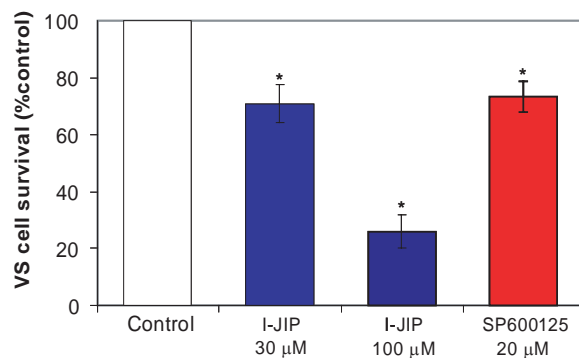ErbB2 antibody followed by non-phosphospecific anti-ErbB2 antibody.

A. pJNK S100 Hoechst VS

B. pJNK S100 Hoechst VN

C. pJNK S100 Hoechst VN

D. pJNK NF200 VN

E. VS GAN — JNK2, pJNK2, JNK1, pJNK1, RhoGDI

F. Relative JNK levels

G. Relative phosphorylated JNK levels

58

Day 1 2 3 4 5 6 7 SKBR3

A.

| - | + | - | + | U0126 |
| - | - | + | + | PD158780 |

pERK

ERK

pAKT

pJNK

B.

| - | + | - | + | LY294002 |
| - | - | + | + | PD158780 |

pAKT

AKT

pERK

C.

-	-	-	-	+	+	LY294002
-	-	+	+	+	-	U0126
-	+	+	-	-	-	PD158780

pJNK

actin

D.

pJNK

pJNK
S100
Hoechst

60

50 μm

61

A.

B.

C.

D.

E.

62

A.

Control	S100 TUNEL Hoechst	Control	pJUN TUNEL
I-JIP	S100 TUNEL Hoechst	I-JIP	pJUN TUNEL

100 μM

B.

percent VS cell nuclei

- pJun-/TUNEL+
- pJun-/TUNEL-
- pJun+/TUNEL-

Control   SP600125   I-IJP
           20 μM   100 μM

63

A.

B.

C.

A. Control | I-JIP | SP600125

0 — 255

B.

relative MitoSOX intensity

Control | SP600125 20 μM | I-JIP 100 μM

C.

TUNEL + VS cells (% control)

control | SP 20 μM | I-JIP 100 μM | control | SP 20 μM | I-JIP 100 μM

AdCon | AdSOD2

D.

S100 TUNEL Hoechst | SP600125 Ad.Con

S100 TUNEL Hoechst | SP600125 Ad.SOD2

65

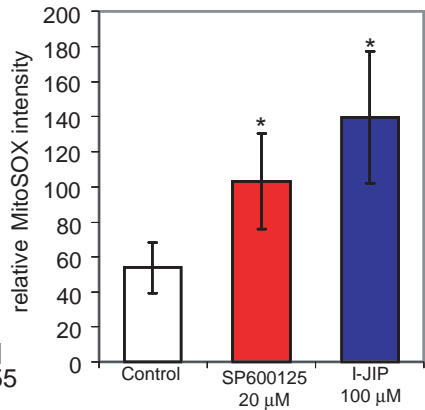100 μM

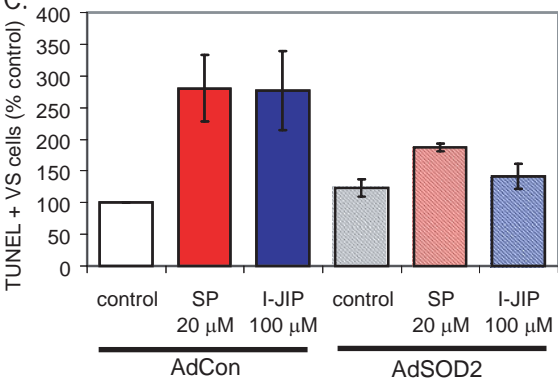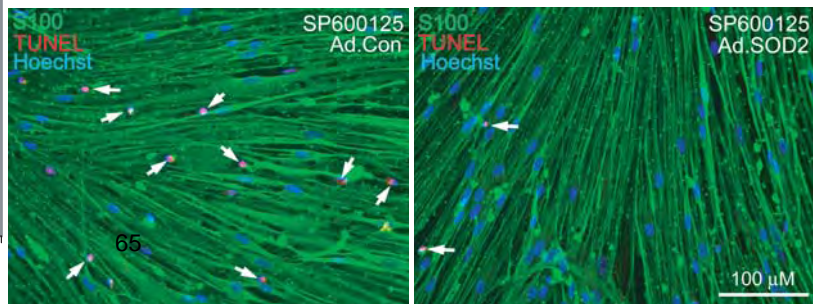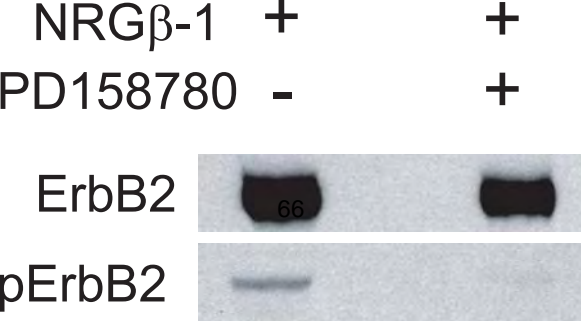| NRGβ-1 | + | | + |
| PD158780 | - | | + |

ErbB2   66

pErbB2

MicroRNA-21 Over-Expression Contributes to Vestibular Schwannoma Cell Proliferation and Survival.

Joseph A. Cioffi[1], Wei Ying Yue[3], Sabrina Mendolia-Loffredo[1], Kameron R. Hansen[3], P. Ashley Wackym[1,2], and Marlan R. Hansen[3]

[1]Department of Otolaryngology and Communication Sciences; and [2]Department of Physiology, Medical College of Wisconsin, Milwaukee, WI 53226, USA, [3]Department of Otolaryngology - Head and Neck Surgery, University of Iowa College of Medicine, Iowa City, IA, USA

Correspondence:
Joseph A. Cioffi, Ph.D.
Department of Otolaryngology and Communication Sciences
Medical College of Wisconsin
9200 W. Wisconsin Avenue
Milwaukee, WI 53226

414-805-3012 (office)
414-805-2888 (fax)
joeciof@aol.com

Abstract:

Vestibular schwannomas (VSs) are benign tumors that arise from the vestibular nerve. Left untreated, VSs can become life threatening. Despite efforts to characterize the VS transcriptome, the molecular pathways that lead to tumorigenesis are not completely understood. MicroRNAs are small RNA molecules that regulate gene expression post-transcriptionally by blocking the production of specific target proteins. We examined microRNA expression in VSs and found consistent over-expression of microRNA-21 (miR-21) when compared to normal vestibular nerve tissue. Furthermore, elevated levels of miR-21 correlated with decreased levels of PTEN; a known molecular target of miR-21. To determine the functional significance of miR-21 expression in VS cells, we transfected primary human VS cultures with anti-miR-21 or control, scrambled oligonucleotides. Anti-miR-21 decreased VS cell proliferation in response to platelet derived growth factor stimulation and increased apoptosis suggesting that increased miR-21 levels contributes to VS growth. Since PTEN regulates signaling through the growth-promoting PI3K/AKT pathway, our findings suggest that miR-21 may be a suitable molecular target for therapies aimed specifically at reducing VS growth.

Introduction

Vestibular schwannomas (VSs) are benign Schwann cell-derived tumors associated with the vestibular nerve and are a hallmark of the autosomal dominant genetic disorder neurofibromatosis type 2 (NF2). NF2 has been linked to mutations in the gene which encodes the tumor suppressor protein "merlin" (aka schwannomin) (1,2). Although the exact mechanisms whereby merlin prevents tumor formation are not completely understood, recent efforts to define the associated genes and molecular pathways involved in tumorigenesis and expansion have met with some success (3). VSs frequently go undiagnosed until clinical symptoms develop such as hearing loss, tinnitus, and balance impairment as the tumors grow larger. Left untreated, vestibular schwannomas can become life threatening. At present, the most common methods of treatment are observation with serial imaging studies, microsurgical removal and stereotactic radiosurgery.

MicroRNAs are evolutionarily conserved, small (~22 nt), non-coding RNA molecules that regulate gene expression post-transcriptionally. Mature microRNAs bind to specific mRNA targets in regions that are significantly complementary to the microRNA and, by a mechanism that is not completely understood, results in translational repression or mRNA degradation (4,5). The human genome encodes more than 1000 microRNAs with tissue- and cell-type specific expression (6). MicroRNAs have been shown to play important roles in such diverse cellular processes as differentiation, development, metabolism, apoptosis and cancer (7). Studies have shown that tumors generally exhibit aberrant microRNA expression profiles, and identified multiple microRNAs with reputed tumor suppressor or oncogenic properties (8-10).

In preliminary studies investigating microRNA expression profiles in four human VSs using a microarray platform, we found that hsa-miR-21 (herein referred to as miR-21) was consistently over-expressed when compared to normal vestibular nerve. Over-expression of miR-21 has been observed in many cancers including breast, liver, and glioblastoma (11-13). PTEN (phosphatase and tensin homolog) tumor suppressor gene has been identified as a target of miR-21 (12). PTEN acts as a tumor suppressor via its inhibitory effect on the PI3K/AKT pathway, which promotes cell survival, cell proliferation, and tumor formation (14). The PI3K/AKT pathway has recently been shown to be active in VSs (15). Therefore, elevated levels of miR-21 in VS may contribute to tumor growth by down-regulating PTEN and consequent hyperactivation of AKT signaling.

The microRNA-21 gene has an upstream enhancer region containing two strictly conserved STAT3 (signal transducer and activator of transcription 3) binding sites and activation of STAT3 has been shown to induce the expression of miR-21 (16). STAT3 is a critical regulator of gene expression in response to many growth factors and cytokines (17). For example, the neuropoietic cytokines ciliary neurotrophic factor (CNTF), leukemia inhibitory factor (LIF) and interleukin 6 (IL-6) bind to specific ligand-binding receptor subunits and share the signal transduction subunit gp130 which signals through the JAK/STAT pathway (18). Interestingly, merlin has been shown to play a role in suppressing STAT3 activation through its interaction with hepatocyte growth factor-regulated tyrosine kinase substrate (HRS) in a human schwannoma cell line (19).

Furthermore, these authors showed that a naturally occurring *NF2* missense mutation interferes with hepatocyte growth factor-regulated tyrosine kinase substrate (HRS) binding and abolishes the ability of merlin to inhibit STAT activation. This raises the possibility that over-expression of miR-21 in VSs may be a consequence of deregulated activation of STAT3 by an autocrine mechanism involving neuropoietic cytokines or other growth factors.

In the present study, we sought to confirm our earlier microarray results showing over-expression of miR-21 in the four original VSs using quantitative real-time polymerase chain reaction assays, measure the expression of PTEN mRNA and protein levels, and determine whether CNTF, LIF, IL-6, the receptor subunits CNTFRα, LIFR, IL-6Rα and gp130, and STAT3 are expressed in these tumors. We also examined miR-21 expression levels in four additional VSs, greater auricular and normal vestibular nerve samples to strengthen our statistical analyses. Finally, we show that transfection human VS cultures with anti-miR-21 oligonucleotides reduces their proliferative potential and promotes apoptosis suggesting that over-expression of miR-21 contributes to VS growth.

Materials and Methods

Procurement of Vestibular Schwannoma Specimens: The human subject protocol for tissue procurement was approved by the Institutional Review Board of the Medical College of Wisconsin and informed consent was obtained from all participating patients.

Quantitative Real-Time RT/PCR: Real-Time RT/PCR was used to confirm previous microarray data showing elevated expression of hsa-miR-21 in VSs. Real-Time RT/PCR reagents for RNU6B (control) and hsa-miR-21 were purchased from Applied Biosystems (Foster City, CA) and the reactions were performed as recommended by the manufacturer. Briefly, RT reactions containing total RNA, stem-looped primers, 1X RT buffer, reverse transcriptase, and RNase inhibitor were incubated for 30 min. each, at 16°C and at 42°C. Stem-looped primers were annealed to miRNA targets and extended by reverse-transcriptase. Reactions containing miRNA-specific forward primer, TaqMan® probe and reverse primers were loaded into a PCR reaction plate in quadruplicate and incubated in a thermocycler (BIO-RAD iCycler iQ) for 10 min. at

95°C followed by 40 cycles of denaturing (15 sec. at 95°C), annealing and extension (60 sec. at 60°C). Experiments were set up in quadruplicate and repeated three times. Mean threshold cycles (C_T) were calculated by averaging the technical replicates for each experiment and then by averaging the mean replicate C_T across the three runs. Quadruplicates with a standard deviation greater than 0.50 were eliminated and these assays repeated. The miR-21 expression was normalized to RNU6B (ΔC_T) for each tissue. Relative expression and fold differences were determined by comparing normalized expression levels between tissues ($\Delta\Delta C_T$) using the $2^{-\Delta\Delta C_T}$ method (20). Statistical significance was determined using the Student's t-test assuming unequal variance.

Reverse Transcriptase/PCR: RT/PCR was used to detect transcripts for PTEN, STAT3, the neuropoietic cytokines LIF, CNTF, and IL-6, and their receptor signaling subunits LIFR, IL-6Rα, CNTFRα, and gp130. NCBI mRNA sequences were obtained from the GenBank database and primer sets were designed using Primer3 software (http://frodo.wi.mit.edu/cgi-bin/primer3/primer3_www.cgi). Gene-specific primer sets and the expected amplicon sizes are listed in Table 1. Approximately 0.5–1µg aliquots of total RNA were used to generate cDNA for these experiments. Total RNA extracted from the tumors using TRIzol Reagent (Invitrogen, Carlsbad, CA) was treated with 1µl RNase-Free DNase I (Promega, Madison, WI) in 1µl RNase-Free DNase 10X Reaction Buffer (Promega, Madison, WI) and incubated for 10 min at 37°C. DNase I was inactivated by adding 1 µl of DNase Stop Solution (Promega, Madison, WI) followed by heating for 10 min at 65°C. RNA was then reverse transcribed using random hexamer primers and the Superscript III kit (Invitrogen, Carlsbad, CA) according to the manufacturer's instructions. Reactions in which reverse transcriptase was omitted served as a negative control for PCR amplification. Amplicons were resolved by agarose gel electrophoresis and visualized using GelStar nucleic acid stain (Lonza, Rockland, ME). Restriction enzyme mapping was used to confirm the authenticity of each amplicon (data not shown).

Sodium Dodecyl Sulfate-Polyacrylamide Gel Electrophoresis and Western Blot

Analysis: Tissue samples were homogenized and lysed using the TRIzol procedure for protein extraction (Invitrogen, Carlsbad, CA). Approximately twenty micrograms of total protein was resolved on a 12% sodium dodecyl sulfate polyacrylamide gel by electrophoresis, transferred to a nitrocellulose membrane (Amersham International, Little Chalfont, UK), and probed for PTEN using 2µg/ml polyclonal rabbit anti-human PTEN (ab23694) (Abcam Inc., Cambridge, MA). All Western blots were stripped using Re-Blot Plus strong antibody stripping solution (Chemicon International, Temecula, CA) and nonspecific sites were blocked using nonfat milk. Blots were then reprobed for beta actin using the monoclonal anti-actin antibody diluted 1:10,000 (CP01) (Calbiochem, San Diego, CA) to ensure equal loading of total protein in all lanes. All antibodies were diluted in phosphate-buffered saline containing 1% (vol/vol) Tween-20. The signal was detected by chemiluminescence using ECL western blotting detection reagents (Amersham International, Little Chalfont, UK).

Primary VS cell cultures: Primary VS cultures were prepared as previously described (21,22). Briefly, acutely resected tumors were cut into 1 mm^3 fragments, digested with collagenase (2 mg/ml, Sigma, St. Louis, MO) and 0.25% trypsin (Sigma) for 45–60 min at 37C, and then put in 10% fetal bovine serum (FBS). Following centrifugation at 800 rpm for 3 min, the cells were resuspended and dissociated by trituration through narrow pipettes. Cell suspensions were plated in 4-well culture slides (Nalge Nunc International, Rochester, NY) pretreated with polyornithine, followed by laminin (20 µg/ml). Cultures were maintained in Dulbecco's modified Eagle's medium (DMEM) with N2 supplements (Sigma), bovine insulin (Sigma, 1 mg/ml) and 10% FBS. The medium was exchanged 2 to 3 days later and when the cells reached 50–70% confluence, they were subsequently maintained in serum-free conditions until used for experiments, typically after 7-10 days. Over 90% of the cells in the cultures were S100-positive. Cultures were maintained in a humidified incubator with 6.0% CO_2 at 37C.

miR-21 knock down: Anti-miR-21 miRCURY LNA™ knockdown probe and control, scrambled miR probe were designed and synthesized by Exiqon (Vedbaek, Denmark).

The miR-21 probe sequence (Exiqon 138102-04) was:

TCAACATCAGTCTGATAAGCTA. The corresponding micro RNA targeting sequence

was: UAGCUUAUCAGACUGAUGUUGA. The scrambled miR probe sequence

(Exiqon 199002-04) was: GTGTAACACGTCTATACGCCCA. When the VS cultures

reached 60-80% confluency, they were maintained in medium without antibiotics for 24

h. Subsequently, the cultures were transfected using Lipofectamine™ RNAiMAX

Transfection Reagent (Invitrogen, Carlsbad, CA) according to the manufacturer's

protocol. Briefly, anti-miR-21 and scrambled probes (2.5 mM) were diluted in Opti-

MEM medium (Opti-MEM, Invitrogen) at 1:50 and mixed with equal volume of

RNAiMAX pre-diluted at 1:50 in Opti-MEM. After 20 min incubation at room

temperature, the complexes were added to the cultures for 12-20 h prior to media

exchange. Preliminary studies using Cy-3-labeled oligonucleotides confirmed that over

90% of VS cells are transfected by RNAiMAX. Both the anti-miR-21 probe and

scrambled probes were 5`-fluorescein labeled and only cultures demonstrating over 85%

of transfected cells were analyzed. Following transfection, cultures were maintained in

serum-free conditions until fixation. PDGF-BB (20 ng/ml) was added to the indicated

cultures 24 h prior to fixation.

Immunostaining: The cultures were fixed with 4% paraformaldehyde, washed with

phosphate-buffered saline (PBS), permeabilized with PBS with 0.1% Triton X-100 for 10

min, blocked with blocking buffer (5% goat serum, 2% bovine serum albumin [BSA],

0.1% Triton- X in PBS) for 30–60 min, and then incubated with anti-BrdU (1:800; clone

G3G4, Hybridoma core, University of Iowa, Iowa City, IA) and anti-S100 (1:400, Sigma

S-2644) antibodies diluted in blocking buffer overnight at 4°C: Following washing,

Alexa 546 and Alexa 647 labeled secondary antibodies (1:800; Invitrogen, Carlsbad, CA)

were incubated at 37C for 1 h. Nuclei were labeled with Hoechst 33342 (10 µg/ml,

Sigma) for 15 min.

Fluorescence images were captured using an inverted Leica DMRIII microscope

(Leica, Bannockburn, IL) equipped with epifluorescence filters and a charge coupled

device camera using Leica FW4000 software and prepared for publication using Adobe

Photoshop (Adobe, San Jose, CA).

VS cell proliferation and apoptosis: VS cultures were labeled with 5-bromo-2-deoxyuridine (BrdU 10 μM, Sigma) for 24 h prior to fixation. Fixed cultures were treated with 2N HCl for 15 min. prior to immunostaining and BrdU uptake was detected by immunostaining as above. The percent of BrdU positive VS cells (S100-positive) nuclei was determined by counting 10 randomly selected fields for each condition. Only S100-positive cells were scored. Apoptotic cells were detected by terminal deoxynucleotidyl transferase dUTP nick end labeling (TUNEL) using the In Situ Cell Death Detection Kit, TMR red kit (Roche Diagnostics) according to the manufacturer's instructions. The percent of apoptotic VS cell (S100-positive) nuclei was determined by counting 10 randomly selected fields for each condition. Criteria for scoring were a TUNEL-positive nucleus with typical condensed morphology in an S100-positive cell. Each condition was repeated on 4 VS cultures derived from separate tumors.

Results

We used quantitative real-time RT/PCR to compare miR-21 expression in a total of eight VSs and fourteen normal nerve specimens (Fig. 1). MiR-21 was consistently over-expressed in all VSs when compared to the mean level of expression in control normal nerve tissues (Fig. 1). Since the level of miR-21 expression in greater auricular nerve was not statistically different from that in normal vestibular nerve, we combined these negative controls for statistical purposes. On average, VSs exhibited ~6.5 fold higher level of expression of miR-21 as compared to the normal nerve control group and this difference was statistically significant ($p < 0.01$) (Fig. 1). These results confirm our previous observations using microRNA microarray profiling which showed elevated expression of miR-21 in the four original tumors (VS1 to VS4) as compared to normal vestibular nerve.

Since miR-21 targets and inhibits tumor suppressor PTEN expression in other cancers, we examined PTEN expression using RT/PCR to detect mRNA and western blots to assess PTEN protein. Although PTEN mRNA was easily detectable by RT/PCR in all four vestibular schwannomas (Fig. 2A), western blot analysis showed that PTEN protein was barely detectable in three out of the four tumors (Fig. 2B). VS4 showed

much higher levels of PTEN protein compared to VS1, VS2, and VS3. Interestingly, VS4 also had the lowest level of miR-21 expression compared to the other three tumors. Rat brain extract served as a positive control for PTEN expression. Beta-actin was used as a sample loading control. Thus, elevated miR-21 expression correlates with decreased levels of PTEN protein, but not mRNA, levels in vestibular schwannomas consistent with the observation that miR-21 reduces PTEN protein expression in tumor cells (12).

The gene encoding miR-21 is predicted to contain STAT3 binding sites and activation of STAT3 has been shown to induce the expression of miR-21 (16). Therefore, we examined the expression of STAT3, and the neuropoietic cytokines and their receptor subunits known to activate STAT3: CNTF, IL-6, LIF, IL6Rα, LIFR, CNTFRα, and gp130 in VS1 to VS4 and normal vestibular nerve. As summarized in Table 2, all of the above genes were found to be expressed in each of the four tumors analyzed. However, we were unable to detect the expression of IL-6, IL-6Rα, LIF and LIFR using pooled total RNA isolated from 3 different normal vestibular nerve samples.

The activated form of STAT3 is phosphorylated (PSTAT3). Therefore, we examined STAT3 by Western blot in VS2 using an antibody that recognizes STAT3 protein regardless of activation state and one that specifically detects activated PSTAT3 (Fig. 3). Activated PSTAT3 can be detected and this correlates with elevated miR-21 expression in this tumor.

To determine the functional significance of miR-21 over-expression in VS cells, we sought to inhibit miR-21 function by transfecting primary cultures derived from acutely resected human VSs cells with anti-miR-21 oligonucleotide probes. We verified the ability to transfect primary VS cultures with oligonucleotides by transfecting cultures with Cy-3 tagged probes. Over 90% of primary VS cells were transfected with the tagged oligonucleotides (Fig. 4).

Transfection of anti-miR-21 significantly reduced the percent of BrdU-positive VS cells in cultures stimulated with PDGF-BB, a VS cell mitogen (23,24), more than 2-fold, but did not decrease proliferation in cultures maintained in basal medium (Fig. 5). Thus, miR-21 contributes to the proliferative potential of primary VS cells. Anti-miR-21 increased the percent of TUNEL-positive, apoptotic VS cells maintained in basal medium by more than 3 fold (Fig. 6), indicating that miR-21 supports VS cell survival. These

observations raise the possibility that over-expression of miR-21 contributes to the VS growth.

Discussion

Using quantitative real-time RT/PCR, we confirmed our previous microarray findings that showed that miR-21 is over-expressed in VSs. Consistent with our results, MicroRNA-21 has been shown to be over-expressed in a variety of solid tumors (25). In addition, important links between miR-21 expression and cancer-related cellular processes such as proliferation, migration, apoptosis and tumor growth have been demonstrated in human breast and hepatocellular cancer cells (12,13). Inhibition of miR-21 in hepatocellular carcinoma cell lines increased expression of tumor suppressor PTEN, and decreased cellular proliferation, migration and invasion; while enhancing miR-21 expression had the opposite effects (12). Despite demonstrating the presence of PTEN mRNA in all four VSs, we observed very low PTEN protein levels in three of the four tumors tested. This may be due to translational suppression by miR-21. VS4 was an exception in that it displayed the highest level of PTEN protein; however, this tumor also exhibited the lowest relative level of miR-21 expression. Alternatively, PTEN mRNA in VS4 may be missing the miR-21 binding site in the 3' untranslated region due to either gene mutations or alternative splicing and thereby escape post-transcriptional regulation. Since PTEN is a strong negative regulator of the AKT pathway, decreased expression of PTEN would enhance signaling through this pathway leading to increased cellular proliferation, decreased apoptosis, or both. Interestingly, the PI3 kinase/AKT pathway has recently been shown to be activated in human VSs (15).

STAT3 is a critical regulator of gene expression in response to many growth factors and cytokines (17). The neuropoietic cytokines IL-6, CNTF, and LIF use the common signal transducing gp130 subunit to mediate STAT1/3 signaling and play important roles in nerve regeneration and repair (18,26). IL-6 has been shown to mediate the activation of STAT3 in adult Schwann cells and rat schwannoma cells (27). Furthermore, activation of STAT3 by IL-6 induces mIR-21 expression in multiple myeloma cells (16). We postulated that VSs may be secreting neuropoietic cytokines and stimulating their own growth through an autocrine pathway mediated, in part, by the

overexpression of miR-21. The detection of mRNAs encoding these cytokines and their receptor subunits in VS supports this possibility. That we were unable to detect the expression of IL-6, IL-6Rα, LIF and LIFR in normal vestibular nerve may reflect the absence or low abundance of these mRNAs in this quiescent, non-proliferative control tissue. Membrane tyrosine kinase receptors such as the platelet derived growth factor receptor (PDGFR), epidermal growth factor receptor (EGFR), and erbB receptors have also been implicated in the activation of STATS (17,28). The EGFR and neuregulin-1/erbB signaling pathways contribute to cell proliferation in NF2-deficient cells and VS primary cultures, respectively (22,29). However, it is not clear to what extent STAT3 activation and miR-21 overexpression mediate this effect. A recently published case study demonstrating some effectiveness of the EGFR inhibitor erlotinib on VS progression in an NF2 patient suggests that targeted therapies for NF2-related tumors hold promise (30).

Recent studies shed additional light on the role of miR-21 in cancer-related processes. MCF-7 breast cancer cells transfected with anti-miR-21 oligonucleotides resulted in increased apoptosis and inhibition of cell growth *in vitro* and tumor growth in a xenograft mouse model (13). Using similar *in vitro* approaches, we found that miR-21 contributes to the proliferative potential and survival of VS cells, confirming the functional significance of miR-21 over-expression in these cells. The tumor suppressor PDCD4 (programmed cell death 4) is an important functional target of miR-21 and the down-regulation of PDCD4 by miR-21 in colorectal cancer stimulated invasion, extravasation, and metastasis (31,32). It would be interesting to know whether PDCD4 is a target of miR-21 in VSs. In addition to supporting VS cell proliferation and survival, there is some evidence suggesting that miR-21 may also contribute to the cystic phenotype that is occasionally observed in more aggressive tumors. MiR-21 increases matrix metalloprotease-2 (MMP-2) expression in cardiac fibroblasts via the PTEN pathway and MMP-2 has been implicated in cyst development in VSs (33,34).

It is clear that miR-21 plays a significant role in the regulation of multiple pathways controlling cell proliferation in many cancers and this attribute makes it a very attractive target for the development of new therapies. Future experiments aimed at manipulating miR-21 expression in xenograft or genetic animal schwannoma models will

allow us to test the relative importance of miR-21 on VS growth *in vivo*. Furthermore, the application of proteomics strategies in these cells should help identify new molecular targets of miR-21 as has been demonstrated in the MCF-7 breast cancer cell line (20,35). These experiments may shed new light on the molecular pathways controlling tumor growth and help identify novel therapeutic targets for the treatment of NF2.

References

1.	Rouleau GA, Merel P, Lutchman M, et al. Alteration in a new gene encoding a putative membrane-organizing protein causes neuro-fibromatosis type 2. *Nature* 1993;363:515-21.

2.	Trofatter JA, MacCollin MM, Rutter JL, et al. A novel moesin-, ezrin-, radixin-like gene is a candidate for the neurofibromatosis 2 tumor suppressor. *Cell* 1993;72:791-800.

3.	Welling DB, Packer MD, Chang LS. Molecular studies of vestibular schwannomas: a review. *Curr Opin Otolaryngol Head Neck Surg* 2007;15:341-6.

4.	Ambros V. The functions of animal microRNAs. *Nature* 2004;431:350-5.

5.	Bartel DP. MicroRNAs: genomics, biogenesis, mechanism, and function. *Cell* 2004;116:281-97.

6.	Landgraf P, Rusu M, Sheridan R, et al. A mammalian microRNA expression atlas based on small RNA library sequencing. *Cell* 2007;129:1401-14.

7.	Hwang HW, Mendell JT. MicroRNAs in cell proliferation, cell death, and tumorigenesis. *Br J Cancer* 2006;94:776-80.

8.	Calin GA, Croce CM. MicroRNA signatures in human cancers. *Nat Rev Cancer* 2006;6:857-66.

9.	Hammond SM. MicroRNAs as oncogenes. *Curr Opin Genet Dev* 2006;16:4-9.

10.	Lu J, Getz G, Miska EA, et al. MicroRNA expression profiles classify human cancers. *Nature* 2005;435:834-8.

11.	Chan JA, Krichevsky AM, Kosik KS. MicroRNA-21 is an antiapoptotic factor in human glioblastoma cells. *Cancer Res* 2005;65:6029-33.

12.	Meng F, Henson R, Wehbe-Janek H, et al. MicroRNA-21 regulates expression of the PTEN tumor suppressor gene in human hepatocellular cancer. *Gastroenterology* 2007;133:647-58.

13.	Si ML, Zhu S, Wu H, et al. miR-21-mediated tumor growth. *Oncogene* 2007;26:2799-803.

14.	Di Cristofano A, Pandolfi PP. The multiple roles of PTEN in tumor suppression. *Cell* 2000;100:387-90.

15.	Jacob A, Lee TX, Neff BA, et al. Phosphatidylinositol 3-kinase/AKT pathway activation in human vestibular schwannoma. *Otol Neurotol* 2008;29:58-68.

16. Loffler D, Brocke-Heidrich K, Pfeifer G, et al. Interleukin-6 dependent survival of multiple myeloma cells involves the Stat3-mediated induction of microRNA-21 through a highly conserved enhancer. *Blood* 2007;110:1330-3.

17. Leaman DW, Leung S, Li X, et al. Regulation of STAT-dependent pathways by growth factors and cytokines. *Faseb J* 1996;10:1578-88.

18. Ernst M, Jenkins BJ. Acquiring signalling specificity from the cytokine receptor gp130. *Trends Genet* 2004;20:23-32.

19. Scoles DR, Nguyen VD, Qin Y, et al. Neurofibromatosis 2 (NF2) tumor suppressor schwannomin and its interacting protein HRS regulate STAT signaling. *Hum Mol Genet* 2002;11:3179-89.

20. Livak KJ, Schmittgen TD. Analysis of relative gene expression data using real-time quantitative PCR and the 2(-Delta Delta C(T)) Method. *Methods* 2001;25:402-8.

21. Hansen MR, Clark JJ, Gantz BJ, et al. Effects of ErbB2 signaling on the response of vestibular schwannoma cells to gamma-irradiation. *Laryngoscope* 2008;118:1023-30.

22. Hansen MR, Roehm PC, Chatterjee P, et al. Constitutive neuregulin-1/ErbB signaling contributes to human vestibular schwannoma proliferation. *Glia* 2006;53:593-600.

23. Ammoun S, Flaiz C, Ristic N, et al. Dissecting and targeting the growth factor-dependent and growth factor-independent extracellular signal-regulated kinase pathway in human schwannoma. *Cancer Res* 2008;68:5236-45.

24. Ammoun S, Ristic N, Matthies C, et al. Targeting ERK1/2 activation and proliferation in human primary schwannoma cells with MEK1/2 inhibitor AZD6244. *Neurobiol Dis*;37:141-6.

25. Volinia S, Calin GA, Liu CG, et al. A microRNA expression signature of human solid tumors defines cancer gene targets. *Proc Natl Acad Sci U S A* 2006;103:2257-61.

26. Ito Y, Yamamoto M, Mitsuma N, et al. Expression of mRNAs for ciliary neurotrophic factor (CNTF), leukemia inhibitory factor (LIF), interleukin-6 (IL-6), and their receptors (CNTFR alpha, LIFR beta, IL-6R alpha, and gp130) in human peripheral neuropathies. *Neurochem Res* 2001;26:51-8.

27. Lee HK, Seo IA, Suh DJ, et al. Interleukin-6 is required for the early induction of glial fibrillary acidic protein in Schwann cells during Wallerian degeneration. *J Neurochem* 2009;108:776-86.

28.   Olayioye MA, Beuvink I, Horsch K, et al. ErbB receptor-induced activation of stat transcription factors is mediated by Src tyrosine kinases. *J Biol Chem* 1999;274:17209-18.

29.   Curto M, Cole BK, Lallemand D, et al. Contact-dependent inhibition of EGFR signaling by Nf2/Merlin. *J Cell Biol* 2007;177:893-903.

30.   Plotkin SR, Singh MA, O'Donnell CC, et al. Audiologic and radiographic response of NF2-related vestibular schwannoma to erlotinib therapy. *Nat Clin Pract Oncol* 2008;5:487-91.

31.   Asangani IA, Rasheed SA, Nikolova DA, et al. MicroRNA-21 (miR-21) post-transcriptionally downregulates tumor suppressor Pdcd4 and stimulates invasion, intravasation and metastasis in colorectal cancer. *Oncogene* 2008;27:2128-36.

32.   Frankel LB, Christoffersen NR, Jacobsen A, et al. Programmed cell death 4 (PDCD4) is an important functional target of the microRNA miR-21 in breast cancer cells. *J Biol Chem* 2008;283:1026-33.

33.   Moon KS, Jung S, Seo SK, et al. Cystic vestibular schwannomas: a possible role of matrix metalloproteinase-2 in cyst development and unfavorable surgical outcome. *J Neurosurg* 2007;106:866-71.

34.   Roy S, Khanna S, Hussain SR, et al. MicroRNA expression in response to murine myocardial infarction: miR-21 regulates fibroblast metalloprotease-2 via phosphatase and tensin homologue. *Cardiovasc Res* 2009;82:21-9.

35.   Yang Y, Chaerkady R, Beer MA, et al. Identification of miR-21 targets in breast cancer cells using a quantitative proteomic approach. *Proteomics* 2009;9:1374-84.

Figure Legends

Figure 1. **A.** Quantitative real-time RT/PCR results showing relative fold increase in expression of miR-21 in each of the eight vestibular schwannomas compared to control pooled normal vestibular and greater auricular nerve samples. **B.** Delta C_T values were used to determine a statistically significant difference in miR-21 expression in tumors compared to normal controls ($p<0.01$) (asterisk).

Figure 2. **A.** Semi-quantitative RT/PCR results showing PTEN gene expression in tumors VS1 to VS4. **B.** PTEN protein detection by Western blot in VS1 to VS4. β-actin served as a loading control.

Figure 3. Western blot showing the detection of STAT3 protein and the phosphorylated form of STAT3 (PSTAT3) in protein extracts derived from VS2.

Figure 4. Transfection of siRNA oligonucleotides in primary vestibular schwannoma cultures. Vestibular schwannoma cultures were transfected with a Cy3-labeled (red) siRNA oligonucleotide. Nuclei were labeled with Hoechst. Over 90% of cells were transfected. Scale bar=50 μm.

Figure 5. Anti-miR-21 suppresses PDGF induced VS cell proliferation. VS cultures were transfected with scrambled or anti-miR-21probes and maintained in the presence or absence of PDGF-BB (20 ng/ml) for 24 hr in the presence of BrdU (10 μM) A-B. Cultures transfected with scrambled (A) or anti-miR-21 (B) probes were immunostained with anti-S100 (green) and anti-BrdU (red) antibodies. Nuclei were labeled with Hoechst (blue). Scale bar=100 μm. C. Mean percent of BrdU positive, S100 positive nuclei for 4 cultures from separate patients for each condition. Error bars present standard deviation. Significance for difference in means determined by two-tailed Student's t-test.

Figure 6. Anti-miR-21 induces VS cell apoptosis. VS cultures were transfected with scrambled or anti-miR-21 probes. Condensed apoptotic nuclei were identified by TUNEL. A-B. Cultures transfected with scrambled (A) or anti-miR-21 (B) probes were

immunostained with anti-S100 antibody (green) and labeled with TUNEL (red). Nuclei were labeled with Hoechst (blue). Scale bar=100 μm. C. Mean percent of TUNEL positive, S100 positive nuclei for 4 cultures from separate patients for each condition. Error bars present standard deviation. Significance for difference in means determined by two-tailed Student's t-test.

84
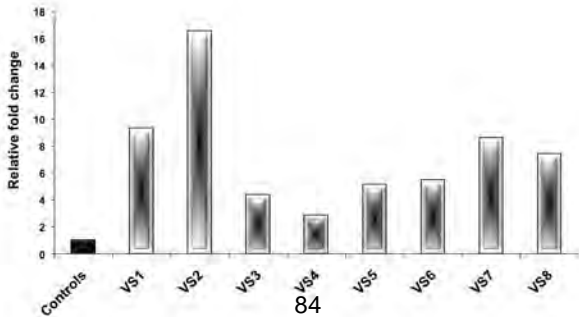
Fig 1A
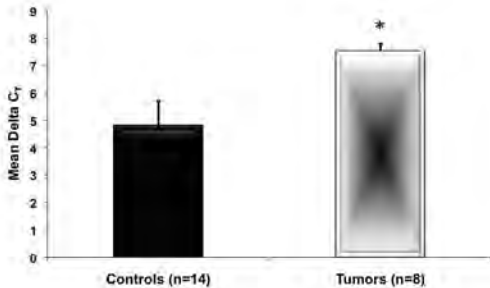
85

Fig 1B

RT/PCR
(362 bp)   A

PTEN
(47 KDa)   B

β-actin
(42 KDa)

RBr   VS1   VS2   VS3   VS4

86
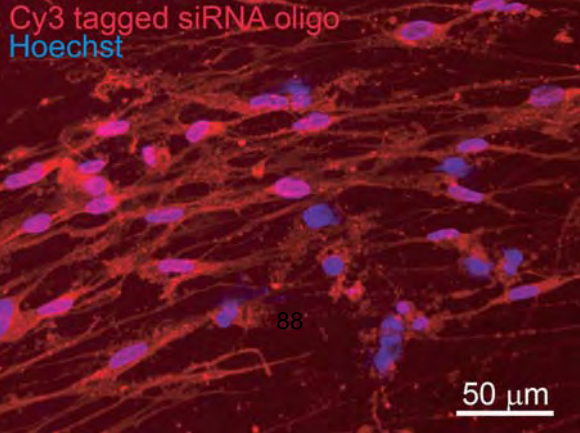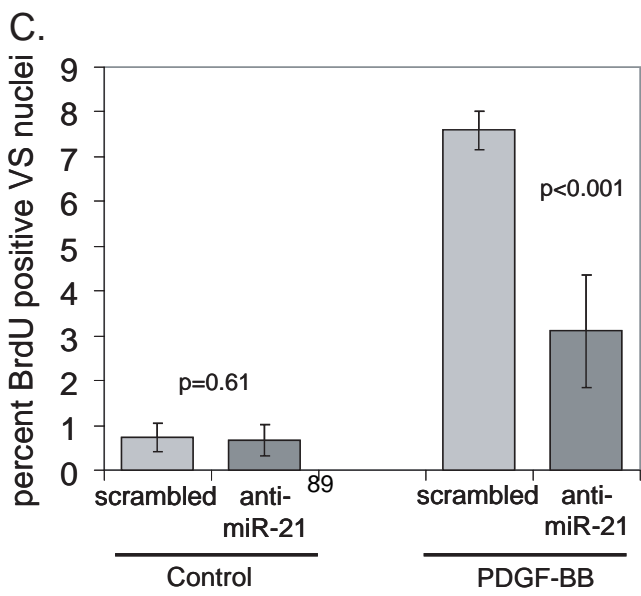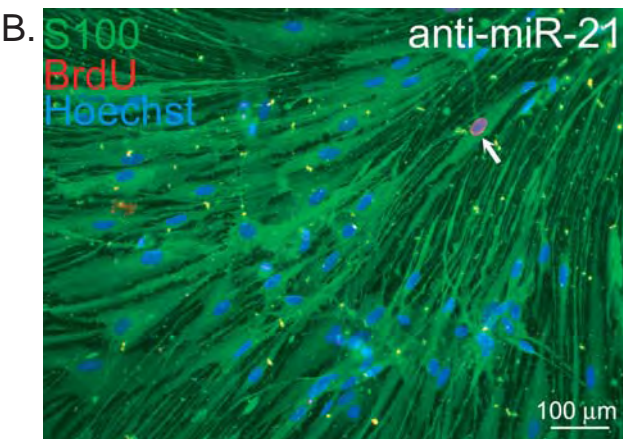
Fig 2

STAT3   PSTAT3

(86 KDa)
(79 KDa)

β-actin
(42 KDa)

87
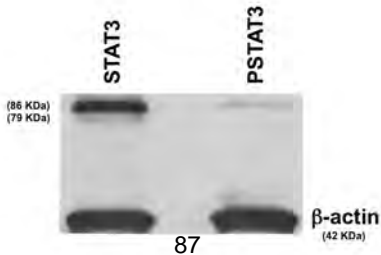
Fig 3

Cy3 tagged siRNA oligo
Hoechst

88

50 μm

A. S100 / BrdU / Hoechst — scrambled

B. S100 / BrdU / Hoechst — anti-miR-21

C.

A. S100 / TUNEL / Hoechst — scrambled

B. S100 / TUNEL / Hoechst — anti-miR-21

C.

p=0.02
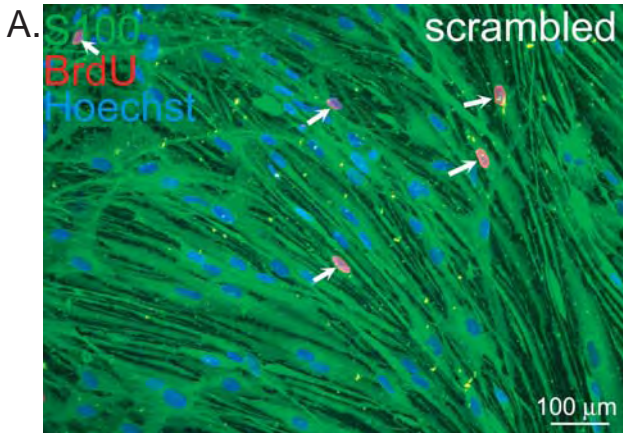
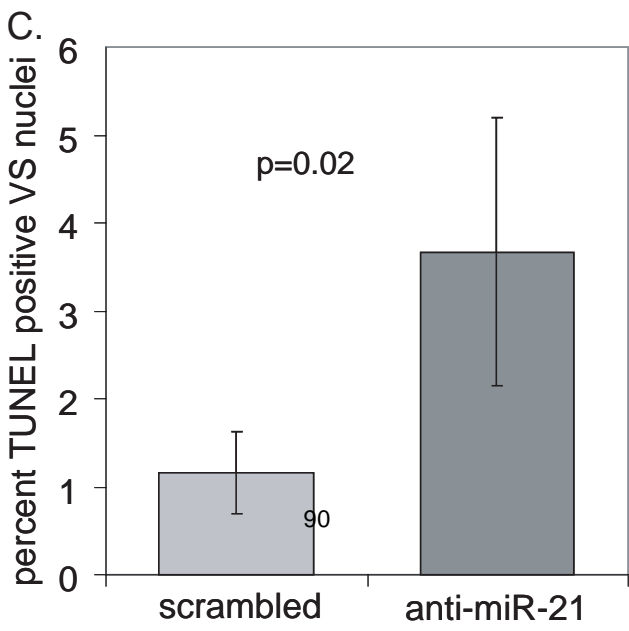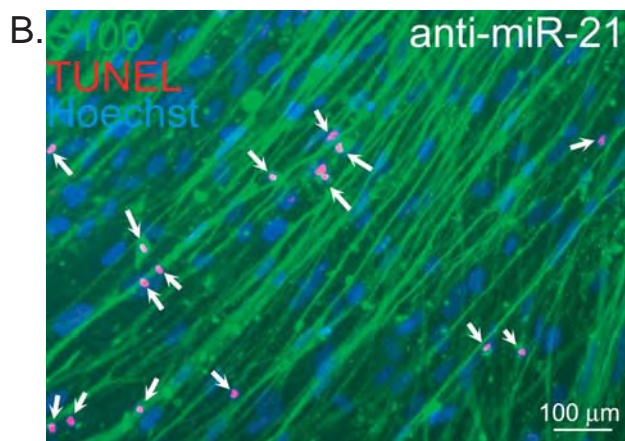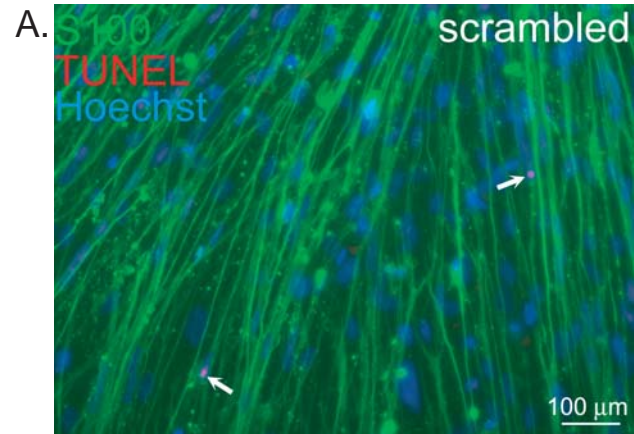**Table 1.** Gene specific reverse transcriptase polymerase chain reaction primer pairs and expected amplicon size.

RT/PCR Primers			
Gene	**Forward Primer (5'-3')**	**Reverse Primer (5'-3')**	**Amplicon Size (BP)**
B2M	TCGCGCTACTCTCTCTTTCTGG	AAAGCAAGCAAGCAGAATTTGG	401
PTEN	TTTGAGTTCCCTCAGCCGTTAC	CTGCTAGCCTCTGGATTTGACG	362
STAT3	GCAAGATCTGAATGGAAACAACC	CCCCTTTGTAGGAAACTTTTTGC	332
CNTF	CAGGGCCTGAACAAGAACAT	AAACGAAGGTCATGGATGGA	410
CNTFR	ATGAGATTGGGACATGGAGTGAC	AGGGTCACAGATCTTCGTGGTAG	158
IL6	AGCCCAGCTATGAACTCCTTCTC	CAGGAACTGGATTCAGGACTTTTG	471
IL6Rα	TTTCAGGGTTGTGGAATCTTGC	TCAGAACAATGGCAATGCAGAG	538
GP130	ATACACAGATGAAGGTGGGAAGG	TTGAAGGATCTGGAACATTAGGC	197
LIF	GTCACAACAACCTCATGAACCAG	GAAGACATCCTTACCCGAGGTG	416
LIFR	GGGCTCCTCATGATTTGAAGTG	CATATCTGAGGCCCAACTCCAG	485

BP = base pairs.

Table 2. Summary of RT/PCR gene expression results for normal vestibular nerve tissue, and VS1 to VS4.

	Normal Vestibular Nerve	VS1	VS2	VS3	VS4
B2M	+	+	+	+	+
STAT3	+	+	+	+	+
CNTF	+	+	+	+	+
CNTFRα	+	+	+	+	+
IL6	−	+	+	+	+
IL6Rα	−	+	+	+	+
GP130	+	+	+	+	+
LIFR	−	+	+	+	+
LIF	−	+	+	+	+
PTEN	+	+	+	+	+

+ = Robust amplification of authentic amplicon; − = Unable to detect amplicon.